

TEMPERATURE CONTROLLABILITY IN CROSS-FLOW HEAT
EXCHANGERS AND LONG DUCTS

A Dissertation

Submitted to the Graduate School
of the University of Notre Dame
in Partial Fulfillment of the Requirements
for the Degree of

Doctor of Philosophy

by

Sorour Abdulhadi Alotaibi, B.S., M.S.

Dr. Mihir Sen, Director

Graduate Program in Aerospace and Mechanical Engineering

Notre Dame, Indiana

June 2003

TEMPERATURE CONTROLLABILITY IN CROSS-FLOW HEAT EXCHANGERS AND LONG DUCTS

Abstract

by

Sorour Abdulhadi Alotaibi

The performance of thermal control systems has, in recent years, improved in numerous ways due to developments in control theory and information technology. However, our understanding of controllability and related questions remain rudimentary. The main characteristics of thermal systems that we are interested in are their distributed nature and delay due to fluid advection from one point to another. Two basic systems, heat exchangers and long ducts, are investigated, and the following issues are addressed. (a) The first is controllability for which conductive-convective systems and cross-flow heat exchangers are examined in detail. In the heat exchanger, controllability results for different choices of the manipulated variable are presented. (b) The second is the control methodology for the outlet temperature in cross-flow heat exchangers. A transient model is developed and tested. The response of this system to control strategies is studied and the performance of a Proportional-Integral (PI) controller to disturbances in the system is presented. (c) The third is the effect of delay in heating or cooling in long ducts in which the flow velocity is the manipulated variable. The governing first-order partial differential equation is transformed to a nonlinear dynamical system represented by an integro-differential equation in the residence time of the fluid in the duct. Both Eulerian and Lagrangian versions of the equation are numerically solved. A PI-based controller

is used to control the duct outlet temperature. Investigation of the linear stability of the system leads to a transcendental equation for which Pontryagin's Theorem can be applied. The stability map for the controller parameters is obtained and the effect of the residence time on the system stability is determined. Simple as well as sub- and super-critical Hopf bifurcations are found.

To my parents.

CONTENTS

FIGURES	vi
ACKNOWLEDGEMENTS	ix
NOMENCLATURE	xi
CHAPTER 1: INTRODUCTION	1
1.1 Background and objectives	1
1.2 Literature review	4
1.2.1 Controllability of thermal systems	5
1.2.2 Simulation of cross-flow heat exchangers	5
1.2.3 Control of cross-flow heat exchangers	6
1.2.4 Modeling, control, and delay in duct flows	7
1.3 Outline of the present work	8
CHAPTER 2: PRELIMINARIES	9
2.1 State-space equation of linear systems	9
2.1.1 Finite-dimensional	10
2.1.2 Infinite-dimensional	13
2.2 Controllability of linear systems	14
2.2.1 Finite-dimensional	14
2.2.2 Infinite-dimensional	16
CHAPTER 3: CONTROLLABILITY OF CONDUCTIVE-CONVECTIVE SYSTEMS	18
3.1 Diffusive-convective system	18
3.2 Distributed control	19
3.2.1 Continuous system	21
3.2.2 Finite-dimensional approximation	23
3.3 Boundary control	24
3.3.1 State controllability	24
3.3.2 Output controllability	25
3.3.3 Optimal control	26
3.4 Constrained control	28
3.5 Conclusions	28

CHAPTER 4: CONTROLLABILITY OF CROSS-FLOW HEAT EXCHANGERS	33
4.1 Governing equations	33
4.2 Manipulated variable: water inlet temperature	38
4.2.1 Finite-dimensional approximation	38
4.2.2 Complete state controllability	40
4.2.3 Output controllability	42
4.3 Manipulated variable: air inlet temperature	47
4.3.1 Complete state controllability	47
4.3.2 Output controllability	47
4.4 Manipulated variable: water velocity	50
4.5 Multi-input controllability	51
4.6 Conclusions	52
CHAPTER 5: NUMERICAL SIMULATION OF THERMAL CONTROL OF CROSS-FLOW HEAT EXCHANGERS	54
5.1 Governing equations	55
5.1.1 Nondimensionalization	57
5.1.2 Boundary conditions	58
5.2 Numerical solutions	58
5.2.1 Validation and convergence	62
5.3 Temperature control	65
5.3.1 Proportional-Integral (PI) control	65
5.3.2 Step change in inlet air temperature	73
5.3.3 Step change in inlet air flow rate	73
5.3.4 Step change in set point	80
5.4 Conclusions	89
CHAPTER 6: FLOW-BASED CONTROL OF TEMPERATURE IN LONG DUCTS	91
6.1 Characteristic solution in duct flow	92
6.2 Governing equations	96
6.3 Numerical solution	98
6.3.1 Eulerian	99
6.3.2 Lagrangian	99
6.3.3 Model validation	100
6.4 Outlet temperature control	107
6.5 Linear stability	108
6.5.1 $\bar{\tau} \ll 1$	109
6.5.2 $\bar{\tau} = O(1)$	111
6.5.3 $\bar{\tau} \gg 1$	119
6.6 Discussion of linear stability	119
6.7 Numerical results	120
6.7.1 Linear	120
6.7.2 Nonlinear	124
6.8 Conclusions	124

CHAPTER 7: CONCLUSIONS AND RECOMMENDATIONS	133
7.1 Conclusions	133
7.2 Recommendations for future work	134
APPENDIX A: NONDIMENSIONALIZATION OF CROSS-FLOW HEAT EXCHANGER GOVERNING EQUATIONS	137
A.1 Air-side equation	137
A.2 Tube-wall equation	137
A.3 Water-side equation	138
BIBLIOGRAPHY	143

FIGURES

2.1	Schematic of room.	12
3.1	One dimensional convection-conduction heat transfer problem.	20
3.2	Variation of boundary condition $u(t)$ with time.	29
3.3	Variation of temperatures at the six nodes with time as a result of varying boundary condition.	30
3.4	Variation of temperatures at the six nodes with time as a result of varying boundary condition.	31
4.1	Single-row cross-flow heat exchanger.	34
4.2	Schematic of single-tube cross-flow heat exchanger.	35
4.3	Effect of number of divisions on condition number when water inlet temperature is manipulated variable.	44
4.4	Effect of air flow rate on condition number.	45
4.5	Effect of water flow rate on condition number.	46
4.6	The effect of the air flow rate on the condition number.	48
4.7	The effect of the water flow rate on the condition number.	49
5.1	Discretization of problem.	60
5.2	Effect of time step on solution at center of pipe.	63
5.3	Effect of time step on solution along heat exchanger pipe wall at 50 sec. and air and water velocity equal to 0.43 m/s and 0.102 m/s respectively.	64
5.4	Outlet air temperature as a function of time step.	66
5.5	Convergence of solution as function of number of nodes.	67
5.6	Possible operating conditions at minimum and maximum air and water Reynolds numbers.	68

5.7	Relation between T_a^{out} and \dot{m}_w for different \dot{m}_a	69
5.8	Behavior of outlet air temperature as function of time at different K_p	70
5.9	Behavior of outlet air temperature as function of time and different K_i	71
5.10	Behavior of outlet air temperature as function of time at constant K_i and different K_p	74
5.11	Behavior of outlet air temperature as function of time at constant K_i and different K_p	75
5.12	Behavior of outlet air temperature as function of time at constant K_i and different K_p	76
5.13	Controlled and uncontrolled outlet air temperature.	77
5.14	Variation of water flow rate with control.	78
5.15	Behavior of outlet air temperature with control and disturbance at 200 sec. due to a step change in air inlet temperature from 25°C to 24.2°C and 25.8°C.	79
5.16	Behavior of outlet air temperature with control and disturbance at 200 sec. due to step change in air inlet flow rate from 20% to 17% and 40%.	81
5.17	Behavior of outlet air temperature with control and disturbance at 200 sec. due to a step change in air inlet flow rate from 20% to 75% of full flow rate.	82
5.18	Behavior of outlet air temperature with control and disturbance at 200 sec. due to step change in set point from 23°C to 22°C.	83
5.19	Variation of water flow rate with control and disturbance at 200 sec. due to step change in set point from 23°C to 22°C.	84
5.20	Behavior of outlet air temperature with control and disturbance at 200 sec. due to step change in set point from 23°C to 24°C.	85
5.21	Variation of water flow rate with control and disturbance at 200 sec. due to step change in set point from 23°C to 24°C.	86
5.22	Behavior of outlet air temperature with control and disturbance at 200 sec. due to step change in set point from 23°C to 21°C	87
5.23	Variation of water flow rate with control and disturbance at 200 sec. due to step change in set point from 23°C to 21°C.	88
6.1	Schematic of duct flow.	93
6.2	Typical characteristic curves.	95
6.3	Flow chart of implicit iterative scheme.	101

6.4	Convergence of Eulerian solution.	102
6.5	Convergence of Lagrangian solution.	103
6.6	Comparison of outlet temperature between Eulerian and Lagrangian methods.	104
6.7	Behavior of temperature with time at different locations in duct.	105
6.8	Behavior of temperature along duct at different times.	106
6.9	Stability regions for $\bar{\tau} \ll 1$; $(K_i \bar{\tau}^3 + 2)/K_p^{cr} > 2(\bar{\tau}^2 - \bar{\tau}^3)$	110
6.10	$F_r(\omega)$ and $F_i(\omega)$ for $k = 1, -2\pi + \pi/4 < \omega < 2\pi + \pi/4$	114
6.11	$F_r(\omega)$ and $F_i(\omega)$ for $k = 2, -4\pi + \pi/4 < \omega < 4\pi + \pi/4$	115
6.12	Condition (ii) in theorem A. $F'_i(\omega)F_r(\omega) - F_i(\omega)F'_r(\omega) > 0$	116
6.13	Real roots of transcendental equation at $K_i > 0$	117
6.14	Stability map.	121
6.15	Effect of delay at constant $K_i = -5$ and variable K_p	122
6.16	Effect of delay at constant $K_p = -5$ and variable K_i	123
6.17	Supercritical Hopf bifurcation at $K_i = -5$ and $K_p = 1.5$ and 2.5	125
6.18	Simple bifurcation at $K_p = 1$ and $K_i = \pm 1$	126
6.19	Supercritical Hopf bifurcation at $K_i = -30$ and $K_p = -5$ and -7	127
6.20	Simple Hopf bifurcation at $K_p = -10$ and $K_i = \pm 5$	128
6.21	Subcritical Hopf bifurcation at $K_p = -15$ and $K_i = -40$	129
6.22	Limit cycles at subcritical Hopf bifurcation at $K_p = -15$ and $K_i = -40$	130
6.23	Nonlinear amplitude and frequency.	131

ACKNOWLEDGEMENTS

It would not have been possible to complete this work without the help of many people. However, there are a special few to whom I am so grateful that I would like to mention individually. First of all, I am so grateful to my advisor Professor Mihir Sen for his guidance, and understanding throughout my research. His stimulating comments and arguments have been a constant source of inspiration not only as a professor but also a friend. Special thanks are due to Professor K.T. Yang for his fruitful discussion and advices. Also, I would like to express my appreciation to Professor Bill Goodwine and Professor Panos Antsaklis for taking the time to read and review my dissertation.

I also thank the Kuwait University for supporting me to pursue my higher education. I also grateful to the staff of the Islamic center of Michiana in South bend for providing me and my family a warm and a comfortable atmosphere for the worship services, which kept me on track with my research.

As always, I thank my family members for their support and prayer. First and foremost to thank are my parents, Abdulhadi and Monirah. My Grand Mom, my brothers, and sisters are also to be thanked. My most tender and thanks go to my beloved wife Wojoud Albateni, who tirelessly helped me, understood me, and encouraged me during the course of the last eight years. I am deeply grateful for you Wojoud. I also thank my sweet sons Abdulhadi, Mohammed, and Abdulwahab and my daughter Razan who's wonderful smiles and noises kept me going toward completion of this work.

Last but not least, all prayers and glories are due to the all mighty Allah (God). Only by his power and guidance was I able to complete my study and finish my dissertation.

NOMENCLATURE

Latin Symbols

A	area [m ²]
\mathbf{A}	matrix operator for system
\mathcal{A}	semigroup operator
A_c	cross-sectional area [m ²]
a	numerical coefficient
\mathbf{B}	matrix operator for manipulated variable
\mathcal{B}	linear operator
\mathbf{b}	vector
\mathbf{C}	matrix operator for output variable
C_M	condition number
c	$\alpha / \Delta x^2$ in Chapter 3
c	specific heat [J/kg K] in Chapters 4 and 5
D	diameter [m]
$D(P)$	domain of operator P
\det	determinant
diag	diagonal matrix
e	error [K]
h	heat transfer coefficient [W/m ² K]
k	thermal conductivity [W/m K]
K_I	integral control constant [kg/s K]

K_P	proportional control constant [kg/s ² K]
L	length [m]
l	dimensionless length
M	mass [Kg]
\mathbf{M}	controllability matrix
\dot{m}	mass flow rate [kg/s]
\mathbf{N}	output controllability matrix
Nu	Nusselt number = hD/k
n	number of finite-difference divisions
P	perimeter [m]
Pe	Peclet number = $Re Pr$
Pr	Prandtl number = ν/α
r	radius [m]
Re	Reynolds number = VD/ν
T	temperature [°C]
t	time [s]
\mathbf{u}	manipulated vector
v	velocity [m/s]
\mathbf{W}	reachability or controllability grammian matrix
x	spatial coordinate [m]
\mathbf{x}	state vector
\mathbf{y}	output vector

Greek Symbols

α	thermal diffusivity [m ² /s]
----------	---

β	dimensionless coefficient
β_m	eigenvalues
ϕ_m	eigenfunctions
γ	thermal diffusivity ratio = α_w/α_t
γ_m	eigenvalues
θ	temperature in Chapter 3
θ	dimensionless temperature in Chapter 5
ρ	density [kg/m ³]
σ	eigenvalue
σ_r, σ_i	real and imaginary parts
τ	dummy variable in Chapter 2
τ	dimensionless time in Chapter 4
τ	residence time in Chapter 7
Δt	time step [s]
Δx	grid spacing
$\Delta \tau$	dimensionless time step size
Δx^*	dimensionless grid spacing
$\delta(P)$	spectrum of the operator P
ζ	parameter representing convection [1/s]

Superscripts

in, out	inlet and outlet respectively
$\overline{(\quad)}$	average value
(\cdot)	dimensional quantity
$'$	small perturbation
t	solution at current time

Subscripts

a	air
f	final
i	in
in	inlet
L	boundary
o	out
T	transpose of matrix
t	tube
w	water
∞	ambient
-1	inverse of matrix

CHAPTER 1

INTRODUCTION

1.1 Background and objectives

The control of thermal components is important in many industrial thermal processes including air conditioning, chemical processes, power generation, etc. Among these components are compact heat exchangers and heating/cooling ducts, which can be found in almost every industrial and residential applications. In many practical thermal systems, it is important that the dynamics of these components in response to changes in other conditions be understood. The controlled variable is usually the exit temperature of one of the fluids in response to disturbances in the inlet conditions. An example of this is a building cooling or heating system where long ducts and water-to-air cross-flow heat exchangers are commonly used. It may then be desired that, in response to arbitrary changes in one or more of the inlet conditions, the discharge air temperature from any one of the heat exchangers be kept constant by manipulating the flow rate of the water.

In order to properly predict the behavior of the control system, it is important that the dynamics of these components in response to these changes in input conditions be understood and calculable. This is difficult due to the distributed and nonlinear nature of these systems. It is described by partial differential equations and the presence of turbulent flow makes it difficult to solve even under steady-state conditions. Sometimes a lumped parameter approximation is used; ordinary differential equations are then obtained but the spatially distributed nature and the

transportation delay in long ducts are ignored. An intermediate approach may be taken by using approximation techniques, but the resulting system with an acceptable accuracy usually has too high an order for easy dynamic analysis and control. Control is also complicated by the fact that the steady state response of the heat exchanger is a nonlinear function of the flow and temperature variables of interest.

Before attempting to design a control strategy for a system to achieve a desired objective, it is clearly sensible to determine whether any control is possible. This can be done by investigating the controllability (or state controllability) of the system. This refers to the ability of the system to reach a specific condition under any control input within a prescribed time interval. Output controllability is a similar concept applied only to the output of the system. In thermal systems, controllability usually means that a system with an initial temperature distribution is able to move to any temperature distribution in finite time by means of a suitable input. The control input could be in the form of flow rate, an applied heat flux or externally applied temperature. A system which is found to be not controllable has a behavior which cannot in general taken from one state to another. Of course this does not imply that the system is not useful.

Controllability must be exactly defined before the given system is tested for it. It is easily tested for systems governed by a system of linear, finite-dimensional ordinary differential equations [1]. The situation is more complicated for linear infinite-dimensional systems such as those governed by partial differential equations (PDEs) [2]. Controllability is exact if the function representing the state can be taken from an initial to a final target state, and approximate if it can be taken to the neighborhood of the target [3]. Determination of approximate controllability is usually sufficient and is the goal here. It only requires that the system reach a small neighborhood of the target state, and makes sense in most engineering problems.

Although an uncontrollable thermal system cannot in general be taken from any state to any other, it is for many applications not necessary since state controllability may be less important than output controllability. For example, Rosenbrock [4] notes that most industrial plants are controlled quite satisfactorily though they are not state controllable. Constrained controllability where the manipulated inputs such as flow rates and temperatures have finite bounds is also very relevant to thermal engineering.

The control of the fluid temperature at a specific location is important. This is often achieved by circulating fluids such as steam or chilled water through long ducts with heat exchangers that can heat or cool the air passing over them. In these cases, sensors and actuators are usually separated, and in addition, fluid mass and energy flows always vary with time. In these long ducts, the fluid takes time to travel these lengths. As a result, a dynamic delay between the inlet and the outlet will occur. This delay will effect the controlled output and may lead to subsequent instability in the system. These aspects should be understood and taken into account in designing a thermal control system.

In the *Hydronics Laboratory* at the University of Notre Dame, the overall objective is the simulation and control of heat exchangers and hydronic networks. Within this framework, the simulation and control of a cross-flow heat exchanger was successfully performed using artificial neural networks [32]. At that time, however, it was not clear whether thermal components were indeed controllable with respect to various inputs. To clarify this is one of the goals of the present work. Thermal systems have some special characteristics that differentiate them from other systems. There is convection which can be modeled by Newton's law of cooling, conduction modeled by Fourier's law which leads to partial differential equations, and advection which can lead to a finite transportation delay. In this dissertation we will look at

the details of these issues using two thermal systems as typical examples, cross-flow heat exchangers and long ducts flow that have convection, conduction, and delay.

The objective of this work is aimed at bringing control theory and heat transfer together to answer some of the questions that fall between the two sciences. It is not easy (and beyond their scope) for a control or a heat transfer engineer to answer those questions related to the controllability of a thermal system. For this reason, two widely used thermal systems, cross-flow heat exchangers and flow in long ducts, are chosen in this dissertation to address some of these questions.

One of main objectives of this work is to develop more accurate transient models to understand their dynamic response for the purpose of control of these two systems. The resultant models are simple and yet effective enough in reflecting the main dynamic characteristics of the cross-flow heat exchangers and flow in long heating/cooling ducts. Since many control theory applications deal with ordinary differential equations rather than partial differential equations, it is our aim to use these models to understand the response of these distributed thermal systems to control strategies.

The second main objective is to understand the controllability of a thermal system from a mathematical and practical point view and to give different controllability results.

A final objective is to provide a physical understanding of the effect of time delay in long heating/cooling ducts. Furthermore, the effect of time delay on the stability of a Proportional-Integral controller is also to be investigated.

1.2 Literature review

The following literature review is divided into four topics that are related to this work. The cited published literature is related to the controllability of thermal systems, simulation of cross-flow heat exchangers, control of cross-flow heat exchangers,

and control and effect of delay in duct flows.

1.2.1 Controllability of thermal systems

In the mid-seventies, the theory of controllability of linear partial differential equations began to be developed. Different papers appeared concerning various kinds of controllability of linear continuous-time dynamical systems defined in infinite-dimensional spaces. Pioneering contributions include the works by Fattorini [5], Russell, and later Triggiani [7]. There are plenty of other results and papers, so that it is impossible to list all of them. Controllability for different kinds of dynamical systems governed by PDEs has been considered in many publications (see [8] for an extensive list). Most of these results are in the framework of abstract equations in Banach and Hilbert spaces. Applications to thermal problems, however, are very limited. There has been some work in the areas of industrial and chemical plants [9] and thermal networks [10]. The controllability of multi-stream heat exchangers, when some operating parameters deviate from their design value, has also been studied recently [11].

1.2.2 Simulation of cross-flow heat exchangers

There is a lot of publication regarding the simulation of heat exchangers. Perhaps the most recent and complete work on the simulation of the dynamic behaviour of heat exchangers was that of Wilfried R. and Yimin X. [12]. But, despite the importance of the simulation of cross-flow heat exchangers, it found relatively less attention compared to other types of heat exchangers.

Much of the early work focussed on parallel- and counter-flow heat exchangers as power plant components. In the literature, there have been several analytical, experimental and numerical studies carried out on the transient response of cross-flow heat exchangers. Several investigators have presented simplified models of cross-

flow heat exchangers. Gartner and Harrison [13, 14] proposed frequency response transfer functions for inlet temperature disturbances for water flowing in a tube in a cross flow of dry air. Myers *et al.* [15] numerically solved partial differential equations for a more general case of a cross-flow response to an inlet temperature disturbance. Further experimental and analytical research [16, 17, 18, 19] extended this to more complex cross-flow geometries and disturbances in the water flow rate. Boot *et al.* [20] studied the outlet air temperature response of single row, multiple-pass, cross-flow heat exchangers to disturbances in the water flow rate. Sundén [21] numerically solved transient conjugate forced convection heat transfer from a circular horizontal thick-walled tube in cross-flow with external forced flow in the range of $5 \leq Re \leq 40$ and with various inner-tube surface thermal conditions changing with time. Underwood and Crawford [22] developed an empirical nonlinear model of a hot-water to air heat exchanger that could be used in nonlinear control. Yamashita *et al.* [23] used a central difference method with a large value of the heat capacity. In [24, 25, 26] the Laplace transform method has been used to obtain a two-dimensional transient temperature distribution of the core wall and both fluids. A review of research carried out in various applications of transient conjugate heat transfer has been given in Refs. [27, 28].

1.2.3 Control of cross-flow heat exchangers

It was pointed out in the previous section that while a lot of works have been published regarding the simulation of the heat exchangers, relatively less work has been done on the simulation of cross-flow heat exchangers. Even fewer work deal with issues relating to the control of cross-flow heat exchangers and its related questions. Most publications focus on shell-and-tube heat exchangers [29, 30, 31]. Artificial neural networks have been used recently in dynamic simulation and control [32].

1.2.4 Modeling, control, and delay in duct flows

Duct flow is usually described by a first order hyperbolic partial differential equation which appears often as a control system model in many engineering and nonengineering processes. This equation has been solved by different numerical algorithms, such as, finite differences [33], method of characteristics [34, 35], Galerkin method with Legendre polynomials [36], and the use of orthogonal collocation [37].

Several flow control algorithms have been proposed to this problem for different controlled outputs. The early research based on the lumped parameter technique [38] followed by the application of control methods for ordinary differential equations. [37] used orthogonal collocation to control first order hyperbolic systems. Recently, the application of distributed parameter systems based on control methods for partial differential equation has been used; see for example [39] and the comprehensive book [40].

The effect of delay has been studied in different fields. However, the literature contains few applications to thermal systems. During the years since Munk [41], a small number of papers concerning thermal delay have appeared in the literature, though there has been some work in the area of heat exchangers that have been studied by Górecki *et al.* [42] and Huang *et al.* [43]. There are fewer publications on heating, ventilating and air-conditioning (HVAC) systems. Zhang and Nelson [44] modeled the effect of a variable-air-volume ventilating system on a building using delay, and Antonopoulos and Tzivanidis [45] developed a correlation for the thermal delay of buildings. Work on duct flows has also been reported. Saman and Mahdi [46] analyzed pipe and fluid temperature variations due to flow, and Chow *et al.* [47] modeled the thermal behavior of fluid conduit flows with transportation delay. The delayed hot water problem has been studied by Comstock *et al.* [48]. Chu [49] described the application of a discrete optimal tracking controller to an

industrial electrical heater with pure delays, and Chu *et al.* [50] studied a time-delay control algorithm for the same industrial electric heater.

Stability analysis for systems with delay usually leads to transcendental equations. In general, these equations have an infinite number of roots. This property of the characteristic equation suggests that a delay system indeed belongs to the class of infinite-dimensional systems. The solution of these equations to locate their roots is of much interest in determining the stability of a system; see for example [51, 53] and the literature cited therein for more details on the solution and the stability of these equations. More explanations with extensive references on these equations and the effect of delay on stability can be found in [54]. In [55], a transcendental equation has been solved to construct a PI controller for stabilizing first-order plants with input delay. In [56], the thermal aspects of long duct flows with constant mass flow has been addressed.

1.3 Outline of the present work

The outline of this dissertation is as follows. In Chapter 2 we present some basic notations, definitions and preliminary results necessary for working with some topics that will be useful. In Chapter 3 we discuss the concept of controllability with application to a conductive-convective system. Chapter 4 extends the problem of controllability to a more complex model representing a cross-flow heat exchanger. Chapter 5 presents the numerical simulation of cross-flow heat exchangers, and their thermal control. Chapter 6 presents simulation of long duct flows and the effect of delay on the stability of the system. Stability maps for Proportional-Integral controllers are also included in this chapter.

CHAPTER 2

PRELIMINARIES

This dissertation makes use of tools and results from the area of mathematical control theory. Here we collect the basic definitions and results so that they can be used later without more detail. Most of the material in this chapter is covered in additional depth in texts by Ansaklis and Michel [1], Klamka [8], and Ray [38].

It turns out that, though these issues are well known in mathematical control theory, they have not received adequate treatment from the thermal engineering point of view. Thus most heat transfer engineers are, by and large, unaware of these ideas and their applications in thermal systems.

2.1 State-space equation of linear systems

Most dynamical systems, either mechanical, thermal or electrical, can be represented by a differential equation. These equations that depend on the physics of the analysis are lumped (finite-dimensional) or distributed parameter (infinite-dimensional), linear or nonlinear, time-dependant or time-independent, and continuous or discrete in time. In this section we will consider linear dynamical systems both finite-dimensional and infinite-dimensional that are continuous in time.

These dynamical systems usually lead to a system of ordinary differential or partial differential equations. In matrix form the state-space equation can be represented by a single equation. In essence, this means that, instead of studying a high-order differential equation, we replace it by a system of first-order differential

equations.

2.1.1 Finite-dimensional

The dynamical system we will consider in this section is linear time-continuous and finite-dimensional. Such systems have no spatial dependence, and sometimes results as a consequence of a linearization of the original nonlinear system. The general form of such systems can be written as

$$\begin{aligned}\dot{x} &= f(x, u, t), \\ y &= g(x, u, t),\end{aligned}\tag{2.1}$$

where x is the state vector which is the variable of the system that needs to be evaluated to determine its future evolution. It could be the position of a moving object, a velocity, or a temperature. u is the system input vector, y is the system output, and f and g are vector-valued functions. These equations are called the state and output equations, respectively. A special case of Equation (2.1) is the time-independent set of equations given by

$$\begin{aligned}\dot{\mathbf{x}}(t) &= \mathbf{A}\mathbf{x}(t) + \mathbf{B}\mathbf{u}(t), \\ \mathbf{y}(t) &= \mathbf{C}\mathbf{x}(t) + \mathbf{D}\mathbf{u}(t),\end{aligned}\tag{2.2}$$

where t is time, $\mathbf{x}(t) \in \mathbb{R}^n$ represents the state of the system, $\mathbf{u}(t) \in \mathbb{R}^m$, $\mathbf{A} \in \mathbb{R}^{n \times n}$, $\mathbf{B} \in \mathbb{R}^{n \times m}$, $\mathbf{C} \in \mathbb{R}^{p \times n}$, and $\mathbf{D} \in \mathbb{R}^{p \times m}$. Matrices \mathbf{A} , \mathbf{B} , \mathbf{C} , and \mathbf{D} are all constant.

The solution of Equation (2.2) for \mathbf{x} can be found. For the homogeneous case, for example, when the input $\mathbf{u} = 0$ with initial condition $\mathbf{x}(0) = \mathbf{x}_0(t)$, the solution is

$$\mathbf{x}(t) = \mathbf{x}_0(t)e^{\mathbf{A}t}.\tag{2.3}$$

If we need the system to start from $t = t_0$, not from $t = 0$, then

$$\mathbf{x}(t) = \mathbf{x}_0(t)e^{\mathbf{A}(t-t_0)}.\tag{2.4}$$

For an inhomogeneous problem, for example, if $\mathbf{u} \neq 0$ this problem has the solution

$$\mathbf{x}(t) = \mathbf{x}_0(t)e^{\mathbf{A}(t-t_0)} + \int_{t_0}^t e^{\mathbf{A}(t-\tau)} \mathbf{B}\mathbf{u}(\tau) d\tau. \quad (2.5)$$

To illustrate how these general results apply, let us consider the following simple heat transfer problem. A room is shown in Figure 2.1 with temperature T_a , wall temperature T_{wall} , and outside temperature T_∞ .

The heat balance equations for this room can be described by the following coupled differential equations. For the walls of the room we have

$$M_w c_w \frac{dT_w}{dt} = h_i A_i (T_a - T_{wall}) + h_o A_o (T_\infty - T_{wall}), \quad (2.6)$$

and for the temperature inside the room we have

$$M_a c_a \frac{dT_a}{dt} = h_i A_i (T_{wall} - T_a), \quad (2.7)$$

where A_i and A_o are the internal and external areas respectively, and h_i is the inside heat transfer coefficient, and h_o is the outside heat transfer coefficient.

The above equations can be rearranged as

$$\frac{dT_w}{dt} = \frac{h_i A_i}{M_w c_w} (T_a - T_{wall}) + \frac{h_o A_o}{M_w c_w} (T_\infty - T_{wall}), \quad (2.8)$$

$$\frac{dT_a}{dt} = \frac{h_i A_i}{M_a c_a} (T_{wall} - T_a). \quad (2.9)$$

Thus, if we define the vector $\mathbf{x} = [T_{wall} \quad T_a]^T$, the matrices

$$\mathbf{A} = \begin{bmatrix} -(h_i A_i + h_o A_o)/(M_w c_w) & (h_i A_i)/(M_w c_w) \\ (h_i A_i)/(M_a c_a) & -(h_i A_i)/(M_a c_a) \end{bmatrix}, \quad (2.10)$$

$$\mathbf{B} = \begin{bmatrix} (h_o A_o)/(M_w c_w) & 0 \end{bmatrix}^T. \quad (2.11)$$

and $\mathbf{u} = T_\infty$ then the model of the system is in the form of Equation (2.2).

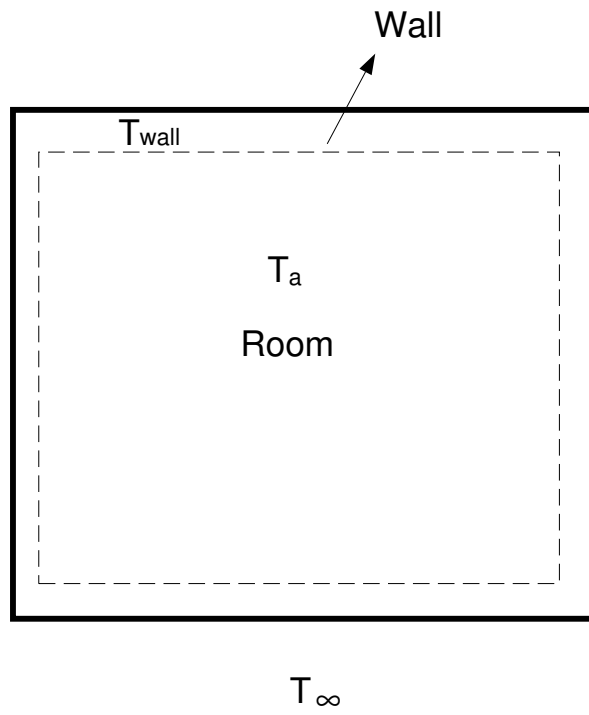


Figure 2.1. Schematic of room.

2.1.2 Infinite-dimensional

Infinite-dimensional or distributed parameter systems are distinguished from the finite-dimensional systems by the fact that the states, input, and the output may depend on spatial position. Thus these systems can be described by partial differential equations, integral equations, or delay differential equations. In general, these systems can be presented in a unified treatment in an abstract formulation using the theory of semigroup operators.

In this dissertation we will encounter one class of infinite-dimensional systems which is described through partial differential equations. The state-space Equation (2.2) can be used where now the dimension of the system is infinite. The state variable $\mathbf{x}(t) \in \chi$ a Banach space, the input $\mathbf{u} \in \mathbf{L}^2([0, \infty), \mathbf{U})$, where $\mathbf{L}^2([0, \infty), \mathbf{U})$ is a space of locally 2-integrable functions with values in \mathbf{U} , \mathbf{U} is a Banach space, $\mathbf{B} \in \mathbf{L}(\mathbf{U}, \chi)$, i.e. $\mathbf{B} : \mathbf{U} \rightarrow \chi$ is a linear and bounded operator, and $\mathbf{A} : \chi \supset D(\mathbf{A}) \rightarrow \chi$ is the infinitesimal generator of a strongly continuous semigroup of linear, bounded operators $\mathbf{S}(t) : \chi \rightarrow \chi$, $t \geq 0$ [6].

For every initial condition $\mathbf{x} \in \chi$ and each input $\mathbf{u} \in \mathbf{L}^2([0, \infty), \mathbf{U})$ there exists a unique solution of this abstract differential equation

$$\mathbf{x}(t) = \mathbf{S}(t)\mathbf{x}(0) = \int_0^t \mathbf{S}(t - \tau)\mathbf{B}\mathbf{u}(\tau)d\tau. \quad (2.12)$$

If the control input space \mathbf{U} is finite-dimensional, i.e. $\mathbf{U} = \mathbb{R}^m$, the dynamical system (2.2) can be written as

$$\dot{\mathbf{x}}(t) = \mathbf{A}\mathbf{x}(t) + \sum_{j=0}^n \mathbf{b}_j u_j(t), \quad (2.13)$$

where $\mathbf{b}_j \in \chi$, and $u_j \in \mathbf{L}^2([0, \infty), \mathbb{R})$ for $j = 1, 2 \dots, n$.

In this case we have the following solution

$$\mathbf{x}(t) = \mathbf{S}(t)\mathbf{x}(0) = \int_0^t \mathbf{S}(t - \tau) \sum_{j=0}^n \mathbf{b}_j u_j(\tau) d\tau. \quad (2.14)$$

2.2 Controllability of linear systems

One of the useful and fundamental concepts in modern mathematical control theory is controllability. Many dynamical systems are such that the control does not affect all the components state of the system but only part of them. Therefore, it is important to know whether or not complete system control is possible. There are many definitions of the controllability of dynamical systems, but generally speaking a system is controllable if there is a control input that is able to steer the system from any initial condition to any other final state in finite time.

Controllability must be exactly defined before the given system is tested for it [2]. Even for linear systems, the controllability criteria for infinite-dimensional systems governed by partial differential equations are different than for finite-dimensional systems. The latter have exact controllability which requires the system to move to an exact final state from any initial state. For infinite-dimensional systems function-space completeness requirements make exact controllability difficult to analyze, so that approximate controllability is usually used. This only requires that the system be in a small neighborhood of the final state and makes sense in most engineering problems.

As in many real applications the control inputs are always bounded between minimum and maximum values due to physical constraints, economics or safety requirements. The controllability of these systems is defined as constrained controllability. In this section the conditions of controllability for some systems will be defined.

2.2.1 Finite-dimensional

In this section we will define the condition for controllability of linear, time-invariant (matrices \mathbf{A} and \mathbf{B} above are constant) dynamical systems. It can be shown [1]

that the system in Equation (2.2) is completely state controllable if and only if the rank of an $n \times nm$ controllability matrix \mathbf{M} is n , where

$$\mathbf{M} = [\mathbf{B} | \mathbf{A}\mathbf{B} | \mathbf{A}^2\mathbf{B} | \dots | \mathbf{A}^{n-1}\mathbf{B}] \in \mathbb{R}^{n \times nm}. \quad (2.15)$$

If this condition is satisfied, the system is controllable; this means that the control input $\mathbf{u}(t)$ can influence all the components of the state $\mathbf{x}(t)$, and is able to move the system to any final state. In the above room example, the control input $\mathbf{u}(t)$ was T_∞ . The controllability criterion may be tested by noting matrices \mathbf{A} and \mathbf{B} as above. The controllability matrix is

$$\mathbf{M} = \begin{bmatrix} (h_o A_o)/(M_w c_w) & -(h_i A_i + h_o A_o)(h_o A_o)/(M_w c_w)^2 \\ 0 & (h_o A_o)(h_i A_i)/(M_a M_w c_a c_w) \end{bmatrix}.$$

Clearly the rank of \mathbf{M} is two for this second-order system, so the system is completely state controllable. This means if the control input T_∞ can be changed by blowing hot or cold air to the room, then the inside and the wall temperatures can be controlled to reach certain values in finite time. Of course in a real situation when the system is of high order it becomes difficult to control all the components of the state of the system simultaneously although it is mathematically possible. In these situations other controllability objectives are practically more useful.

In many situations the output $\mathbf{y}(t)$ of the system is needed to be controlled rather than the state of the system. In these situations the controllability has to be defined as the output controllability. The condition for a system to be output controllable is that the rank of the $p \times nm$ output controllability matrix \mathbf{N}

$$\mathbf{N} = [\mathbf{C}\mathbf{B} | \mathbf{C}\mathbf{A}\mathbf{B} | \mathbf{C}\mathbf{A}^2\mathbf{B} | \dots | \mathbf{C}\mathbf{A}^{n-1}\mathbf{B}] \in \mathbb{R}^{p \times nm} \quad (2.16)$$

is p .

Matrices \mathbf{A} and \mathbf{B} are fixed, but matrix \mathbf{C} will depend on the output of the system. In the above example, if two temperatures, T_a and T_w , are needed to be

controlled, then $\mathbf{C} = [1 \ 1]$. If we want to control only one temperature, then $\mathbf{C} = [0 \ 1]$, and $[1 \ 0]$ for the room and wall temperature respectively.

2.2.2 Infinite-dimensional

In general it is very difficult to satisfy all the conditions for controllability in infinite-dimensional systems. Here we will consider the controllability of only one type of infinite-dimensional systems, systems governed by parabolic partial differential equations. Consider the state-space system in Equation (2.13)

$$\dot{\mathbf{x}}(t) = \mathbf{A}\mathbf{x}(t) + \sum_{j=0}^n \mathbf{b}_j u_j(t).$$

If the operator \mathbf{A} satisfies the following assumptions, then we can obtain simple and easily computable criteria for approximate controllability of the above system [8].

- (a) Spectrum $\delta(\mathbf{A})$ of the operator \mathbf{A} is a point spectrum consisting entirely of β_m , $m = 1, 2, \dots$, which are distinct, isolated, real eigenvalues of the operator \mathbf{A} , each with multiplicity $r(m)$, $m = 1, 2, \dots$, equal to the dimensionality of the corresponding eigenmanifolds.
- (b) There is a corresponding complete orthogonal set ϕ_{mk} , $m = 1, 2, \dots$, $k = 1, 2, \dots, r(m)$, of the eigenfunctions of \mathbf{A} .
- (c) There is a semigroup $\mathbf{S}(t)$ given by

$$\mathbf{S}(t)\mathbf{x} = \sum_{m=1}^{\infty} e^{\beta_m t} \sum_{k=1}^{r(m)} \langle \mathbf{x}, \phi_{mk} \rangle \phi_{mk}, \quad t \geq 0.$$

To simplify the notation we will introduce the following $r(m) \times n$ dimensional matrix \mathbf{B}_m [8]

$$\mathbf{B}_m = \begin{bmatrix} \langle \mathbf{b}_1, \phi_{m1} \rangle & \langle \mathbf{b}_2, \phi_{m1} \rangle & \cdots & \langle \mathbf{b}_n, \phi_{m1} \rangle \\ \vdots & \vdots & \vdots & \vdots \\ \langle \mathbf{b}_1, \phi_{mr(m)} \rangle & \langle \mathbf{b}_2, \phi_{mr(m)} \rangle & \cdots & \langle \mathbf{b}_n, \phi_{mr(m)} \rangle \end{bmatrix}, m = 1, 2, \dots$$

where $\langle \cdot, \cdot \rangle$ is a Hilbert space inner product. It is known that the system is approximately state controllable if and only if for all m , the rank of $\mathbf{B}_m = r(m)$. If all eigenvalues are singular, we have of course $r(m) = 1$ for all $m = 1, 2, \dots$. Then the condition for approximate controllability reduces to

$$\sum_{j=1}^n \langle \mathbf{b}_j, \phi_{mj} \rangle \neq 0, \quad m = 1, 2, \dots.$$

If we have only one control input, the condition for controllability is to check that the inequality

$$\langle \mathbf{b}, \phi_m \rangle \neq 0, \quad m = 1, 2, \dots$$

holds. In general, this procedure to check the controllability of a given system is not as straightforward as for finite-dimensional systems.

CHAPTER 3

CONTROLLABILITY OF CONDUCTIVE-CONVECTIVE SYSTEMS

3.1 Diffusive-convective system

The control of a heat diffusion-convection process is needed frequently in many applications. Heat exchangers, for example, have many of the aspects to be considered here. To give another example, in steel-making plants it is necessary to estimate the temperature distribution of metal slabs based on measurements at certain points on the surface [57]. In this chapter we will investigate the controllability of a mathematical model representing a one-dimensional conduction-convection system. This is an approximate model of a heat exchanger in which we have neglected the advective effect of the in-tube fluid. We will determine controllability using finite-difference and continuous approaches and compare the results. For a controllable system, since there exists an input that is able to steer the system from any given initial condition to any other desired condition within a finite time, we will calculate the inhomogeneous boundary condition that will do this using linear systems theory. It is easy to understand that in real systems this input control function is bounded, and hence some limitations should be placed on it.

Consider the fin equation, which is a one-dimensional conduction-convection system that gives a single second-order PDE [59]. Though the controllability of this system has been analyzed previously [8], it will be shown that it can be studied using either infinite- or finite-dimensional approaches.

A conductive bar of length L that is being cooled or heated from the side as

schematically shown in Figure 3.1 is considered. There is conduction along the bar as well as convection to the surroundings from the side. The temperature distribution is governed by

$$\frac{\partial T}{\partial t} = \alpha \frac{\partial^2 T}{\partial x^2} - \zeta(T - T_\infty), \quad (3.1)$$

where $T(x, t)$ is the temperature distribution along the bar representing the state of the system, T_∞ is the temperature of the surroundings, t is time, and x is the longitudinal coordinate. α is the thermal diffusivity, and $\zeta = hP/\rho cA_c$ where h is the convective heat transfer coefficient, A is the constant cross-sectional area of the bar, P is the perimeter of the cross section, ρ is the density, and c is the specific heat. For simplicity it will be assumed that ζ is independent of x .

The system is assumed to be initially at a uniform temperature. This does not imply any loss of generality since if a linear system is indeed controllable it can be taken from any state to any other. An adiabatic condition at the end $x = 0$ will be assumed so that $(\partial T/\partial x)(0, t) = 0$. Either the surrounding temperature T_∞ or the temperature of the other end $T(L, t)$ can be used as a manipulation variable for control purposes. These two single-input methods are known as distributed and boundary control since the manipulated variable enters through the equation and the boundary condition, respectively. They will be analyzed separately.

3.2 Distributed control

In this section the controllability of the system will be analyzed in two different ways: as a continuous system and using a finite-dimensional approximation. The manipulated variable is the ambient temperature $T_\infty(t)$ with a constant boundary condition $T(L, t) = T_L$. Using T_L as a reference temperature and defining $\theta = T - T_L$, Equation (3.1) becomes,

$$\frac{\partial \theta}{\partial t} = \alpha \frac{\partial^2 \theta}{\partial x^2} - \zeta \theta + \zeta \theta_\infty(t), \quad (3.2)$$

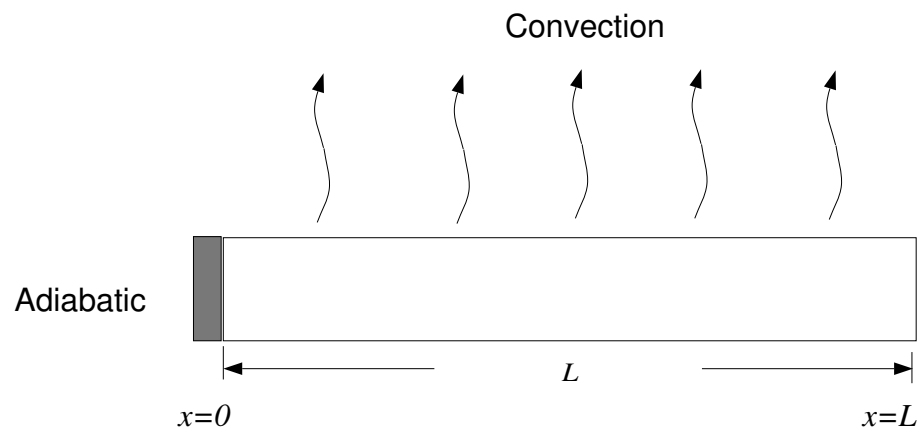


Figure 3.1. One dimensional convection-conduction heat transfer problem.

with the following homogeneous boundary and initial conditions

$$(\partial\theta/\partial x)(0, t) = 0,$$

$$\theta(L, t) = 0,$$

and

$$\theta(x, 0) = 0.$$

3.2.1 Continuous system

Consider a system governed by

$$\frac{\partial\theta}{\partial t} = \mathcal{A}\theta + \mathcal{B}u, \quad (3.3)$$

with suitable boundary and initial conditions, where, $\theta \in \Theta$ (Banach space representing the state space), the manipulated variable $u \in \mathbf{U}$ (Banach space corresponding to the control space), $\mathcal{B} \in L(\mathbf{U}, \Theta)$. $\mathcal{B} : \mathbf{U} \rightarrow \Theta$ is a linear bounded operator on u . \mathcal{A} is a bounded semi-group operator. \mathcal{A} operates on elements of a vector space of functions that satisfy the homogeneous spatial boundary conditions. If \mathcal{A} is self-adjoint, then it has real eigenvalues β_m , with $m = 0, 1, 2, \dots$, and a complete orthonormal set of eigenfunctions $\phi_m(x)$ which forms a spatial basis for θ .

Therefore, from Equation (3.2) we have an eigenvalue problem with the following operator

$$\mathcal{A}(\theta) = \alpha \frac{\partial^2\theta}{\partial x^2} - \zeta\theta. \quad \zeta > 0$$

Then the general solution can be written as

$$\theta(x) = a \sin \sqrt{-(\zeta + \beta)/\alpha}x + b \cos \sqrt{-(\zeta + \beta)/\alpha}x. \quad (3.5)$$

Thus, we can obtain the following eigenvalues

$$\beta_m = -\frac{(2m+1)^2\pi^2}{4L^2} - \zeta, \quad m = 0, 1, 2, 3, \dots \quad (3.6)$$

and the normalized eigenfunctions

$$\phi_m = \sqrt{\frac{2}{L}} \cos \frac{(2m+1)\pi x}{2L}. \quad (3.7)$$

We can now use the controllability criterion for infinite-dimensional systems. From the results of Chapter 2, the system is state controllable if for all m the rank of matrix $\mathbf{B}_m = r(m)$.

In the present case

$$\begin{aligned} \mathcal{A} &= \alpha \frac{\partial^2}{\partial x^2} - \zeta, \\ \mathcal{B} &= \zeta, \\ u &= \theta_\infty. \end{aligned}$$

The eigenvalues and eigenfunctions are

$$\begin{aligned} \beta_m &= -\frac{(2m+1)^2\pi^2}{4L^2} - \zeta, \\ \phi_m &= \sqrt{\frac{2}{L}} \cos \frac{(2m+1)\pi x}{2L}. \end{aligned}$$

In this problem we have only one control input, thus $n = 1$, and \mathcal{A} is self-adjoint. Thus, it has real and singular eigenvalues β_m , with $m = 0, 1, 2, \dots$, and $r(m) = 1$. Thus, the controllability condition reduces to the following inner products

$$\begin{aligned} \langle \mathcal{B}, \phi_m \rangle &= \int_0^L \mathcal{B} \phi_m \, dx \\ &= \int_0^L \zeta \sqrt{\frac{2}{L}} \cos \frac{(2m+1)\pi x}{2L} \, dx \\ &\neq 0. \end{aligned} \quad (3.8)$$

The controllability inequalities (3.8) are satisfied for all m , so the system is indeed state controllable.

3.2.2 Finite-dimensional approximation

Though the continuous-systems approach worked for this simple problem, it is desirable to develop a numerical approximation for the controllability test which can also be used for more complicated problems.

Dividing the domain $[0, L]$ into n equal parts of size Δx , a finite-difference spatial discretization of Equation (3.2) gives

$$\frac{d\theta_i}{dt} = -(2c + \zeta)\theta_i + c(\theta_{i-1} + \theta_{i+1}) + \zeta\theta_\infty,$$

where $c = \alpha/\Delta x^2$.

The nodes are $i = 1, 2, \dots, n + 1$, where $i = 1$ is at the left and $i = n + 1$ at the right end. The boundary conditions used at the two ends are $\theta_0 = \theta_1$ and $\theta_{n+1} = 0$, respectively. Collecting the equations for all the nodes

$$\frac{d\theta}{dt} = \mathbf{A}\theta + \mathbf{B}u, \quad (3.9)$$

where

$$\theta(t) = [\theta_1, \theta_2, \dots, \theta_n]^T \in \mathbb{R}^n \quad (3.10)$$

and $u(t) = T_\infty \in \mathbb{R}$. Also

$$\mathbf{A} = \begin{bmatrix} -(2c + \zeta) & 2c & 0 & \cdots & 0 \\ c & -(2c + \zeta) & c & & \vdots \\ 0 & \ddots & \ddots & \ddots & \\ \vdots & & & & c \\ 0 & \cdots & 0 & c & -(2c + \zeta) \end{bmatrix} \in \mathbb{R}^{n \times n}, \quad (3.11)$$

$$\mathbf{B} = \zeta[1, \dots, 1]^T \in \mathbb{R}^n,$$

where the boundary conditions have been applied to make \mathbf{A} non-singular.

It is known [1] that the state of a system of the form of Equation (3.9) is completely controllable if and only if the matrix

$$\mathbf{M} = [\mathbf{B} | \mathbf{A}\mathbf{B} | \dots | \mathbf{A}^{n-1}\mathbf{B}] \in \mathbb{R}^{n \times n} \quad (3.12)$$

is of full rank. In this case it can be shown that

$$\begin{aligned}\det \mathbf{M} &= (-1)^{\lfloor n/2 \rfloor} c^{n(n-1)/2} \zeta^n, \\ \text{rank } \mathbf{M} &= n,\end{aligned}$$

where $\lfloor \cdot \rfloor$ is the floor function. The matrix \mathbf{M} is of full rank, indicating that the state of the system is controllable, a conclusion that is also obtained from the eigenfunction expansion. This lends support to the use from now on of the finite-difference approximation to analyze controllability.

3.3 Boundary control

Here the boundary condition $T(L, t) = T_L(t)$ will be the manipulated variable through which control is exercised. Now, using the constant outside temperature T_∞ as reference and defining $\theta = T - T_\infty$, Equation (3.1) becomes,

$$\frac{\partial \theta}{\partial t} = \alpha \frac{\partial^2 \theta}{\partial x^2} - \zeta \theta, \quad (3.13)$$

with the following initial and boundary conditions

$$\begin{aligned}(\partial \theta / \partial x)(0, t) &= 0, \\ \theta(L, t) &= T_L(t) - T_\infty,\end{aligned}$$

and

$$\theta(x, 0) = 0.$$

3.3.1 State controllability

Equation (3.13) can be discretized to take the form of Equation (3.9), where $\theta(t)$ is given by Equation (3.10). \mathbf{A} is given by Equation (3.11), $u(t) = \theta(L, t) \in \mathbb{R}$ and

$$\mathbf{B} = [0, \dots, c]^T \in \mathbb{R}^n. \quad (3.14)$$

At the left end the adiabatic condition is the same as before. However, the temperature at right end θ_{n+1} is not known but is the manipulated variable u .

The controllability matrix \mathbf{M} is

$$\mathbf{M} = \begin{bmatrix} 0 & \cdots & \cdots & 0 & c^n \\ 0 & \cdots & 0 & c^{n-1} & \cdots \\ \vdots & \vdots & \vdots & \vdots & \vdots \\ 0 & 0 & c^3 & \cdots & \cdots \\ 0 & c^2 & -2c^2(2c + \zeta) & \cdots & \cdots \\ c & -c(2c + \zeta) & c^3 + c(2c + \zeta)^2 & \cdots & \cdots \end{bmatrix},$$

so that

$$\begin{aligned} \det \mathbf{M} &= (-2)^{\lfloor n/2 \rfloor} c^{(n^2+n)/2}, \\ \text{rank } \mathbf{M} &= n. \end{aligned}$$

Thus \mathbf{M} is of full rank, indicating that the state of the system is boundary controllable.

3.3.2 Output controllability

Up to now control of the complete state of the system has been considered. In thermal systems, however, it is unusual to be able to observe the complete temperature distribution. Most of the times users are interested in or able to work with only a vector $\mathbf{y} \in \mathbb{R}^p$, called the output, where

$$\mathbf{y}(t) = \mathbf{C}\theta(t), \tag{3.15}$$

with $\mathbf{C} \in \mathbb{R}^{p \times n}$. Output controllability refers to the ability of a suitable control input $u(t)$ to be able to take the output $y(t)$ from one point to another. The system represented by Equations (3.9) and (3.15) is output controllable [63] if and only if

the rank of the matrix

$$\mathbf{N} = [\mathbf{CB} | \mathbf{CAB} | \dots | \mathbf{CA}^{n-1}\mathbf{B}] \in \mathbb{R}^{p \times n}$$

is p . If, for example, it is desired to control the temperature at $x = 0$ which is θ_1 , then

$$\mathbf{C} = [1, 0, \dots, 0] \in \mathbb{R}^{1 \times n}.$$

Thus

$$\mathbf{N} = [0, \dots, 0, 2c^n].$$

which has a rank equal to $p = 1$ indicating that this output is controllable.

3.3.3 Optimal control

Since the system is boundary controllable, there exists a control function $T_L(t)$ which transfers the system from the initial state $\theta_0 = \theta(x, 0)$ to the target state $\theta_f = \theta(x, t_f)$ within a finite time t_f . Following [61], the solution of Equation (3.13) is

$$\theta(x, t) = e^{-\zeta t} \left[\frac{2\alpha}{L} \sum_{m=0}^{\infty} e^{-\alpha\gamma_m^2 t} (-1)^m \cos(\gamma_m) \gamma_m \int_{t'=0}^t e^{\alpha\gamma_m^2 t'} (T_L(t') - T_\infty) dt' \right],$$

where $\gamma_m = (2m + 1)\pi/2L$, $m = 0, 1, 2, 3, \dots$. Although Equation (3.13) has been solved analytically, it is hard to find an expression for $T_L(t)$ from the above solution. This is an ill-posed problem known in thermal science as a boundary inverse heat transfer problem. Finding $T_L(t)$ from the above solution requires the solution of this Fredholm integral equation of the first kind, and there are ways to solve it numerically [62]. However, it is obvious that the control input, i.e. the temperature at the boundary, is not unique.

With a finite-dimensional approximation, however, optimal control theory [1] can be used to get

$$u(t) = \theta(L, t) = \mathbf{B}^T e^{\mathbf{A}^T(t-t_f)} \mathbf{W}^{-1}(0, t) [\theta_0 - e^{\mathbf{A}t} \theta_f],$$

where $e^{\mathbf{A}t} = \sum_{k=0}^{\infty} (t^k/k!) \mathbf{A}^k$. θ_0 and θ_f are n -dimensional vectors representing the initial and target temperatures respectively. $\mathbf{W}^{-1}(0, t)$ is a $n \times n$ matrix called the reachability grammian or controllability grammian of the system defined by

$$\mathbf{W}(0, t) = \int_0^t e^{(s-t_f)\mathbf{A}} \mathbf{B} \mathbf{B}^T e^{(s-t_f)\mathbf{A}^T} ds.$$

For the system to be controllable this matrix should be nonsingular for any $t > 0$.

It is obvious that the open-loop control input, i.e. the temperature at the boundary, is not unique and that other temperature functions will be able to do the job. But this control input from the above solution has been proved to use the minimum control effort. Actually it minimizes $\| u \|$ which expresses the cost of the control. For more detail on the above optimal solution see for example [64].

Thus, starting from a zero temperature distribution, any given temperature distribution in the finite-dimensional approximation can be reached at a given time by varying only the temperature at one end of the bar.

As a special case, if it is desired that the output of the system be the temperature distribution along the bar, then \mathbf{C} in Equation (3.15) is the identity matrix. This, of course, is state controllability which has already been confirmed. For example, the system can be discretized in a small number of divisions, say $n = 6$, and it may be required that the temperatures at these locations be changed from the initial values of (say) $\theta = 0^\circ\text{C}$ to the final temperature of $\theta_f = 25^\circ\text{C}$ in a time interval $t_f = 20$ s. For illustration, numerical values of the parameters are set at $\zeta = 0.0118 \text{ s}^{-1}$ and $\alpha/\Delta x^2 = 1 \text{ s}^{-1}$. \mathbf{M} is found to have a rank equal to $n = 6$, indicating that the system is controllable. The results of optimal control are shown in Figure 3.2 and Figure 3.3. Figure 3.2 shows the variation of the temperature at the end of the bar that will take the temperature distribution to the target. In Figure 3.3 the variation of the temperature with time at each of the six nodes is plotted. In Figure 3.4 the temperatures at the six nodes are plotted as a function of time and position, where

the temperature numbered 6 is the closest to the control input.

What we have seen in this section is an optimal open-loop control. In practical applications open-loop control can be used if the relation between the input and the output is known. If this relation is unknown, feedback control should be designed to continuously change the control input based on the system output.

3.4 Constrained control

As we have seen from the controllability of the conductive-convective system, this controllability guarantees only the ability of a system to transfer the state from the initial condition to the final state. But the controllability itself does not imply the capability of the system to attain any arbitrary state.

In practical situations, there is always a constrained control input, which is bounded between two given values. These inputs may prevent the states from being as close as possible from the final condition. So, a system which is completely state controllable may not practically be so. Therefore the concept of controllability may not be very useful in these situations.

Additional complications arise in that in heat transfer problems the temperature must be constrained to positive values. Consideration of these constraints on the system shows that a controllable system may not be controllable over the entire range of states used in the above controllability tests even if the system meets all the criteria for controllability.

3.5 Conclusions

In this chapter the concept of controllability is investigated for a conductive-convective system. State controllability tells us whether a system can reach a specific target condition. We have presented in this chapter two type of controls, distributed and boundary control. The system is state controllable in both distributed and bound-

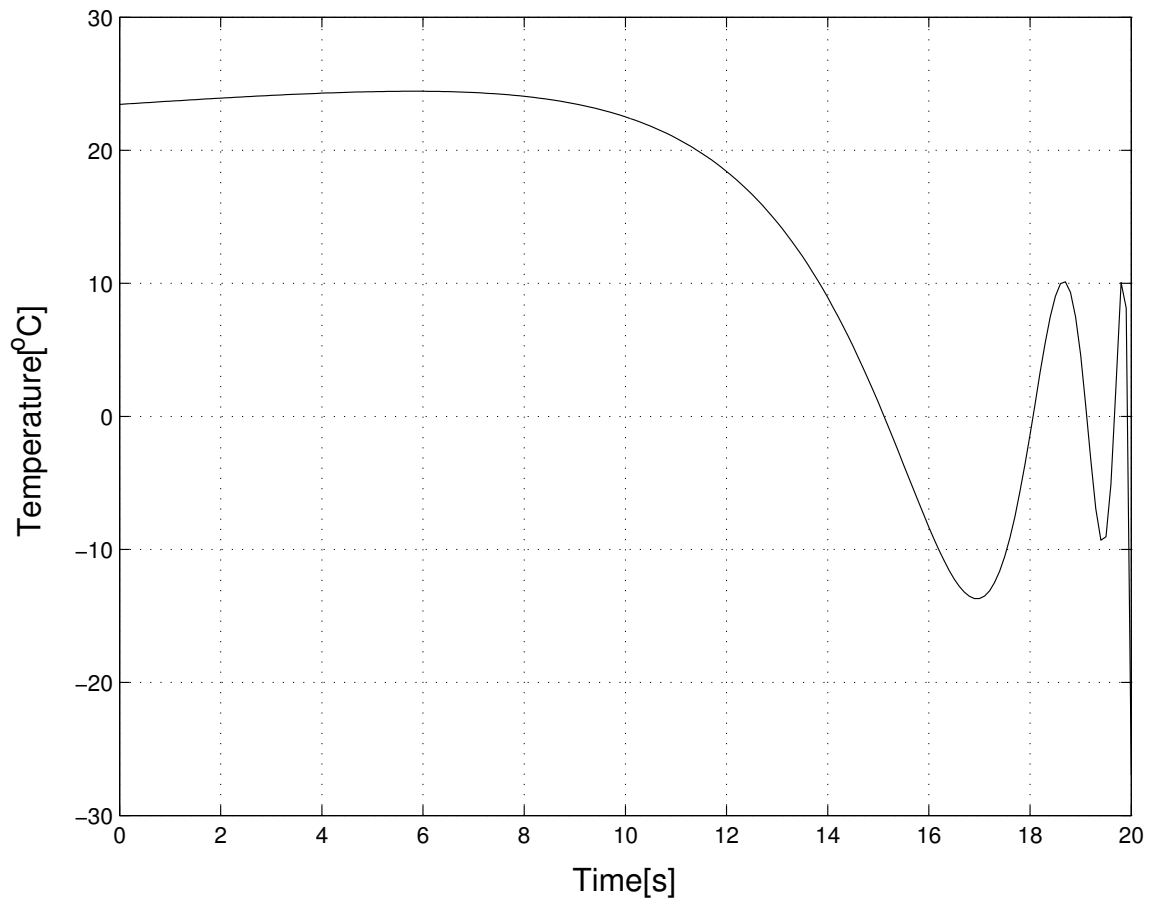


Figure 3.2. Variation of boundary condition $u(t)$ with time.

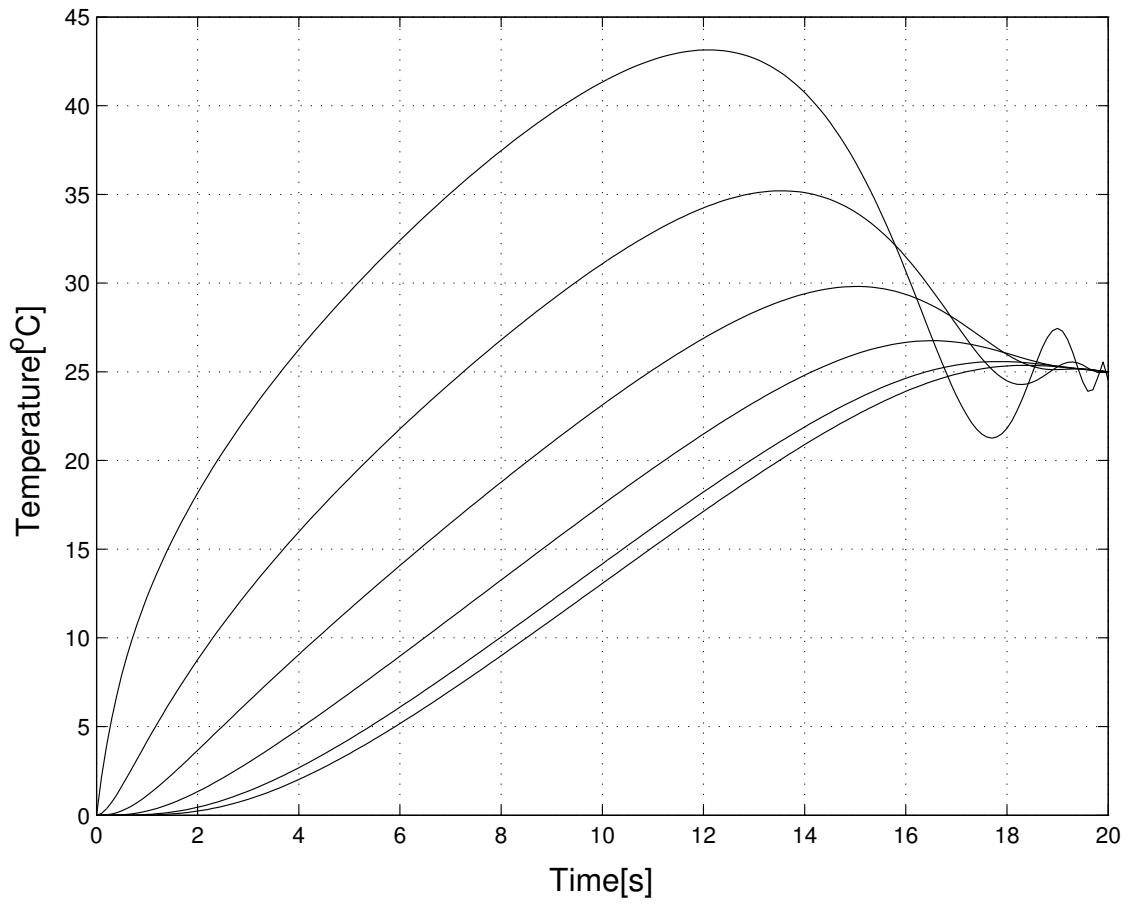


Figure 3.3. Variation of temperatures at the six nodes with time as a result of varying boundary condition.

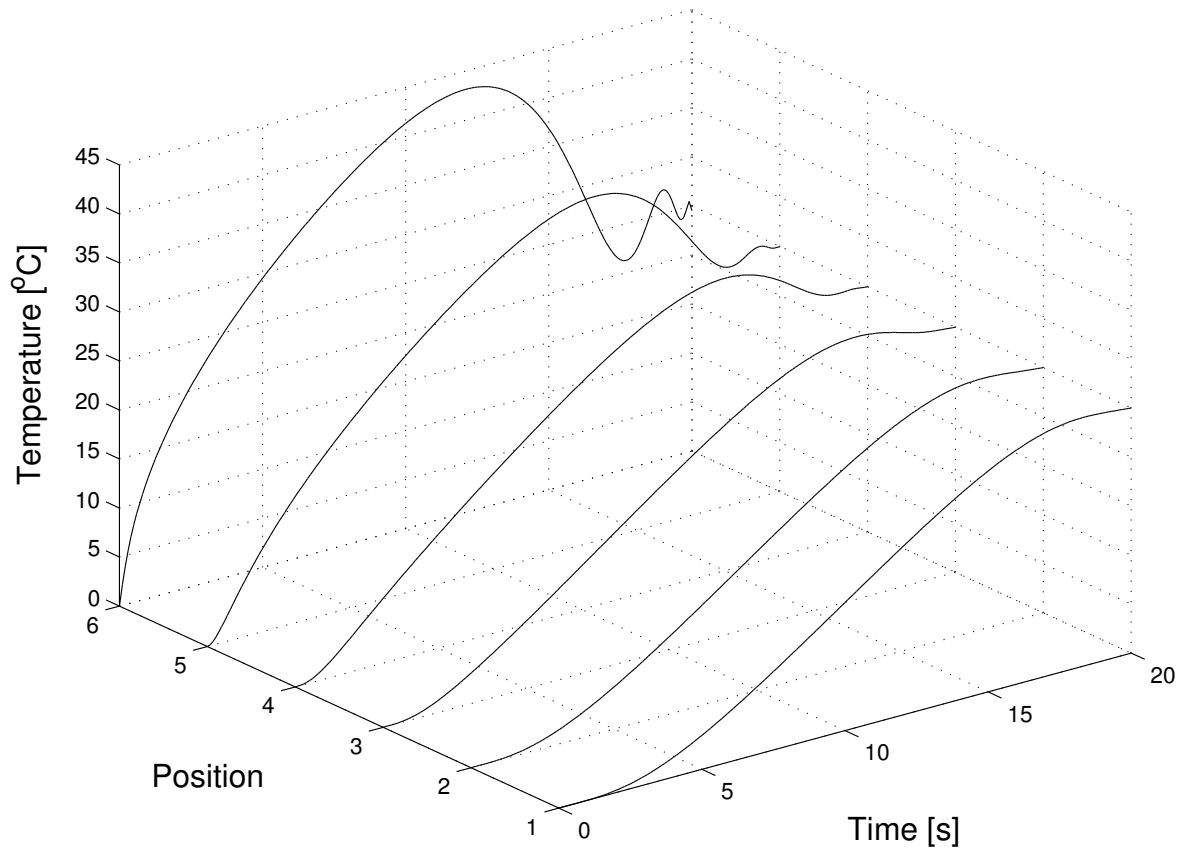


Figure 3.4. Variation of temperatures at the six nodes with time as a result of varying boundary condition.

ary control cases. The output controllability, on the other hand, is more important if the complete state of the system is not what we desire to control. We have seen that the system is output boundary controllable when the output is a temperature at the other boundary.

We have shown that both infinite-dimensional and finite-dimensional models lead to the same controllability results. The effect of manipulating the boundary condition on the controllability has also been shown. Furthermore, we have calculated the required boundary condition that will steer the system to the final condition. Finally, the effect of constrained control inputs on controllability is discussed. This work is a base for a more complex model representing a cross-flow heat exchanger that we will deal with in the next chapter.

CHAPTER 4

CONTROLLABILITY OF CROSS-FLOW HEAT EXCHANGERS

In the previous chapter the controllability of a conductive-convective system which shares a lot of the aspects of a heat exchanger is discussed. In this chapter we extend the analysis to a more complex thermal system representing a cross-flow heat exchanger.

Among the many kinds of water-to-air heat exchangers (e.g. Figure 4.1), the cross-flow geometry is very common. Though they sometimes have multiple rows and/or circuits, we will consider here the simplest geometry that can be easily computed, i.e. a single tube with water flow inside and cross flow of air outside. A schematic of this arrangement is shown in Figure 4.2. Although a straight geometry is shown, the tube may zig-zag over the face of the heat exchanger so as to make it more compact. We will use an approach based on a finite-difference approximation of the governing equations to study the controllability.

4.1 Governing equations

To enable a one-dimensional analysis, we make the simplifying assumptions that the flow is hydrodynamically and thermally fully developed, and that the velocity and temperature are uniform over the cross section of the pipe. The physical properties of the fluid are also time-independent. In this problem, there is convective heat transfer between the water and the tube wall, conduction along the tube wall, and convection between the tube wall and the surrounding air.

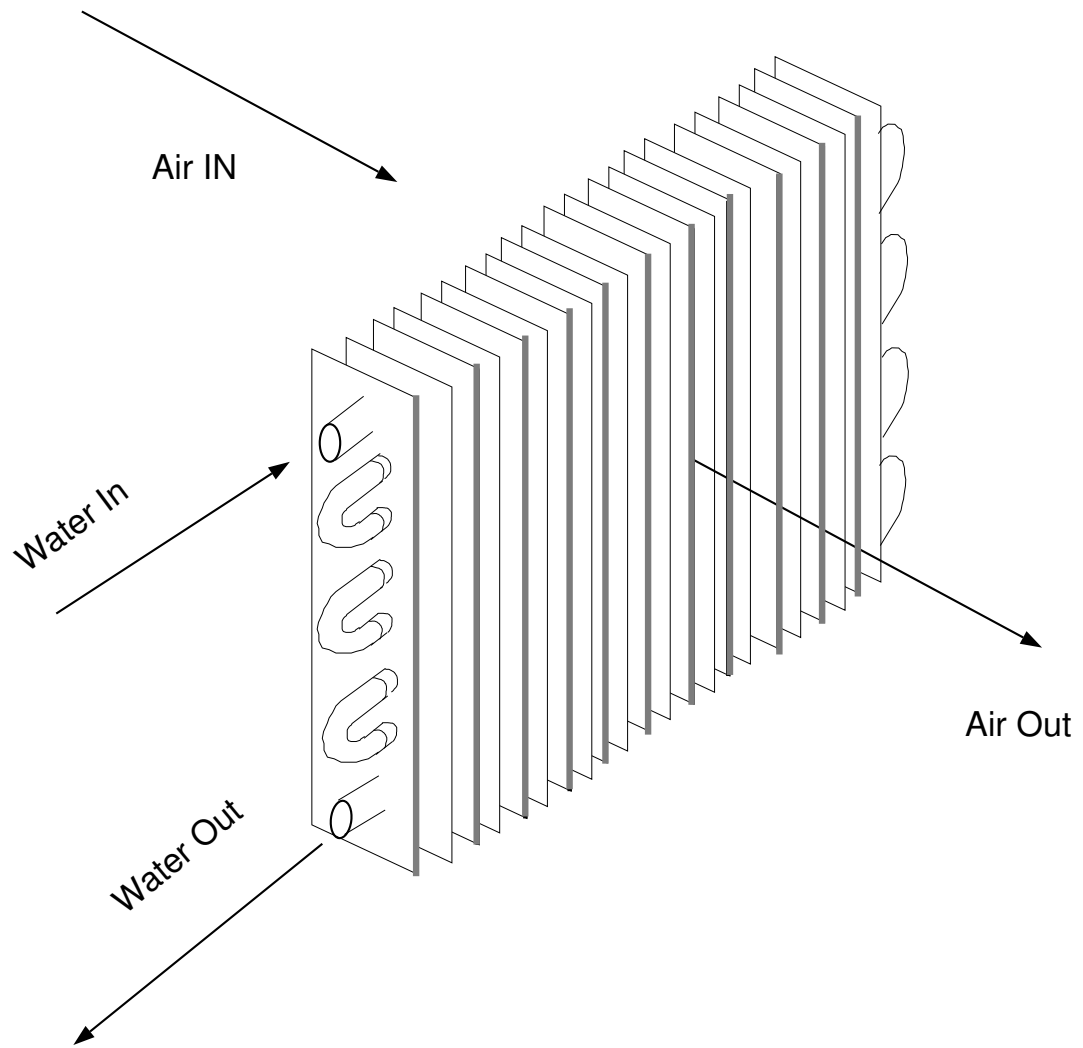


Figure 4.1. Single-row cross-flow heat exchanger.

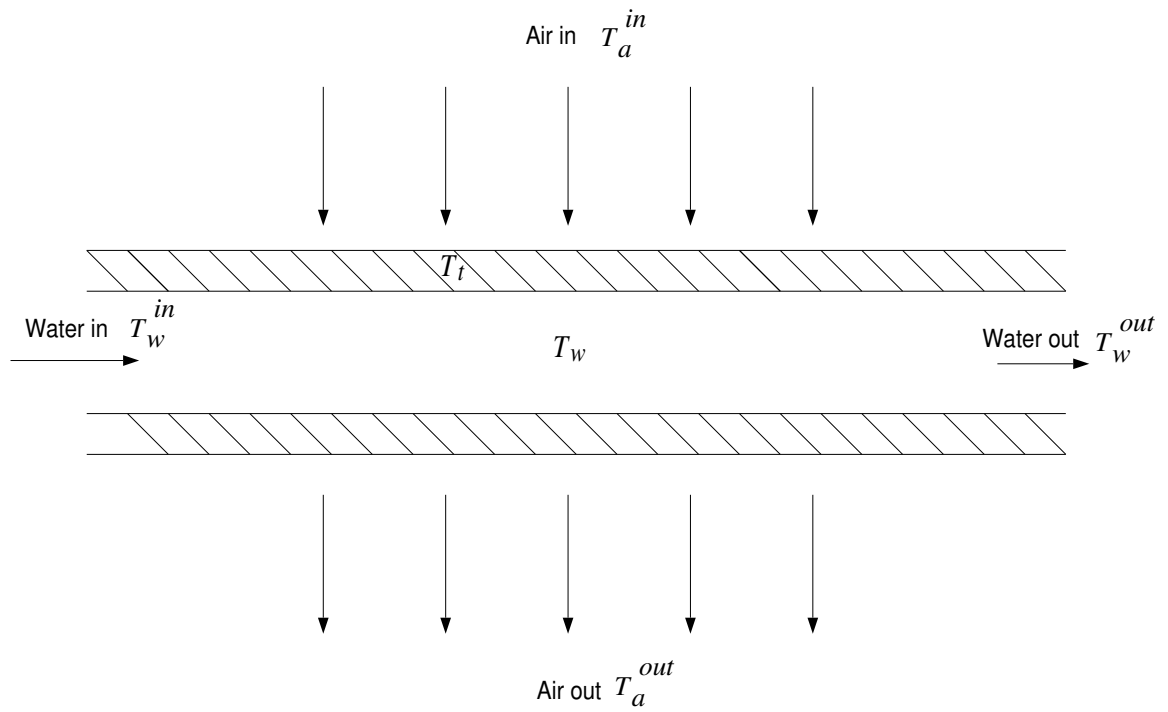


Figure 4.2. Schematic of single-tube cross-flow heat exchanger.

Based on the conservation of energy, the dynamic behavior of the heat exchanger can be described mathematically by coupled partial differential equations and an algebraic equation. In these governing equations several assumptions have been made. These assumptions include (1) all physical properties of the air, tube wall and water are time-independent; (2) the water enters and leaves the tube with uniform temperature and velocity profiles; (3) axial conduction of the water is negligible. The following are the governing equations for this problem with the boundary conditions that need to be analyzed.

First, on the outside of the tube, there is heat transfer by convection from the air to the tube. We assume that there is no air-temperature gradient, and we are dealing with dry air only, i.e. there is no moist air and condensation outside the tube.

Energy balance for the air side thus gives

$$\frac{\dot{m}_a}{L}c_a(T_a^{in} - T_a^{out}) = h_o2\pi r_o(T_a - T_t), \quad (4.1)$$

where L is the length of the tube, \dot{m}_a is the mass flow rate of air, c_a is its specific heat, T_a^{in} and T_a^{out} are the incoming and outgoing air temperatures, h_o is the heat transfer coefficient in the outer surface of the tube, r_o is the outer radius of the tube, T_a is the air temperature surrounding the tube, and T_t is the tube wall temperature.

Second, in the wall of the tube itself we have to consider conduction along it as well as forced convection with both fluids. Neglecting conduction in the circumferential direction compared to the conduction in the radial direction, we get

$$\rho_w c_w \pi (r_o^2 - r_i^2) \frac{\partial T_t}{\partial t} = k_t \pi (r_o^2 - r_i^2) \frac{\partial^2 T_t}{\partial x^2} + 2\pi r_o h_o (T_a - T_t) - 2\pi r_i h_i (T_t - T_w), \quad (4.2)$$

where ρ_w is the water density, c_w is its specific heat, and \dot{m}_w is the water mass flow rate. In these equations $T_t = T_t(x, t)$, $T_w = T_w(x, t)$, $T_a^{out} = T_a^{out}(t)$, $T_a = T_a(t)$ in

general. The boundary and initial conditions are

$$T_t(x, 0) = T_w(x, 0) = T_w^{in},$$

$$T_t(x, L) = T_w(x, L),$$

and $T_t(0, x) = T_w(0, x) = 25^\circ\text{C}$ (arbitrarily).

Lastly, the flow within the pipe is assumed to be incompressible, and fully developed. We have the heat transfer from the tube wall to the water inside. We neglect axial conduction through the water compared to the bulk motion. The temperature of the water considered here is the bulk temperature. So we get

$$\rho_w c_w \pi r_i^2 \frac{\partial T_w}{\partial t} + \dot{m}_w c_w \frac{\partial T_w}{\partial x} = h_i 2\pi r_i (T_t - T_w), \quad (4.3)$$

where ρ_t is the density of the tube material, c_t is its specific heat, k_t is its thermal conductivity, r_i is the inner radius of the tube, h_i is the heat transfer coefficient in the inner surface of the tube, and T_w is the water temperature.

We assume that the local air temperature around the tube, T_a , in Equations (4.1) and (4.2) is the average between its inlet and outlet values so that

$$T_a = \frac{T_a^{in} + T_a^{out}}{2}, \quad (4.4)$$

which can be substituted into the Equations (4.1) and (4.2) above to remove T_a as a variable.

Since the convective heat transfer coefficients depend upon the mass flow rates of air and water, they can be evaluated from the following standard dimensionless relations [66]. For laminar flow on the water side, we have

$$Nu_i = \begin{cases} 1.86(Re_w Pr_w)^{1/3} (D_i/L)^{1/3} (\mu_w/\mu_t)^{0.14} & \text{for } Re_i Pr_w (D_i/L) > 10 \\ 3.66 & \text{for } Re_i Pr_w (D_i/L) < 10. \end{cases} \quad (4.5)$$

For turbulent flow on the water side

$$Nu_i = 0.027 Re_i^{0.8} Pr_w^{1/3} (\mu_w/\mu_t)^{0.14} \text{ for } Re_i > 2300. \quad (4.6)$$

For the air side [67]

$$Nu_o = 0.683 Re_o^{0.466} Pr_a^{1/3} \text{ for } 40 < Re_o < 4000. \quad (4.7)$$

Apart from geometry and material properties, there are four parameters in Equations (4.1)–(4.3), two mass flow rates and two inlet temperatures for water and air, that can be used for control purposes as the manipulated variable. Two single-input cases will be analyzed for the purpose of controlling the fluid outlet temperatures. First, when the mass flow rates \dot{m}_a and \dot{m}_w are constant and control of the heat exchanger outlet temperatures T_a^{out} and T_w^{out} is accomplished by manipulating either T_a^{in} or T_w^{in} . Second, when the flow rates (\dot{m}_w will be used as an example) are used as a manipulated variable; the problem is nonlinear and linear theory cannot be used then.

4.2 Manipulated variable: water inlet temperature

The controllability of the heat exchanger can be studied with different manipulated variables. In this section we will use the water inlet temperature T_w^{in} as a manipulated variable. All other inputs like T_a^{in} , \dot{m}_w , and \dot{m}_a will be constant.

4.2.1 Finite-dimensional approximation

Dividing the computational domain into n parts, and using finite-differences technique, Equations (4.1)–(4.3) can be put in the state-space form

$$\frac{dT}{dt} = \mathbf{A}T + \mathbf{B}u. \quad (4.8)$$

This is done by approximating first and second-order derivatives by upwind and central differences, respectively, for Equations (4.2) and (4.3), and eliminating the

algebraic Equation (4.1) to give

$$\frac{dT_{t,i}}{dt} = a_1 T_{t,i} + c_t (T_{t,i+1} + T_{t,i-1}) + a_2 T_{w,i} + a_3 T_a^{in}, \quad (4.9)$$

$$\frac{dT_{w,i}}{dt} = -b_1 T_{w,i} + b_2 T_{w,i-1} + a_4 T_{t,i}, \quad (4.10)$$

where the parameters in these equations are defined as

$$\begin{aligned} a_1 &= \frac{2\pi r_o h_o}{\rho_t c_t \pi (r_o^2 - r_i^2)} \left(\frac{a_5}{2 + a_5} - 1 \right) - \frac{2\alpha_t}{\Delta x^2} - a_2, \\ a_2 &= \frac{2\pi r_i h_i}{\rho_t c_t \pi (r_o^2 - r_i^2)}, \\ a_3 &= \frac{2\pi r_o h_o}{\rho_t c_t \pi (r_o^2 - r_i^2)} \left(\frac{1}{2} + \frac{1 - a_5/2}{2 + a_5} \right), \\ a_4 &= \frac{4h_i}{\rho_w c_w D_i}, \\ a_5 &= \frac{2\pi r_o h_o L}{\dot{m}_a c_a}, \\ b_1 &= \frac{\dot{m}_w}{\rho_w \pi r_i^2 \Delta x} + a_4, \\ b_2 &= \frac{\dot{m}_w}{\rho_w \pi r_i^2 \Delta x}, \\ c_t &= \frac{\alpha_t}{\Delta x^2}. \end{aligned}$$

At each spatial point we have the above two coupled equations, one for the tube and the other for the water. The boundary conditions are

$$T_{t,0} = T_{w,0} = T_w^{in}, \quad (4.11)$$

$$T_{t,n} = T_{w,n}. \quad (4.12)$$

In the following the variables

$$T(t) = [T_{t,1}(t), T_{w,1}(t), T_{t,2}(t), T_{w,2}(t), \dots, T_{w,n}(t)]^T \in \mathbb{R}^{(2n-1) \times 1} \quad (4.13)$$

$$\mathbf{A} = \begin{bmatrix} a_1 & a_2 & c_t & 0 & \dots & & & & & 0 \\ a_4 & -b_1 & 0 & \dots & & & & & & 0 \\ c_t & 0 & a_1 & a_2 & c_t & 0 & \dots & & & 0 \\ 0 & b_2 & a_4 & -b_1 & 0 & \dots & & & & 0 \\ 0 & 0 & c_t & 0 & a_1 & a_2 & c_t & 0 & \dots & 0 \\ 0 & 0 & 0 & b_2 & a_4 & -b_1 & 0 & \dots & & 0 \\ \vdots & \ddots & \ddots & \ddots & \ddots & \ddots & \ddots & \ddots & \ddots & \vdots \\ 0 & \dots & & & & & 0 & b_2 & a_4 & -b_1 \end{bmatrix}, \quad (4.14)$$

are used, where the dimension of \mathbf{A} is $(2n-1) \times (2n-1)$, and the boundary conditions have been included. The order of the system is $2n - 1$, where n is the number of nodes used for the discretization. \mathbf{B} will depend on the choice of the manipulated variable. In the following sections \mathbf{B} will change based on what control inputs will be used.

4.2.2 Complete state controllability

To use the linear controllability theory, the flow rates should be kept relatively constant. The only manipulated variable is the inlet water temperature, T_w^{in} . Therefore, in this situation the state-space equation can be written as

$$\frac{dT}{dt} = \mathbf{A}T(t) + \mathbf{B}u(t) + \mathbf{F}, \quad (4.15)$$

where $T(t)$ and \mathbf{A} are given by Equations (4.13) and (4.14), and

$$\begin{aligned}\mathbf{B} &= \left[\frac{\alpha_t}{\Delta x^2}, \frac{\dot{m}_w}{\rho_w \pi r_i^2 \Delta x}, 0, \dots, 0 \right]^T \in \mathbb{R}^{2n-1 \times 1}, \\ \mathbf{F} &= [a_3, 0, a_3, 0, \dots, a_3, 0]^T T_a^{in} \in \mathbb{R}^{2n-1 \times 1}, \\ u &= T_w^{in}.\end{aligned}$$

Since \mathbf{A} is non-singular the transformation

$$\tilde{\theta} = \mathbf{A}^{-1}\mathbf{F} + \theta \quad (4.16)$$

can be introduced to write Equation (4.15) in the form of Equation (4.8). Thus

$$\frac{d\tilde{\theta}}{dt} = \mathbf{A}\tilde{\theta} + \mathbf{B}u. \quad (4.17)$$

For any n , it can be shown by computation that the controllability matrix \mathbf{M} defined in the previous chapters has a full rank, indicating that $\tilde{\theta}$ is controllable.

As the number of divisions of the spatial domain n increases, the size of \mathbf{M} also increases. The range of eigenvalues increases correspondingly and the rank becomes difficult to compute numerically. More importantly, however, this also means that the system needs large values of the control input which may not be available in practice. The condition number of \mathbf{M} , C_M , being the ratio of the largest to smallest singular values, is thus an indicator of the degree to which the system may be controlled with a bounded input. Of course, \mathbf{M} is singular and not of full rank if C_M is infinite. Figure 4.3 shows the effect of n on C_M . As n increases, it becomes increasingly difficult to take the system to a desired $\tilde{\theta}$.

Let us now see the effect of the flow rate and the heat transfer on the controllability. So far air and water flow rates have been fixed. We will test different combinations of the air and water flow rates in each case. Figures 4.4 and 4.5 show the effect of the flow rates on the condition number of the controllability matrix. Figure 4.4 shows the effect of varying air velocity on C_M . It is not appreciable. On

the other hand the water velocity is seen to have much more influence, as shown in Figure 4.5. This means the water velocity has more effect on the heat exchanger tube and water temperatures, and hence on the outlet temperatures than the air flow rate. At the minimum C_M the system is the most controllable. Thus the condition number provides information on the best flow rate for control of the heat exchanger when the inlet water temperature is used as a manipulated variable. It is clear that the lowest condition number and hence the most controllable case occurs at water velocity equal to 0.5 m/s with any air flow rate. Therefore, when the inlet water temperature is used as a manipulated variable, this test provides us with information regarding the optimum flow rates of the heat exchanger.

Apart from the above difficulties in executing an accurate rank test, this test assumes unconstrained control inputs. In this model if \mathbf{M} has a full rank this means the heat exchanger is controllable and any temperature distribution along the tube wall and in the water can be reached. This is mathematically true, but physically impractical. We must now examine a case in which the foregoing results might be changed in real thermal system.

4.2.3 Output controllability

Output controllability refers to the system ability to control the output $\mathbf{y}(t)$ by suitable control input function $u(t)$. In most applications, the output controllability is more important than the state controllability. Sometimes a system which is not completely state controllable may not be output controllable and vice versa. The criterion for determining the output controllability is related to the previous matrices $\mathbf{A} \in \mathbb{R}^{2n-1 \times 2n-1}$ and $\mathbf{B} \in \mathbb{R}^{2n-1 \times m}$, and also $\mathbf{C} \in \mathbb{R}^{p \times 2n-1}$ that depends on the output. The system is output controllable if the rank of the \mathbf{N} matrix is equal to p where

$$\mathbf{N} = [\mathbf{CB} | \mathbf{CAB} | \mathbf{CA}^2\mathbf{B} | \dots | \mathbf{CA}^{2n-2}\mathbf{B}] \in \mathbb{R}^{p \times (2n-1)m}. \quad (4.18)$$

There are many different possibilities of outputs that may be controlled. Some of the those that may have practical use are the following.

(a) One example of an output of the system is the heat exchanger tube wall temperature distribution, for which

$$\mathbf{C} = \text{diag}[1, 0, 1, \dots, 0] \in \mathbb{R}^{(2n-1) \times (2n-1)}.$$

The matrix \mathbf{N} has the same size as \mathbf{C} . However, \mathbf{N} is not of full rank, so that the output is not controllable.

(b) Another is the outlet water temperature T_w^{out} , so that

$$\mathbf{C} = [0, \dots, 0, 1] \in \mathbb{R}^{1 \times 2n-1},$$

where in this case $p = 1$, for which

$$\mathbf{N} = \left[0, \dots, \left(\frac{\alpha_t}{\Delta x^2} \right)^{n-1} \frac{\dot{m}_w}{\rho_w \pi r_i^2 \Delta x} + \left(\frac{\dot{m}_w}{\rho_w \pi r_i^2 \Delta x} \right)^{n-1} \frac{4h_i}{\rho_w c_w D_i}, \dots \right].$$

It is obvious that matrix \mathbf{N} has a rank equal $p = 1$. Thus, the output of the system is controllable.

(c) A third example that is also of practical interest is the average outlet air temperature

$$\bar{T}_a^{out}(t) = \frac{1}{L} \int_0^L T_a^{out}(x, t) dx, \quad (4.19)$$

where

$$T_a^{out}(x, t) = \frac{(1 - a_5/2)T_a^{in} + a_5 T_t}{1 + a_5/2}$$

is used with the trapezoidal rule for integration. The matrix

$$\mathbf{C} = \Delta x \left[\frac{1}{2}, 0, 1, 0, \dots, 1, 0, \frac{1}{2} \right] \in \mathbb{R}^{1 \times (2n-1)} \quad (4.20)$$

with $p = 1$. The output controllability matrix is

$$\mathbf{N} = \Delta x \left[\frac{\alpha_t}{2\Delta x^2}, \dots \right].$$

\mathbf{N} has a rank equal to p , indicating that the system is output controllable.

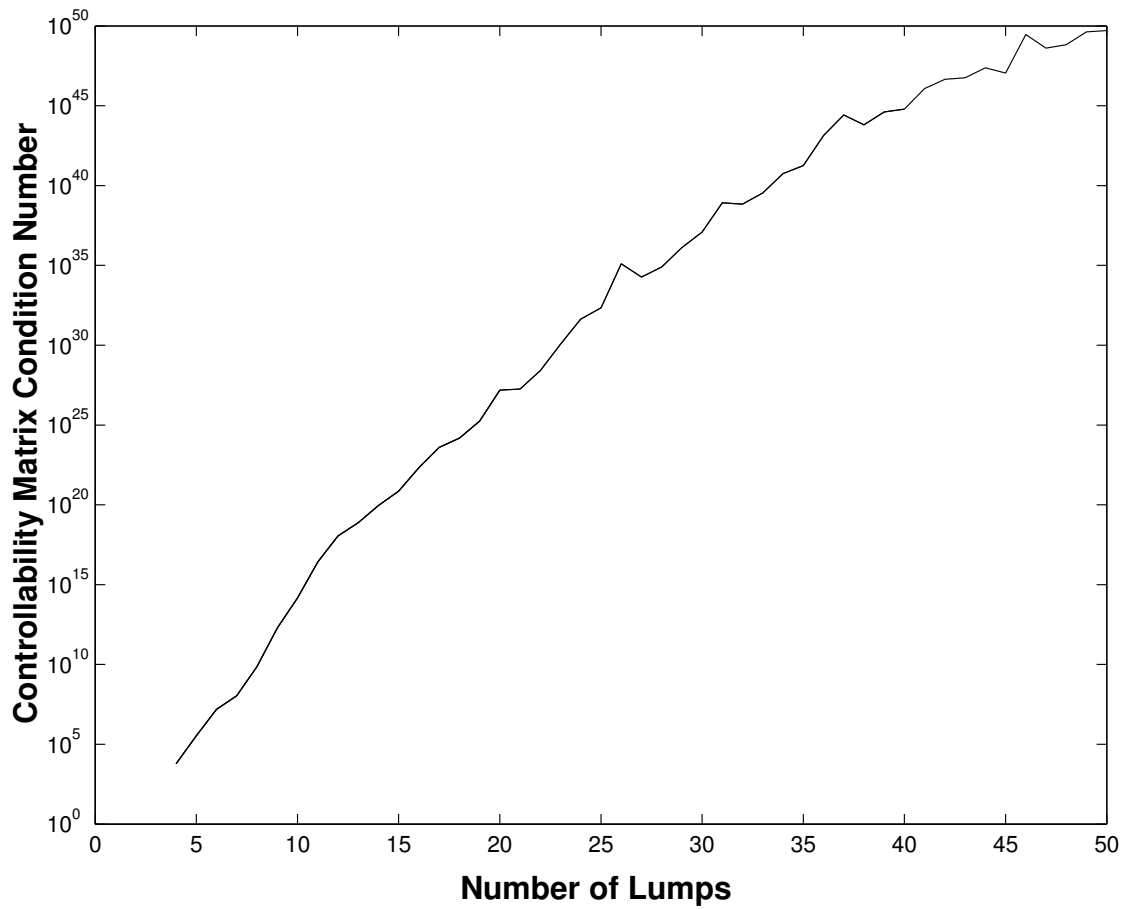


Figure 4.3. Effect of number of divisions on condition number when water inlet temperature is manipulated variable.

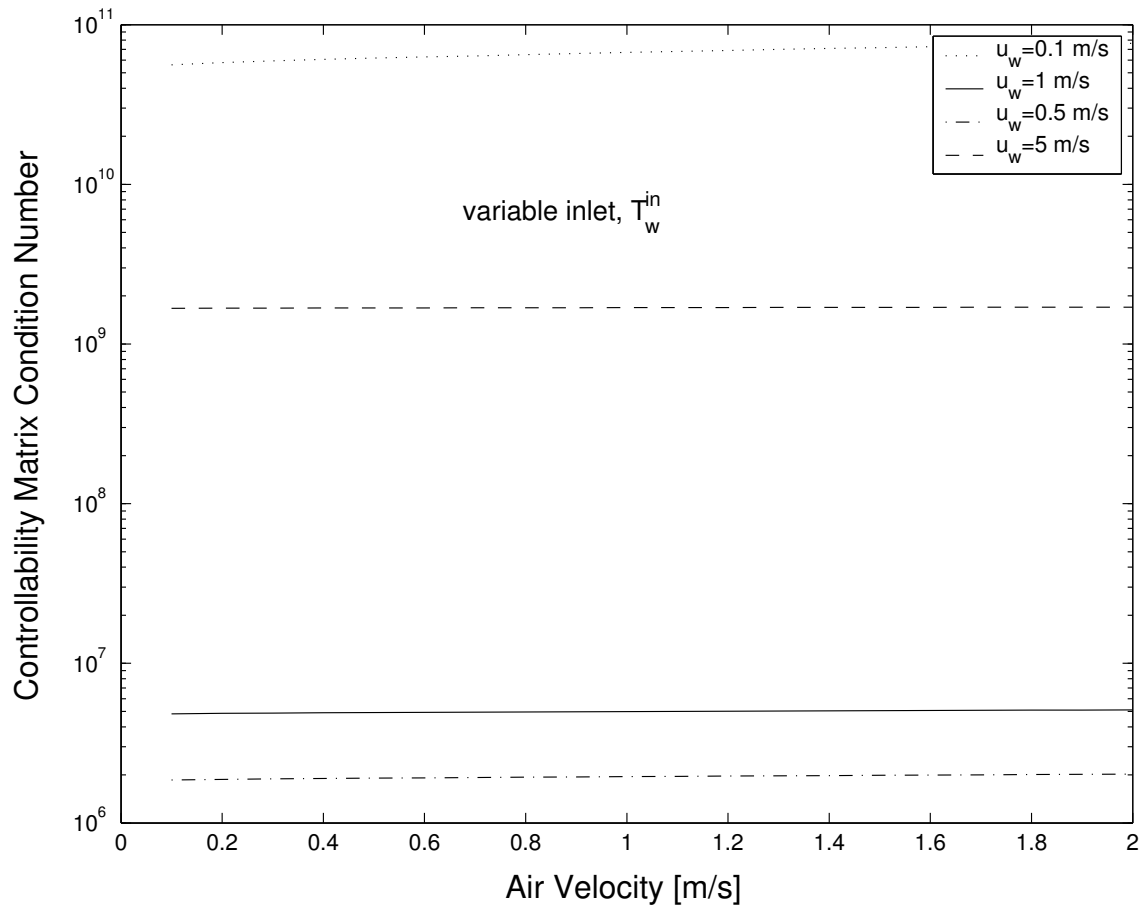


Figure 4.4. Effect of air flow rate on condition number.

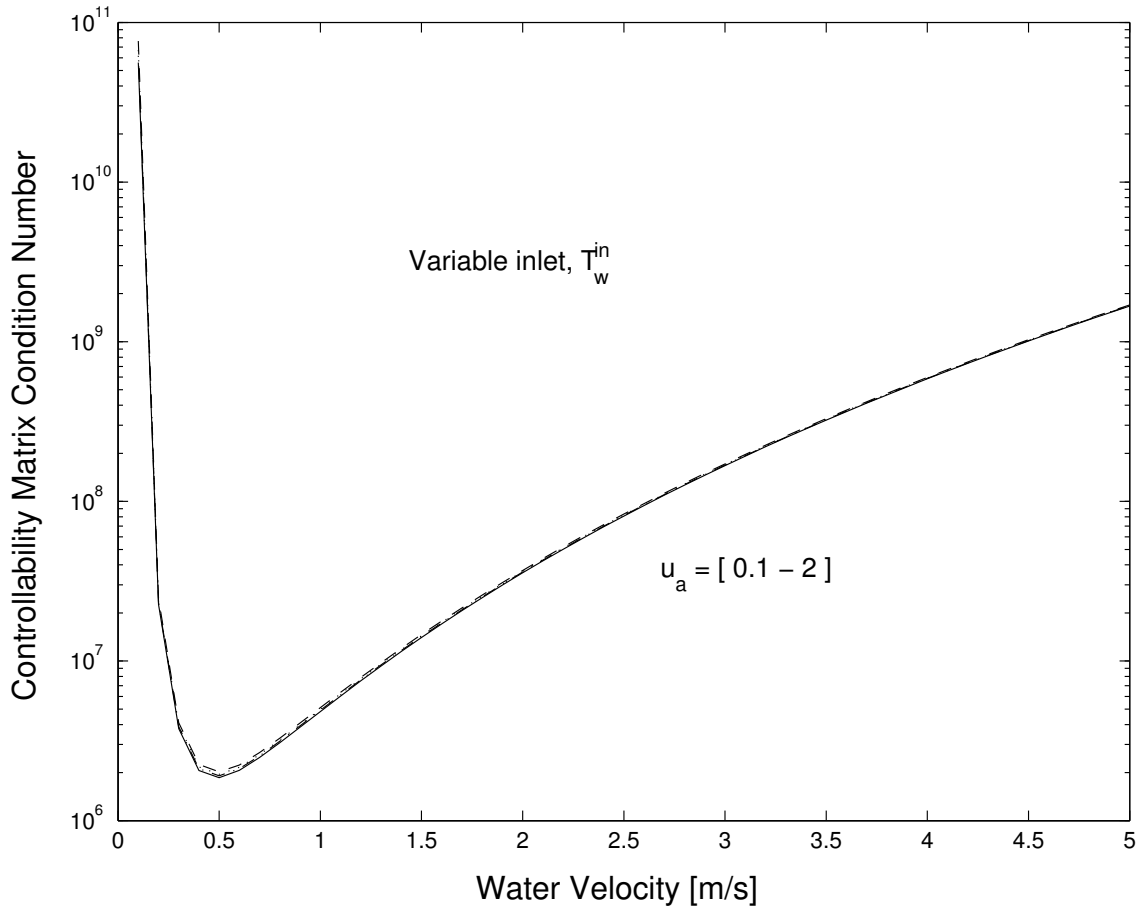


Figure 4.5. Effect of water flow rate on condition number.

4.3 Manipulated variable: air inlet temperature

In this section the controllability of the heat exchanger will be discussed when the inlet air temperature T_a^{in} is used as a manipulated variable. It is also common to have the inlet air temperature T_a^{in} as a manipulated variable.

4.3.1 Complete state controllability

Matrix \mathbf{A} is still as shown in Equation (4.14) but

$$\begin{aligned}\mathbf{B} &= [a_3, 0, a_3, 0, \dots, a_3]^T \in \mathbb{R}^{2n-1 \times 1}, \\ \mathbf{F} &= \left[\frac{\alpha_t}{\Delta x^2} T_w^{in}, \frac{\dot{m}_w}{\rho_w \pi r_i^2 \Delta x} T_w^{in}, 0, \dots, 0 \right]^T \in \mathbb{R}^{2n-1 \times 1}, \\ u &= T_a^{in}.\end{aligned}$$

With the transformation of Equation (4.16), the governing equation can be reduced to the form of Equation (4.8) and the controllability matrix defined in previous chapters can be computed. It is found that \mathbf{M} has a full rank, indicating the system is controllable: by changing T_a^{in} any set of water and tube wall temperatures at a finite number of points can be reached in finite time. When different water and air velocity are used, the same phenomenon occurs as in Section (4.2.2) when the water temperature was the manipulated variable. The results of varying the air and water flow rates on C_M are shown in Figures 4.6 and 4.7 respectively. Again the water flow rate is found to have a significant effect but not the air flow. There is an optimum water flow rate at which the system is the most controllable.

4.3.2 Output controllability

If the output is the average outlet air temperature defined by Equation (4.19), it can be calculated as the above case with the same \mathbf{C} matrix in Equation (4.20). In this case the first element of the output controllability matrix \mathbf{N} can be written in

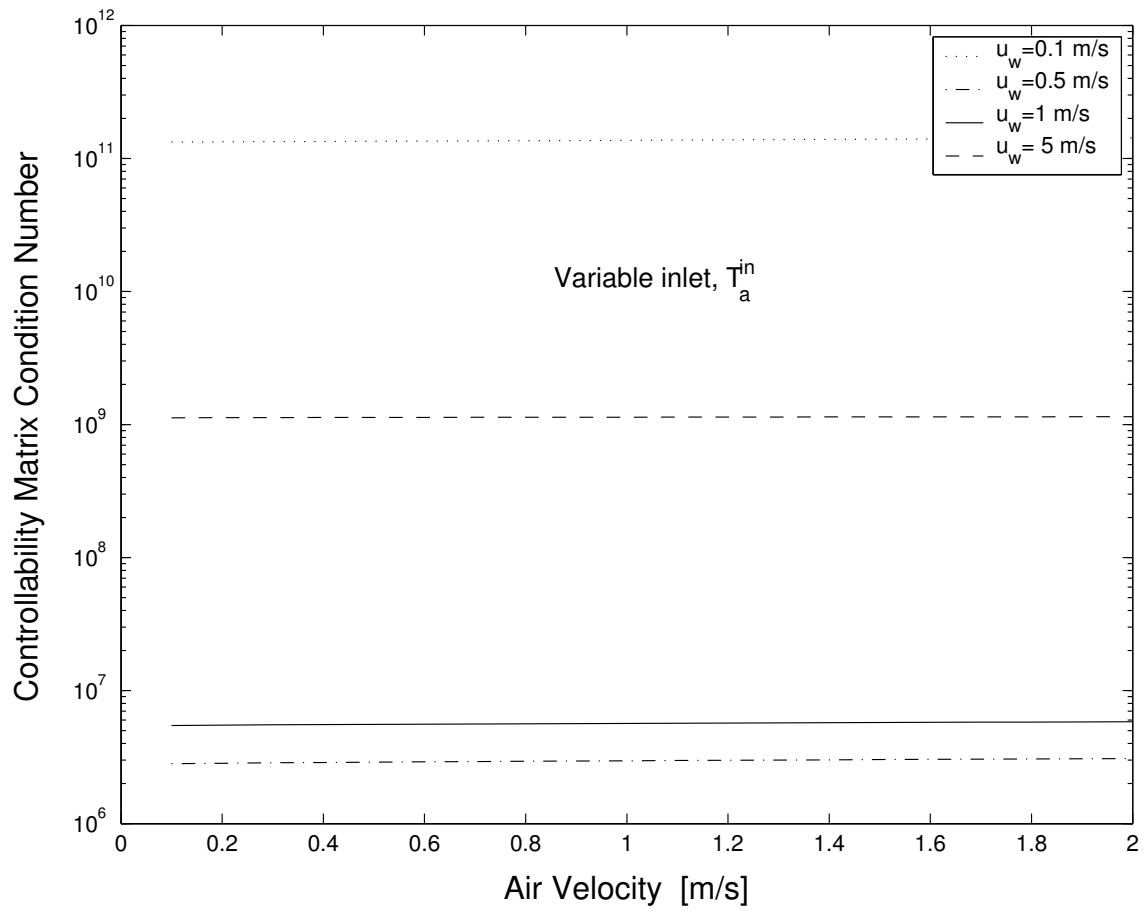


Figure 4.6. The effect of the air flow rate on the condition number.

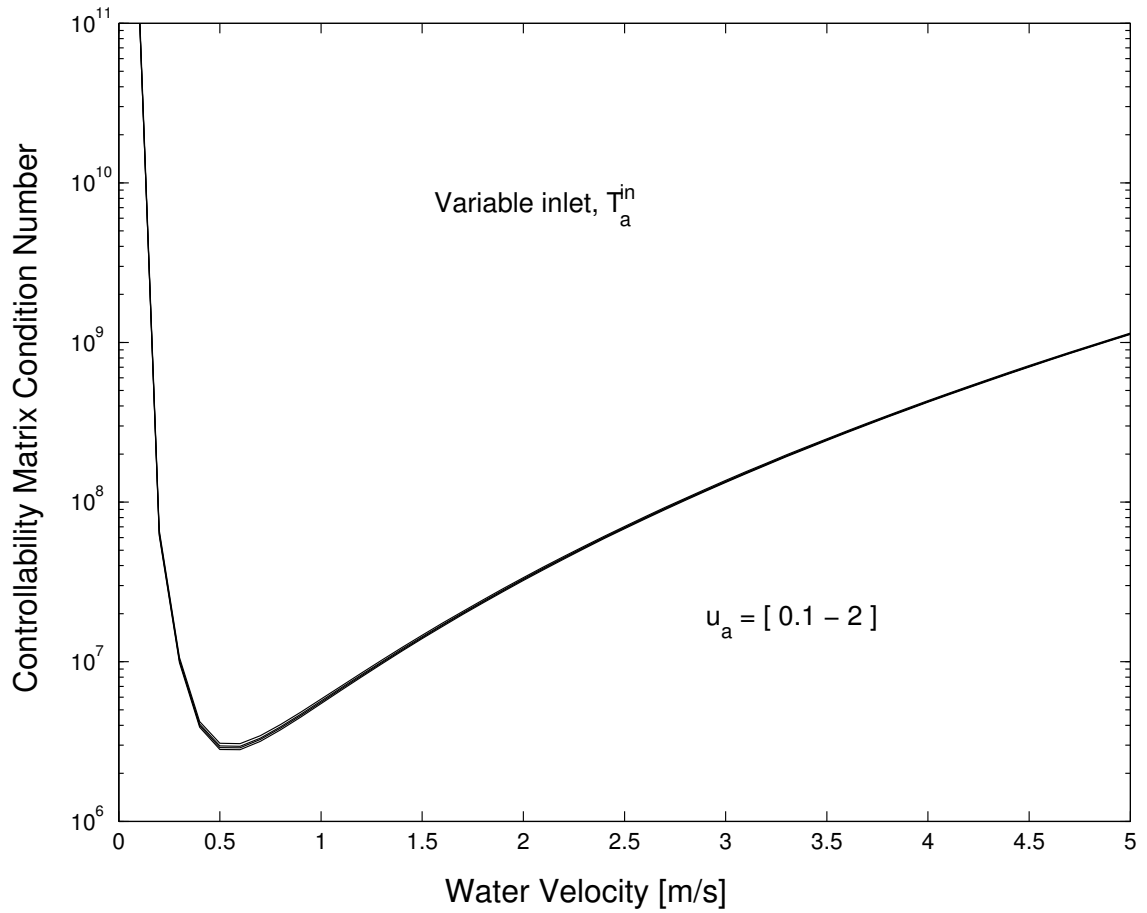


Figure 4.7. The effect of the water flow rate on the condition number.

general form as

$$\mathbf{N} = \Delta x [(n - 1)a_3, \dots].$$

Thus \mathbf{N} is found to have a rank equal to p , indicating that the system is output controllable.

4.4 Manipulated variable: water velocity

The objective here is to control the outlet water temperature T_w^{out} by manipulating the water flow rate \dot{m}_w while keeping constant the air flow rate \dot{m}_a , and the inlet air and water temperatures T_a^{in} and T_w^{in} , respectively. If the water velocity is used as a manipulated variable, the situation is entirely different from those treated before. The control problem is nonlinear since the manipulated variable \dot{m}_w appears as a product with the unknown temperature $T_w(x, t)$ in Equation (4.3). The previously used linear controllability ideas cannot be globally applied in this situation.

To find the range of T_w^{out} by solving Equations (4.1)–(4.2) turns out to be a difficult task. However, it is obvious that by manipulating the water velocity even over the entire range of positive real numbers one cannot reach all possible water outlet temperatures. Two steady state extremes can be considered. When the water flow rate is small the advective term in the steady state version of Equation (4.3) is also small, so that $T_t = T_w$. Substituting this in steady Equation (4.2) where the conduction along the tube wall is now negligible, we have $T_t = T_a$. Since this cannot satisfy the boundary conditions there is a thin boundary layer near the entrance $x = 0$. The water temperature at the outlet is $T_w^{out} = T_a^{in}$. Similarly at the other extreme, for large flow rates Equations (4.2) and (4.3) give $T_w^{out} = T_w^{in}$. Thus, in general, in the steady state T_w^{out} is between the two temperatures, T_a^{in} and T_w^{in} . Since this range of temperatures can be reached in the steady state, it follows that these states are controllable.

The arguments above are not valid for unsteady situations where the dynamics of the control system should be taken into account. However, one can invoke the laws of thermodynamics to assert that the local, instantaneous temperature at any point within the heat exchanger cannot be outside the (T_a^{in}, T_w^{in}) range. Thus T_w^{out} is controllable only within this range and is not globally controllable if \dot{m}_w is the manipulated variable.

4.5 Multi-input controllability

It is also possible to study the controllability with two control inputs to the system. In this section we will briefly discuss this situation. The water and air flow rates \dot{m}_w and \dot{m}_a will be used as a manipulated variables.

We have seen in the previous section that when the water flow rates is used as a control input the control problem is nonlinear. To study the controllability in this case, a linearization of this quasi-linear model need to be performed at the steady-state point. First, a discretization of these equations is needed to put the system in the following form

$$\dot{x} = f(x, u). \quad (4.21)$$

where u is the input and x is the temperature. At the steady-state we have $\dot{x} = 0$ so that

$$0 = f(\bar{x}, \bar{u}). \quad (4.22)$$

Putting $x = \bar{x} + \delta x$, and $u = \bar{u} + \delta u$, we get

$$\delta \dot{x} = f(\bar{x} + \delta x, \bar{u} + \delta u), \quad (4.23)$$

where $(\bar{\cdot})$ is the steady-state.

Using a Taylor series about the equilibrium point and truncating the higher-order terms results in the following linearized equations valid in the vicinity of the

equilibrium point

$$\delta\dot{\mathbf{x}}(\mathbf{t}) = \mathbf{A}\delta\mathbf{x}(\mathbf{t}) + \mathbf{B}\delta\mathbf{u}(\mathbf{t}), \quad (4.24)$$

where $\delta\mathbf{x}(\mathbf{t})$, $\delta\mathbf{u}(\mathbf{t})$ are the perturbations of the vectors about the equilibrium point. The linearized system matrices are given in terms of $\mathbf{f}(\cdot)$ as follows: $\mathbf{A} = \partial\mathbf{f}/\partial\mathbf{x}$, and $\mathbf{B} = \partial\mathbf{f}/\partial\mathbf{u}$, where \mathbf{x} is the temperatures, and \mathbf{u} is the control input to the system. The two control inputs are \dot{m}_w and \dot{m}_a ; matrices \mathbf{A} and \mathbf{B} can be written as

$$\mathbf{A} = \begin{bmatrix} \partial\mathbf{f}_1/\partial\mathbf{x}_1 & \dots & \partial\mathbf{f}_1/\partial\mathbf{x}_{2n-1} \\ \vdots & & \vdots \\ \partial\mathbf{f}_{2n-1}/\partial\mathbf{x}_1 & \dots & \partial\mathbf{f}_{2n-1}/\partial\mathbf{x}_{2n-1} \end{bmatrix} \in \mathbb{R}^{2n-1 \times 2n-1},$$

$$\mathbf{B} = \begin{bmatrix} \partial\mathbf{f}_1/\partial\dot{m}_w & \partial\mathbf{f}_1/\partial\dot{m}_a \\ \vdots & \vdots \\ \partial\mathbf{f}_{2n-1}/\partial\dot{m}_w & \partial\mathbf{f}_{2n-1}/\partial\dot{m}_a \end{bmatrix} \in \mathbb{R}^{2n-1 \times 2}.$$

The system now described by a state-space representation and the controllability matrix can be constructed with matrices \mathbf{A} and \mathbf{B} as before to study the controllability of this linearized system. In some cases linearization does not capture the controllability well enough, so a controllable system may not be so if the system is linearized about some operating point. Nonlinear controllability analysis is needed in these cases to show that the system is indeed controllable.

4.6 Conclusions

The controllability of cross-flow heat exchangers is investigated from a theoretical and practical point of view. This property guarantees the ability of the heat exchanger to transfer a system from an initial to a final state. However, this does

not imply that the system will stay there. State controllability is for the complete system while output controllability refers to the output only. A finite-difference approach has been introduced for the analysis of system governed by a coupled set of PDEs. Two fundamentally different problems arise when the water/air inlet temperatures and the water flow rates are used as a manipulated variables. The former is linear, and the latter nonlinear. Cases of controllability with respect to different manipulated variables were analyzed here. The heat exchanger was found to be less controllable with high air and water flow rates. There is also the issue of practical controllability that can be quantified on the basis of the condition number. It is found that there is an optimum water flow rate at which the heat exchanger is the most controllable.

In linear controllability it is assumed that the dependent variables are allowed to vary over an infinite range. There are practical restrictions to this since the temperatures and flow rates can take on only positive values. Thus the constraints $T_w > 0$, $T_t > 0$, $\dot{m}_w > 0$ and $\dot{m}_a > 0$ impose restrictions on the range over which the heat exchanger is controllable. There is an even greater restriction on the manipulated variables; they cannot be varied in an infinite range even if positive. In this sense all the input variables are constrained: the inlet air and water temperatures are between certain bounds as are the air and water flow rates. This also reduces the controllability of the system. So, a system that is theoretically controllable may not practically be so because of these limitations on both the system and manipulated variable. Finally, we briefly discuss the controllability of a multi-input systems when the system is nonlinear.

CHAPTER 5

NUMERICAL SIMULATION OF THERMAL CONTROL OF CROSS-FLOW HEAT EXCHANGERS

The previous chapter analyzes the controllability of the cross-flow heat exchanger. We have seen that when the water flow rate is a manipulated variable, the problem is nonlinear and we only know that the outlet air temperature cannot exceed some limits by the laws of thermodynamics. But the control of the outlet air temperature using the water flow rate as a manipulated variable turns out to be a difficult task, since the heat exchanger model is a coupled set of PDEs where the input-output relation is nonlinear.

In this chapter a control methodology is presented to numerically simulate the control behavior of the cross-flow heat exchangers and overcome these difficulties. We present the results of numerical simulation of a Proportional-Integral (PI) controller for regulating the cross-flow heat exchanger outlet air temperature. First, we will develop a numerical method to simulate the dynamics of the heat exchanger, then this model will be used to compute the heat exchanger response to a controller.

As we mentioned in Section 1.2, there are several studies that have been carried out on the transient response of heat exchangers. In general the exact simulation of cross-flow heat exchangers is very complicated. They sometimes have fins, multiple rows and/or multiple circuits, and only for some special cases it is possible to simulate their dynamics. In this chapter we will consider the simplest geometry that can be easily computed, i.e. a single tube with water flow inside and cross flow of

air outside. This is schematically shown in Figure 4.2. We assume that the inlet water is cold and inlet air hot. Unlike most previous analysis we will take into account the history and thermal capacity of the tube and the thermal capacity of the fluid. There will be convective heat transfer between the water and the tube wall, conduction along the tube wall, and convection between the tube wall and the surrounding air.

5.1 Governing equations

The governing equations for the cross-flow heat exchanger are those considered in Chapter 4. For convenience, we will rewrite these equations in this chapter.

On the outside of the tube

$$\frac{\dot{m}_a}{L}c_a(T_a^{in} - T_a^{out}) = h_o2\pi r_o(T_a - T_t), \quad (5.1)$$

where L is the length of the tube, \dot{m}_a is the mass flow rate of air, c_a is its specific heat, T_a^{in} and T_a^{out} are the incoming and outgoing air temperatures, h_o is the heat transfer coefficient in the outer surface of the tube, r_o is the outer radius of the tube, T_a is the air temperature surrounding the tube, and T_t is the tube wall temperature. For convenience, the air temperature can be assumed to be approximately

$$T_a = \frac{T_a^{in} + T_a^{out}}{2} \quad (5.2)$$

which can be substituted in Equation (5.1). In the wall of the tube

$$\rho_t c_t \pi (r_o^2 - r_i^2) \frac{\partial T_t}{\partial t} = k_t \pi (r_o^2 - r_i^2) \frac{\partial^2 T_t}{\partial x^2} + 2\pi r_o h_o (T_a - T_t) - 2\pi r_i h_i (T_t - T_w). \quad (5.3)$$

ρ_t is the density of the tube material, c_t is its specific heat, k_t is its thermal conductivity, r_i is the inner radius of the tube, h_i is the heat transfer coefficient in the inner surface of the tube, and T_w is the water temperature. Finally, in the water

$$\rho_w c_w \pi r_i^2 \frac{\partial T_w}{\partial t} + \dot{m}_w c_w \frac{\partial T_w}{\partial x} = h_i 2\pi r_i (T_t - T_w), \quad (5.4)$$

where ρ_w is the water density, c_w is its specific heat, and \dot{m}_w is the water mass flow rate. In these equations $T_t = T_t(x, t)$, $T_w = T_w(x, t)$, $T_a^{out} = T_a^{out}(t)$, $T_a = T_a(t)$ in general. The boundary and initial conditions are

$$T_t(x, 0) = T_w(x, 0) = T_w^{in},$$

$$T_t(x, L) = T_w(x, L),$$

and $T_t(0, x) = T_w(0, x) = 25^\circ\text{C}$ (arbitrarily).

Also, the heat transfer coefficients are calculated from the following standard dimensionless relations [66]. For laminar flow on the water side, we have

$$Nu_i = \begin{cases} 1.86(Re_w Pr_w)^{1/3} (D_i/L)^{1/3} (\mu_w/\mu_t)^{0.14} & \text{for } Re_i Pr_w (D_i/L) > 10 \\ 3.66 & \text{for } Re_i Pr_w (D_i/L) < 10. \end{cases} \quad (5.5)$$

For turbulent flow on the water side

$$Nu_i = 0.027 Re_i^{0.8} Pr_w^{1/3} (\mu_w/\mu_t)^{0.14} \text{ for } Re_i > 2300. \quad (5.6)$$

For the air side [67]

$$Nu_o = 0.683 Re_o^{0.466} Pr_a^{1/3} \text{ for } 40 < Re_o < 4000. \quad (5.7)$$

Apart from geometrical quantities and material properties, there are four basic variables in the heat exchanger system that can be externally determined, i.e. mass flow rate of the water, \dot{m}_w , mass flow rate of air, \dot{m}_a , inlet air temperature, T_a^{in} , and inlet water temperature, T_w^{in} . These are all considered to be independent of position, i.e. uniform, but in general depend on time t . For a given heat exchanger, these quantities then determine the two fluid outlet temperatures: the water temperature, T_w^{out} , and the air temperature, T_a^{out} . The outlet air temperature is the only one of these quantities that depends on position, i.e. $T_a^{out} = T_a^{out}(x, t)$. For purposes of controlling a single variable, we will determine the mean temperature of the outlet air, \overline{T}_a^{out} and try to control it later.

In the complete set of equations, the unknowns are $T_t(x, t)$, $T_a^{out}(x, t)$ and $T_w(x, t)$.

5.1.1 Nondimensionalization

To solve this problem for general parameters, the governing Equations (5.1)–(5.4) need to be nondimensional. We define the following dimensionless quantities.

Spatial coordinate

$$x^* = x/L. \quad (5.8)$$

Time

$$\tau = t\alpha_w/L^2, \quad (5.9)$$

and finally the temperatures

$$\theta = (T - T_w^{in})/(T_a^{in} - T_w^{in}). \quad (5.10)$$

Therefore, we have the following nondimensional governing equations. On the air side we have

$$Pe_a(\theta_a^{in} - \theta_a^{out}) = \beta_1\left(\frac{\theta_a^{in} + \theta_a^{out}}{2} - \theta_t\right). \quad (5.11)$$

And in the wall of the tube we get

$$\gamma\frac{\partial\theta_t}{\partial\tau} + \beta_2(\theta_t - \theta_w) = \frac{\partial^2\theta_t}{\partial x^{*2}} + \beta_3\left(\frac{\theta_a^{in} + \theta_a^{out}}{2} - \theta_t\right). \quad (5.12)$$

And in the water side we get

$$\frac{D_i}{L}\frac{\partial\theta_w}{\partial\tau} + Pe_w\frac{\partial\theta_w}{\partial x^*} = \beta_4(\theta_t - \theta_w). \quad (5.13)$$

The nondimensionalization of the above governing equations is explained in more detail in Appendix A. The coefficients in these equations are

$$\beta_1 = Nu_o(2\pi r_o L/A), \quad (5.14)$$

$$\gamma = \alpha_w/\alpha_t, \quad (5.15)$$

$$\beta_2 = Nu_i(A_i/A_t)(k_w/k_t)(L/D_i), \quad (5.16)$$

$$\beta_3 = Nu_o(A_o/A_t)(k_a/k_t)(L/D_o), \quad (5.17)$$

$$\beta_4 = Nu_i(A_i/A_w). \quad (5.18)$$

where the areas are tube wall cross-sectional area $A_t = \pi(r_o^2 - r_i^2)$, tube outside area $A_o = 2\pi r_o L$, tube inside area $A_i = 2\pi r_i L$, and water flow area $A_w = \pi r_i^2$.

5.1.2 Boundary conditions

Equations (5.11-5.13) represent a set of coupled equations where a unique solution exists if appropriate initial and boundary conditions are specified. The water enters and leaves the tube with uniform temperature and velocity profiles. At the entrance, it is assumed to be at a prescribed temperature, and at the outlet it is set equal to the tube temperature.

The initial condition is

$$\theta_t(x^*, 0) = \theta_i(x^*), \quad (5.19)$$

and the boundary conditions are

$$\theta_t(0, \tau) = \theta_{w1}, \quad (5.20)$$

$$\theta_t(1, \tau) = \theta_{wn}, \quad (5.21)$$

where $\theta_i(x^*)$ is the initial temperature distribution, and θ_{w1} and θ_{wn} are the temperatures at the two ends.

The mean air temperature downstream of the tube is calculated as

$$\bar{\theta}_a^{out} = \frac{1}{L} \int_0^1 \theta_a^{out} dx^*. \quad (5.22)$$

In the simulations the following set of values for the parameters were assumed: $A = 0.13 \text{ m}^2$, $\gamma = 0.001$, $L = 7.32 \text{ m}$, $D_i/D_o = 0.9$, $T_a^{in} = 25^\circ\text{C}$, $T_w^{in} = 1^\circ\text{C}$, and $\dot{m}_a = 0.0609 \text{ kg/s}$ corresponding to 20% of full flow rate, and a steady uniform stream of air is flowing normal to the tube at the ambient temperature.

5.2 Numerical solutions

We have three coupled equations, two partial differential equations for the fluid and the tube wall and one algebraic equation in the air side. Since the θ_a^{out} is a function

of θ_a^{in} and θ_t , then the air side equation Equation (5.11) can be solved for θ_a^{out} . We get

$$\theta_a^{out} = \frac{\theta_a^{in}(Pe_a - \beta_1/2) + \beta_1\theta_t}{Pe_a + \beta_1/2}. \quad (5.23)$$

This equation can be substituted into the tube wall Equation (5.12) to reduce the number of equations to two with two unknown θ_t and θ_w .

A finite-difference method is used to calculate the time-dependent solution numerically. Forward differences in time and a second order fully implicit method in the spatial direction were used for numerical stability. The $0 < x^* < 1$ domain is divided into N equal parts and the unknowns at each point are to be determined. Equation (5.24) is example of this approach. Referring to the mesh of Figure 5.1 which shows a typical grid point S with its two immediate neighbors, we have the discretized form of the equation for the tube as

$$\begin{aligned} \frac{\gamma}{\Delta\tau} \left(\theta_{t(i)}^\tau - \theta_{t(i)}^{\tau-\Delta\tau} \right) + \beta_2(\theta_{t(i)} - \theta_{w(i)}) &= \frac{1}{\Delta x} \left(\theta_{t(i+1)}^\tau - 2\theta_{t(i)}^\tau + \theta_{t(i-1)}^\tau \right) \\ + \beta_3 \left(\frac{\theta_{a(i)}^{in}}{2} + \frac{\theta_{a(i)}^{in}(Pe_a - \beta_1/2) + \beta_1\theta_{t(i)}^\tau}{2Pe_a + \beta_1} - \theta_{t(i)} \right) & \quad (5.24) \end{aligned}$$

which can be written as

$$a_s\theta_{s(i)}^\tau = a_{i-1}\theta_{s(i-1)}^\tau + a_{i+1}\theta_{s(i+1)}^\tau + \beta_2\theta_{w(i)}^\tau + \beta_5\theta_{a(i)}^{in} + a^{\tau-\Delta\tau}\theta_{s(i)}^{\tau-\Delta\tau}, \quad (5.25)$$

where

$$\begin{aligned} a_{i+1} &= 1/\Delta x^{*2}, \\ a_{i-1} &= 1/\Delta x^{*2}, \\ a^{\tau-\Delta\tau} &= \gamma/\Delta\tau, \\ \beta_5 &= \beta_3 \left(1/2 + \frac{Pe_a - \beta_1/2}{2Pe_a + \beta_1} \right), \\ a_s &= a_{i+1} + a_{i-1} + a^{\tau-\Delta\tau} + \beta_2 + \beta_3 \left(-\frac{\beta_1}{2Pe_a + \beta_1} + 1 \right), \end{aligned}$$

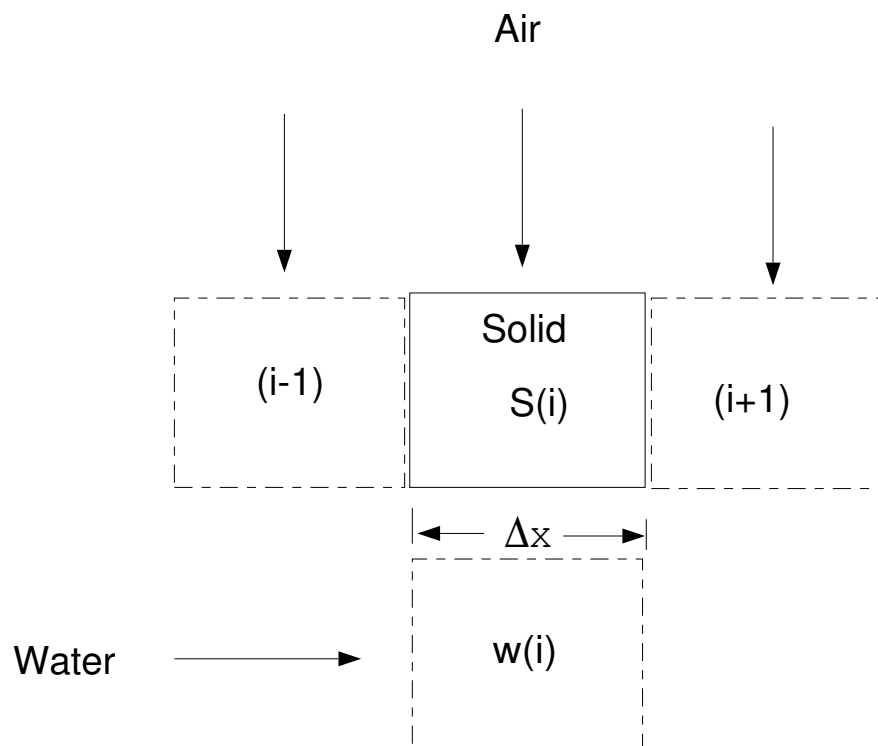


Figure 5.1. Discretization of problem.

where a_s is the coefficient of the variable at the grid point under consideration and the parameters on the right side of the equation are the coefficients of the four immediate neighbors. At the boundary nodes, $a_{i-1} = 0$ and $a_{i+1} = 0$ for nodes number 1 and N respectively. Similarly on the water side we have

$$a_w \theta_{w(i)}^\tau = \beta_4 \theta_{s(i)}^\tau + \frac{RePr}{\Delta x^*} \theta_{w(i-1)}^\tau + a_w^{\tau-\Delta\tau} \theta_{w(i)}^{\tau-\Delta\tau}, \quad (5.26)$$

where

$$\begin{aligned} a_w^{\tau-\Delta\tau} &= D_i / L \Delta\tau, \\ a_w &= a_w^{\tau-\Delta\tau} + \beta_4 + RePr / \Delta x^*. \end{aligned}$$

Applying the initial and boundary conditions, we have a set of coupled equations Equations (5.25) and (5.26) at each node which can be solved simultaneously at each time step for the new temperatures. The number of such equations is equal to twice the number of nodes in the calculation domain. The system matrix is banded and the LU decomposition method is used for solution.

Initially the system is at an ambient temperature of 25°C which corresponds to $\theta = 1$. θ_a^{in} is maintained at this temperature. At the inlet of the tube, water and tube temperatures are maintained at 1°C, i.e. $\theta = 0$, while at the outlet they are equal to each other.

After solving these two equations for the two unknown $\theta_w(t, x)$ and $\theta_t(t, x)$ we can calculate the outlet air temperature $\theta_a^{out}(t, x)$ from Equation (5.23) and then the average air outlet temperature $\bar{\theta}_a^{out}$ calculated from Equation (5.22)

Because θ_a^{out} measurements were located downstream of the tube, the calculated air temperature was delayed by a certain time based on the air speed.

5.2.1 Validation and convergence

The heat exchanger model is verified by comparing the simulation results to some analytical solutions that exist for some limiting cases. The first situation is the steady-state case, where the results can be checked by heat balances across all the thermal resistances. In this case we will have two coupled ordinary differential equations for the tube and water sides which have a known analytical solution. The second case was the very large water flow rate and a negligible tube wall thermal resistance, i.e. $k_t = 0$. In this case we have two coupled ordinary differential equations which also have a known solution. For all the cases tested above and depending on the model parameters, the numerical simulation and the analytical solutions agreed within 1.5 – 4.4%.

The time scale of the temperature is generally different in the fluids and in the tube wall. Within the tube, the dimensionless time of diffusion is proportional to the thermal diffusivity ratio γ . This means that if γ is large, the heat transfer will be slow while if γ is small a rapid process will result. This makes the choice of time step $\Delta\tau$ is very critical in this dynamic problem; a large time-step size gives inaccurate information for short time events, while a small time step size increases the computation time. The time step employed here is 10^{-9} , which corresponds to 0.1 s in real time. Figure 5.2 shows the effect of this time step on the temperature at the center of the tube wall. Also, in order to see if this time step has a different effect along the tube wall, we calculate the temperature along the tube at different time steps, this can be shown in Figure 5.3. The outlet air temperature as a function of time step is also shown in Figure 5.4.

To analyze the numerical convergence we refine the spatial discretization and compare the results. Different number of nodes have been used. Figure 5.5 shows this convergence test. The number of nodes used is $N = 250$ with a spatial segment

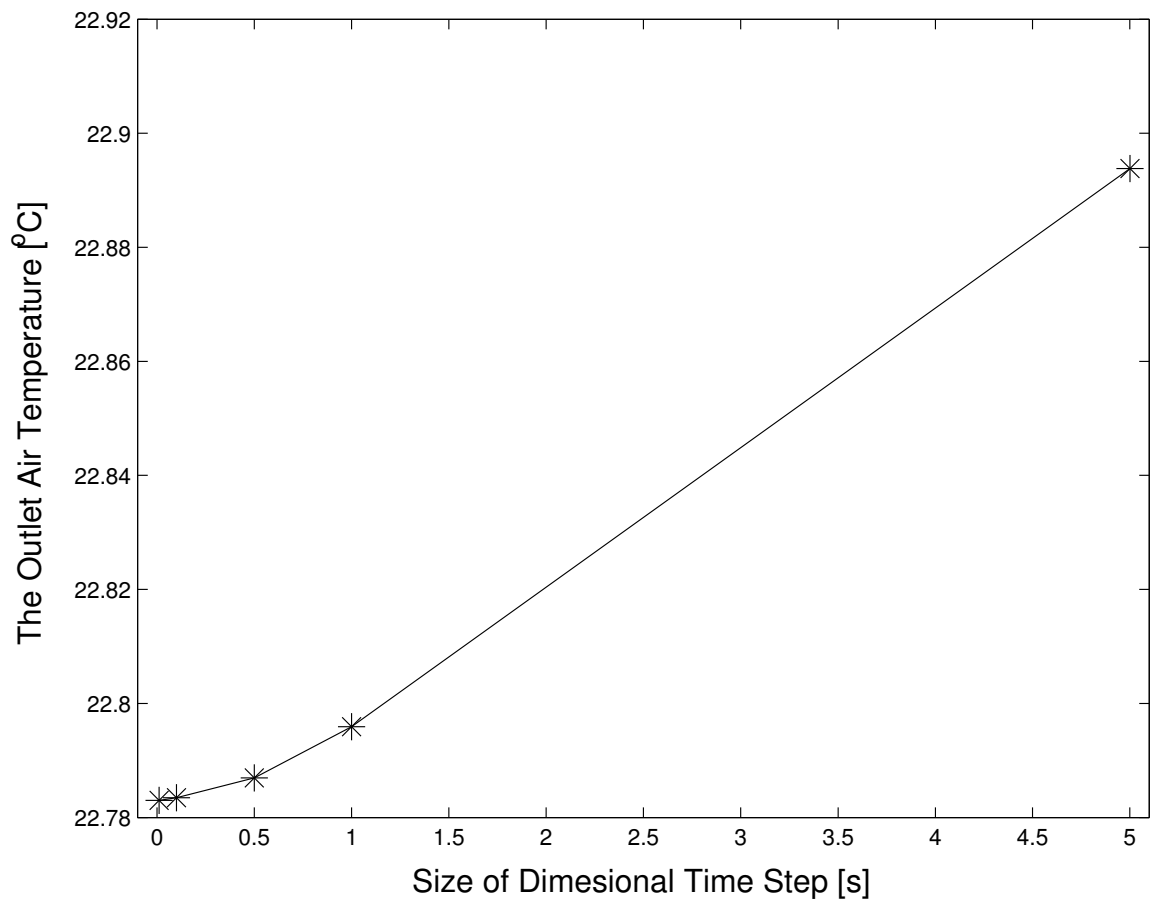


Figure 5.2. Effect of time step on solution at center of pipe.

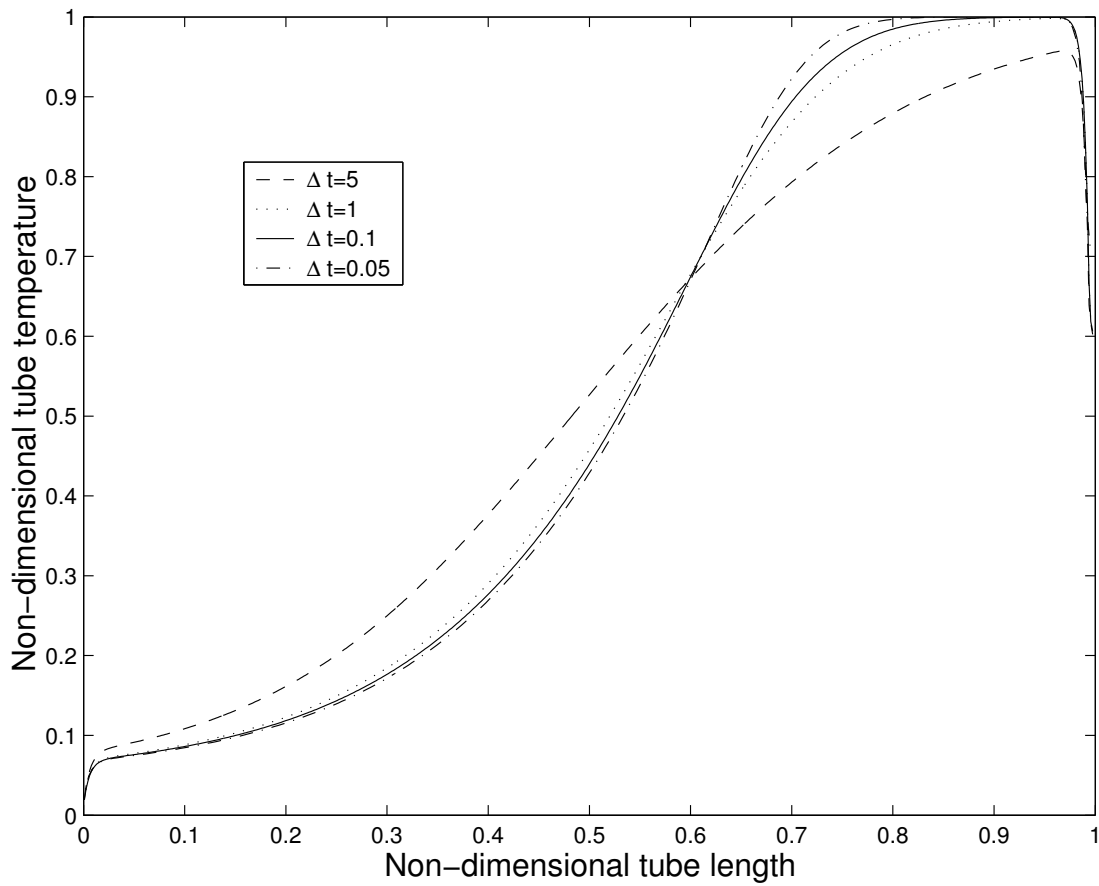


Figure 5.3. Effect of time step on solution along heat exchanger pipe wall at 50 sec. and air and water velocity equal to 0.43 m/s and 0.102 m/s respectively.

size of $2/N$. With this choice, the solution shows that these values give nondimensional temperatures to within 4% of the correct values.

5.3 Temperature control

Based on the dynamic model of the heat exchanger developed in the previous sections, a control scheme can be used to control the air outlet temperature. For purposes of controlling a single variable, we will determine the mean temperature of the outlet air, \overline{T}_a^{out} and try to control it. To be realistic we will place the temperature sensors that will provide the controlling signal a certain distance downstream of the tube. There will thus be a time delay between the instant the air leaves the tube and when it reaches the sensors.

The purpose of the control procedure is to obtain and stabilize a prescribed temperature of the outlet air by acting on other inlet conditions; here we have specifically chosen to control using the water flow rate. Control limits are set by the range of variation of the outlet air temperature that is physically possible. This is shown in Figure 5.6 for both water and air at their maximum and minimum flow rates. This defines the range of air temperatures beyond which the heat exchanger cannot be controlled. Furthermore, since the thermal capacity of the water is much larger than that for air, the air outlet temperature is very insensitive to the water flow rate. The strongly nonlinear nature of the system is clear from Figure 5.7, where \overline{T}_a^{out} is seen to change slope considerably until it finally becomes insensitive to any further change in \dot{m}_w .

5.3.1 Proportional-Integral (PI) control

The objective of the control will be to maintain the average outlet air temperature as close as possible to a prescribed value even in the presence of disturbances. Proportional-Integral (PI) control will be used for this purpose and the water flow

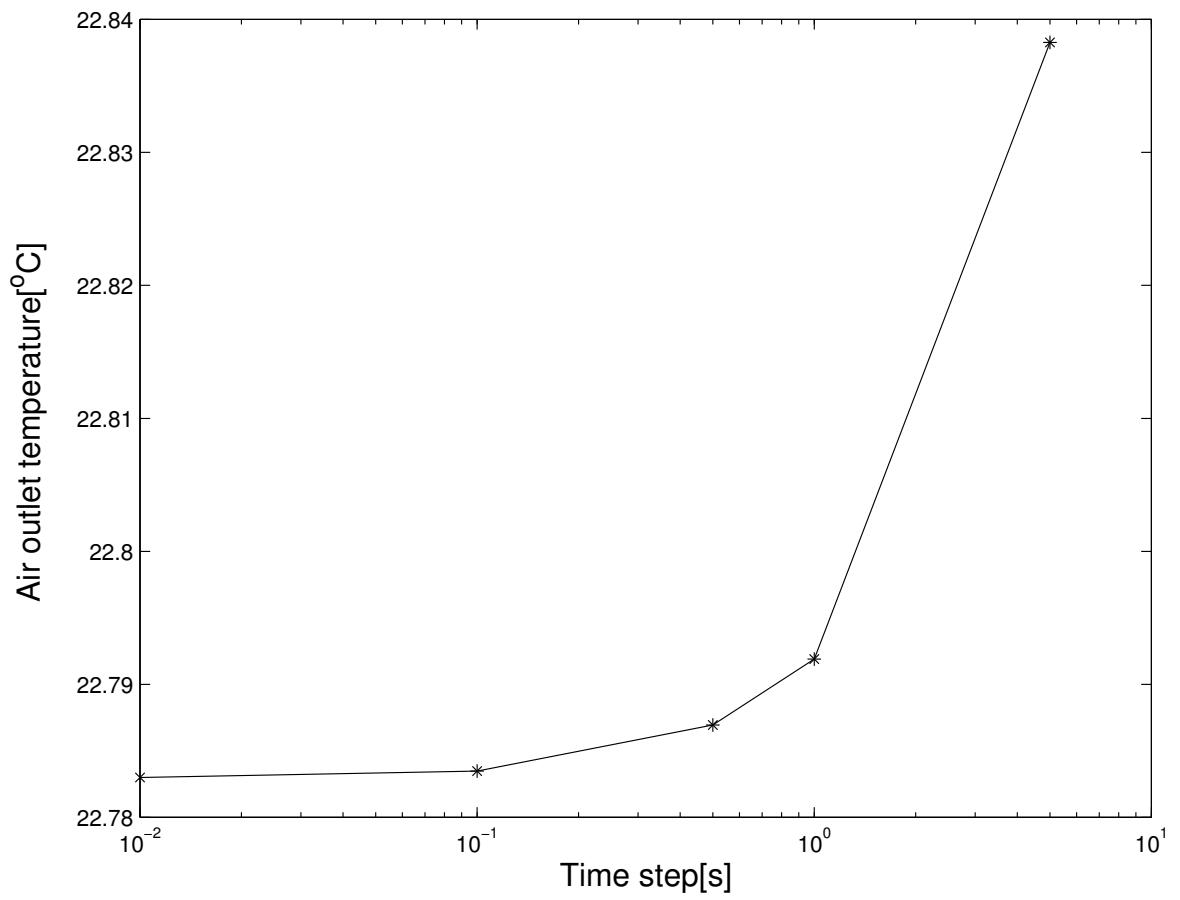


Figure 5.4. Outlet air temperature as a function of time step.

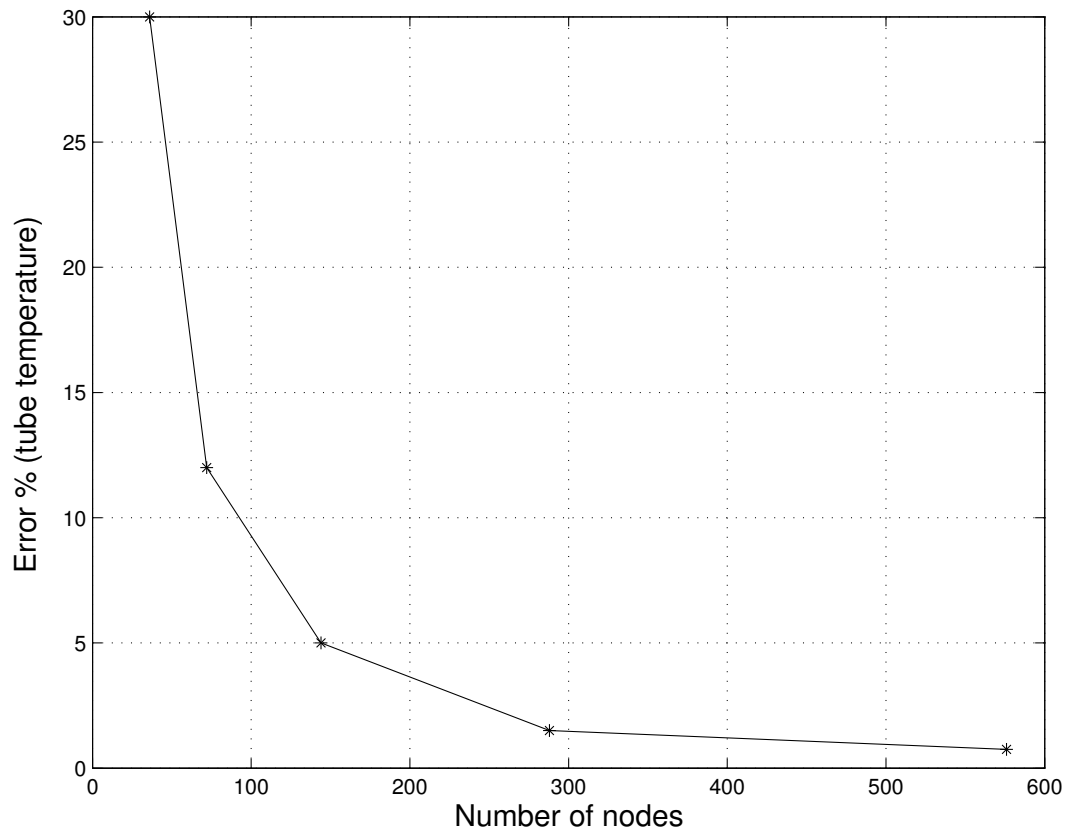


Figure 5.5. Convergence of solution as function of number of nodes.

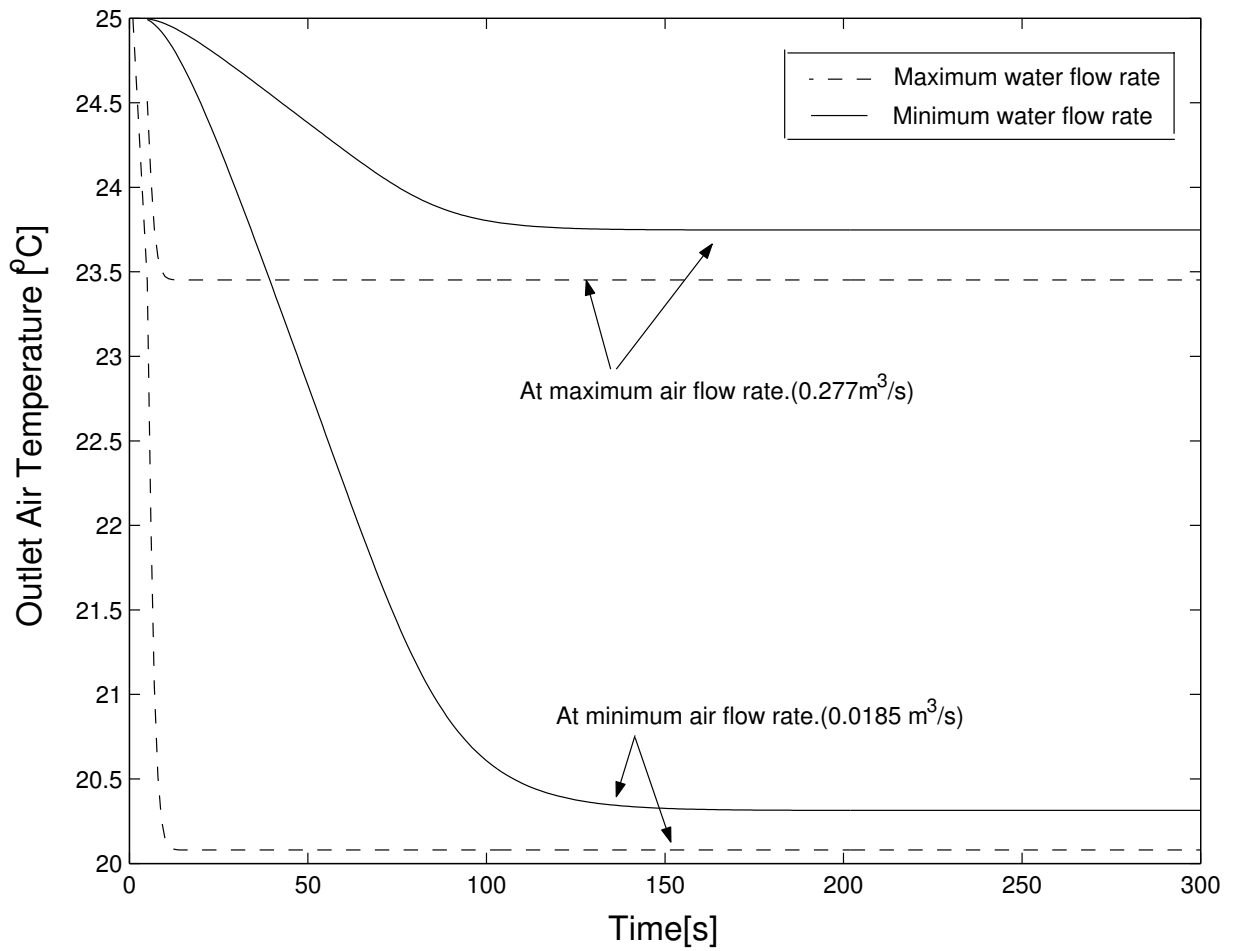


Figure 5.6. Possible operating conditions at minimum and maximum air and water Reynolds numbers.

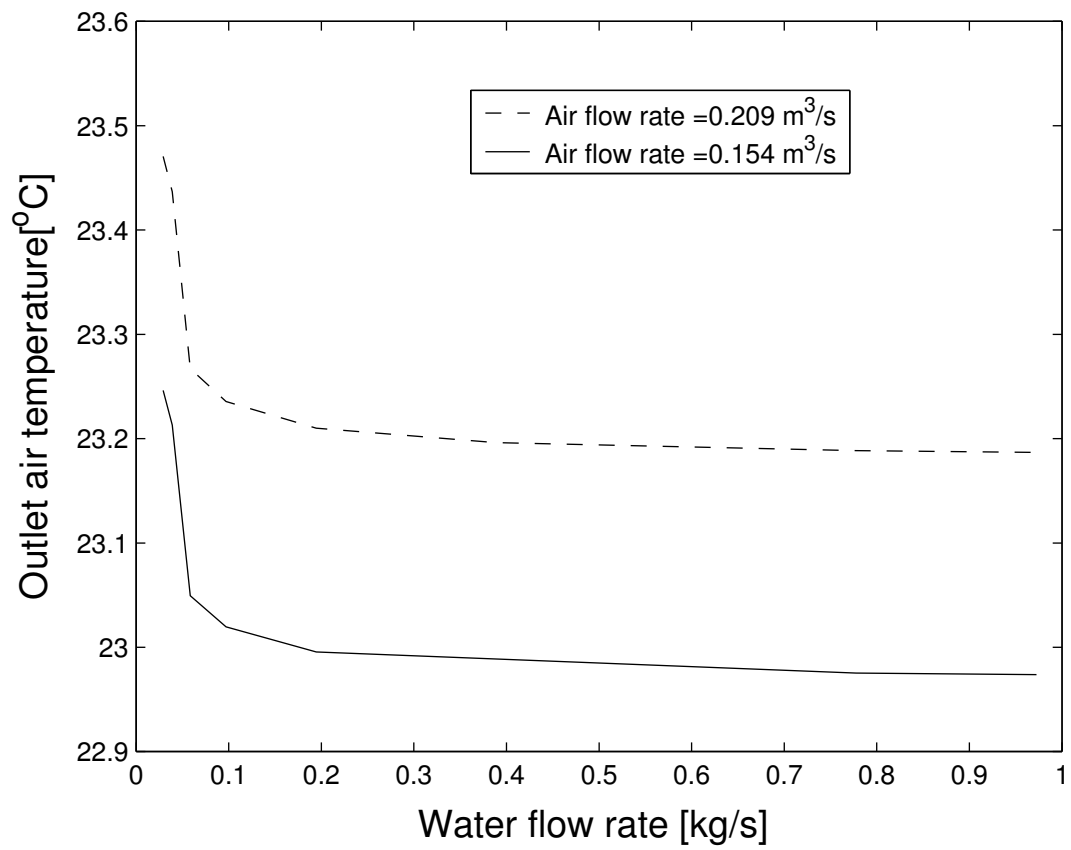


Figure 5.7. Relation between T_a^{out} and \dot{m}_w for different \dot{m}_a .

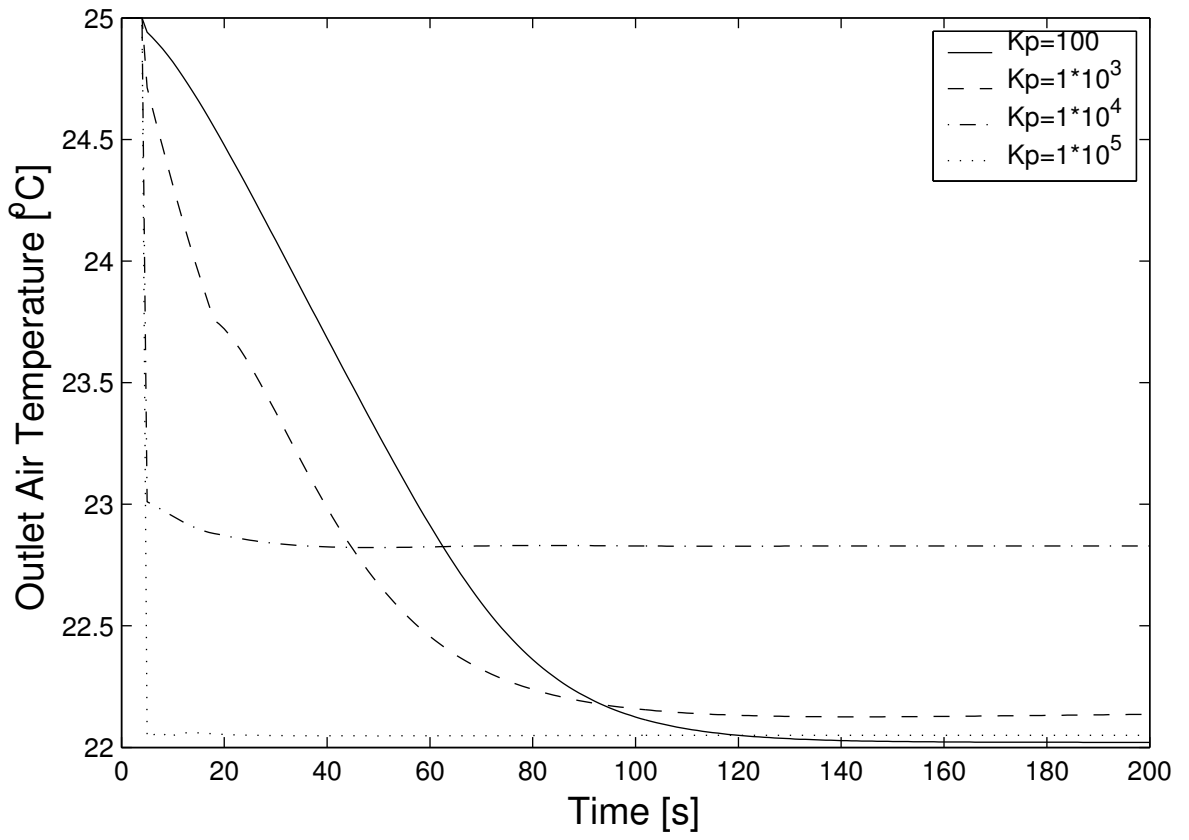


Figure 5.8. Behavior of outlet air temperature as function of time at different K_p .

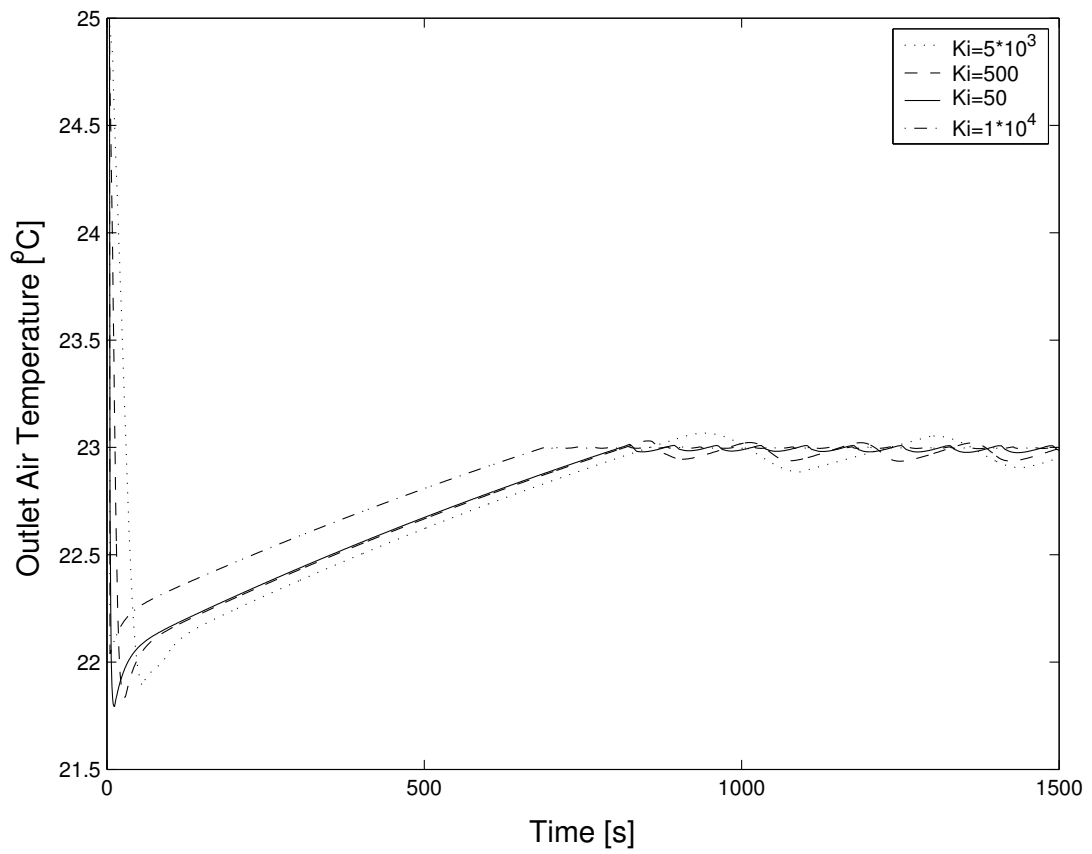


Figure 5.9. Behavior of outlet air temperature as function of time and different K_i .

rate will be modified using

$$\frac{d\dot{m}_w}{dt} = K_I e + K_P \frac{de}{dt}. \quad (5.27)$$

The error signal is $e = T_s - \bar{T}_a^{out}$, where T_s is the desired average temperature. The corresponding time-discretized equation is

$$\dot{m}_w^{t+\Delta t} = \dot{m}_w^t + [K_I e^t + K_P (\Delta e / \Delta t)^t] (\Delta t), \quad (5.28)$$

where K_I and K_P are constants that will be selected on the basis of a compromise between speed and accuracy of response.

First, proportional and integral controls are introduced separately to regulate the cold water flow rate. Their performances are shown in Figure 5.8 and Figure 5.9. Then PI control logic was implemented. Initially the system starts with a flow that produces a different outlet air temperature than the target one. Then, at every time step, the program computes this outlet air temperature and the error which, using Equation (5.27), changes the flow rate to be supplied to the heat exchanger. This regulation of the flow rate will continue until the error reaches a very small value or the outlet air temperature reaches the desired value.

In order to select the constants in Equation (5.27), a wide range of values was investigated, i.e. $K_I = 50, 500, 5 \times 10^3, 5 \times 10^4 \text{ s}^{-1}$ and $K_P = 100, 10^3, 10^4, 10^5$. A typical set of results are shown in Figure 5.10 which gives the outlet air temperatures as a function of time for different values of K_I and K_P . The target temperature was set at $T_a^{out} = 23^\circ\text{C}$, and we can see that the system response is faster as K_P and K_I are increased. At a smaller value of these parameters a high overshoot is reached with a high time between 600 s and 700 s to raise the temperature near 23°C , while the overshoot and the time constant are reduced for $K_P = 10^4$. For low values of K_I there is a high overshoot with an oscillation of 0.05°C around the set-point. However, when K_I is increased, the system response is much better. On

further increase of K_I the system response is far from the set-point. Further results are shown in Figures 5.11 and 5.12. The choice of $K_I = 500 \text{ s}^{-1}$ and $K_P = 2.75 \times 10^4$ was then selected as the best compromise for the given initial conditions.

The performance of the control system at the selected parameters along with the uncontrolled case is shown in Figure 5.13, and the corresponding regulated water flow rate is shown in Figure 5.14 which brings the temperature to the set point in about 20 s without overshoot.

In the following sections, the performance of the above controller will be tested under the influence of disturbances. Different disturbances in the flow rates and temperatures are introduced to check the ability of the controller to return the temperature to the desired one.

5.3.2 Step change in inlet air temperature

In Figure 5.15 at 200 s after starting the control, and after the target temperature is reached, a disturbance from 25°C to 24.2°C in the inlet air temperature is introduced. The temperature returns to the set-point very slowly; this is because the system is at the minimum water flow rate in order to raise the outlet air temperature. Also, due to the fact that this heat exchanger is operating in a cooling mode, it takes much longer to raise the air temperature than to decrease it. In contrast, if a higher inlet air temperature disturbances of 25.8°C is made, the temperature rapidly returns to the set-point in about 40 s without overshoot. This fast return is expected because of the high cooling capacity rate of the water.

5.3.3 Step change in inlet air flow rate

In this case the initial air flow rate is at about 20% of the maximum possible. In Figure 5.16 a step change in the inlet air flow rate is shown at 200 s to about 17% of the maximum. Again, the system response is slow in raising the temperature of the

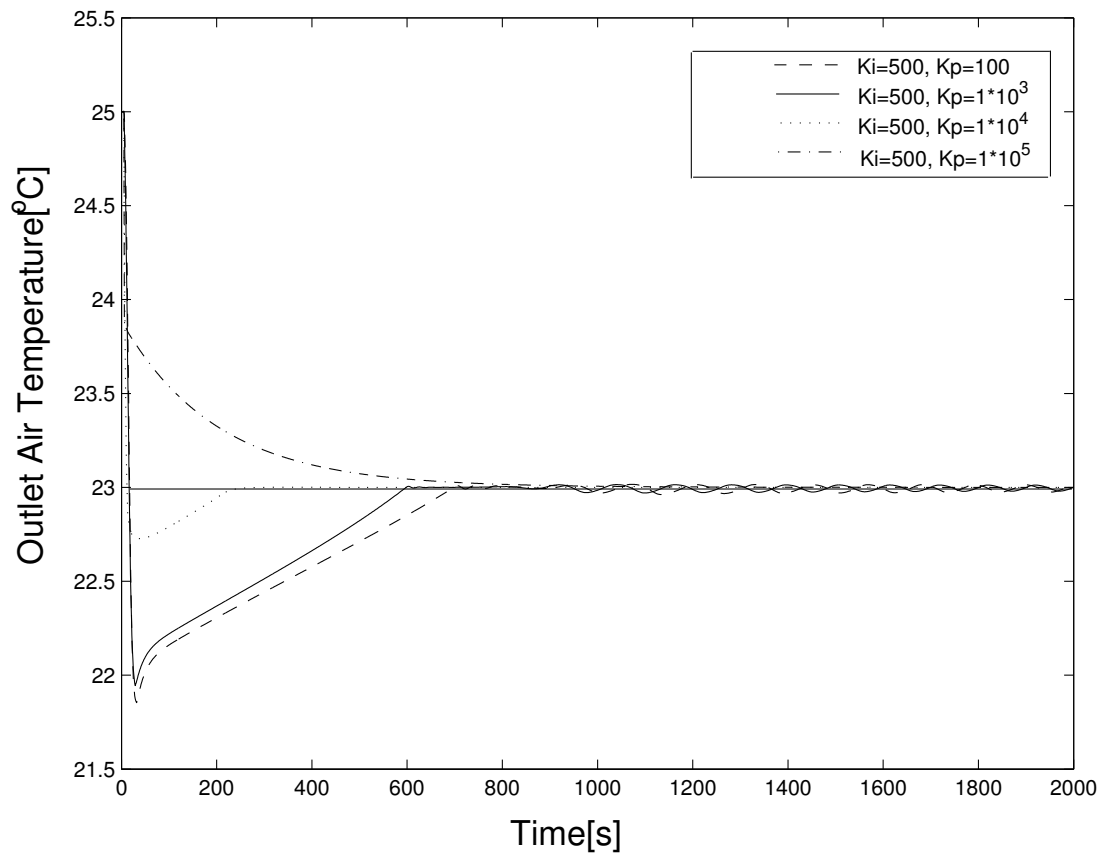


Figure 5.10. Behavior of outlet air temperature as function of time at constant K_i and different K_p .

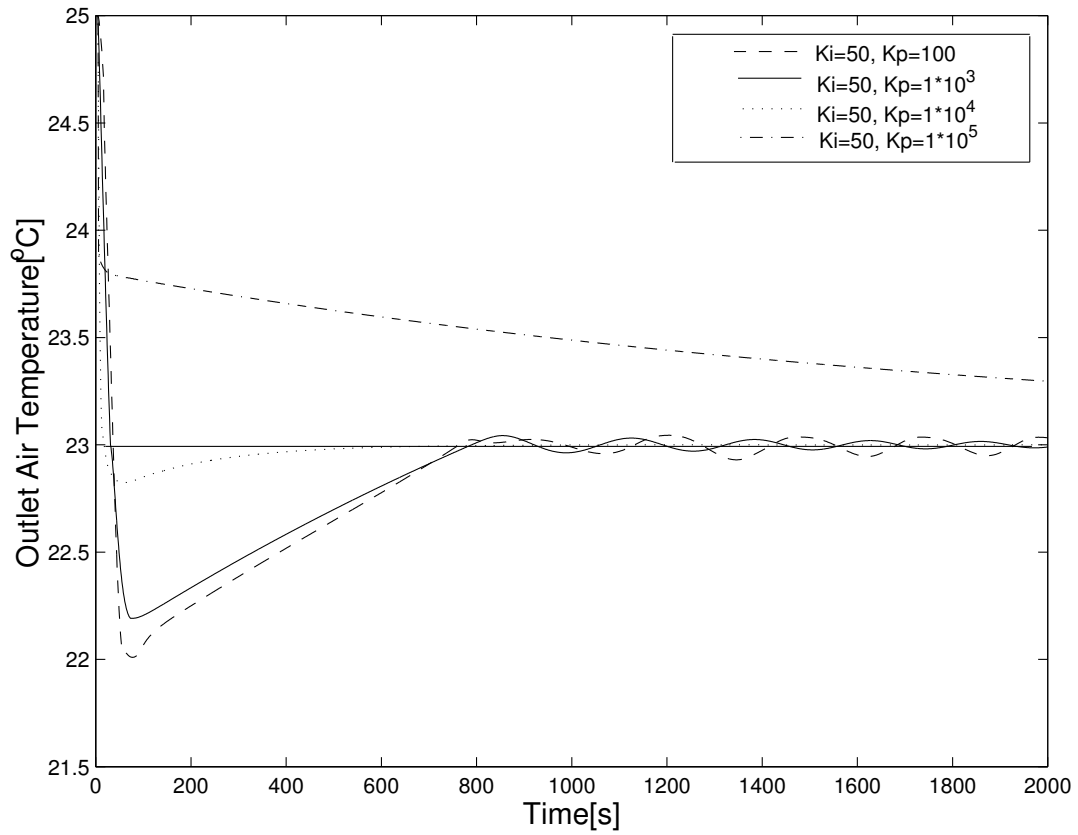


Figure 5.11. Behavior of outlet air temperature as function of time at constant K_i and different K_p .

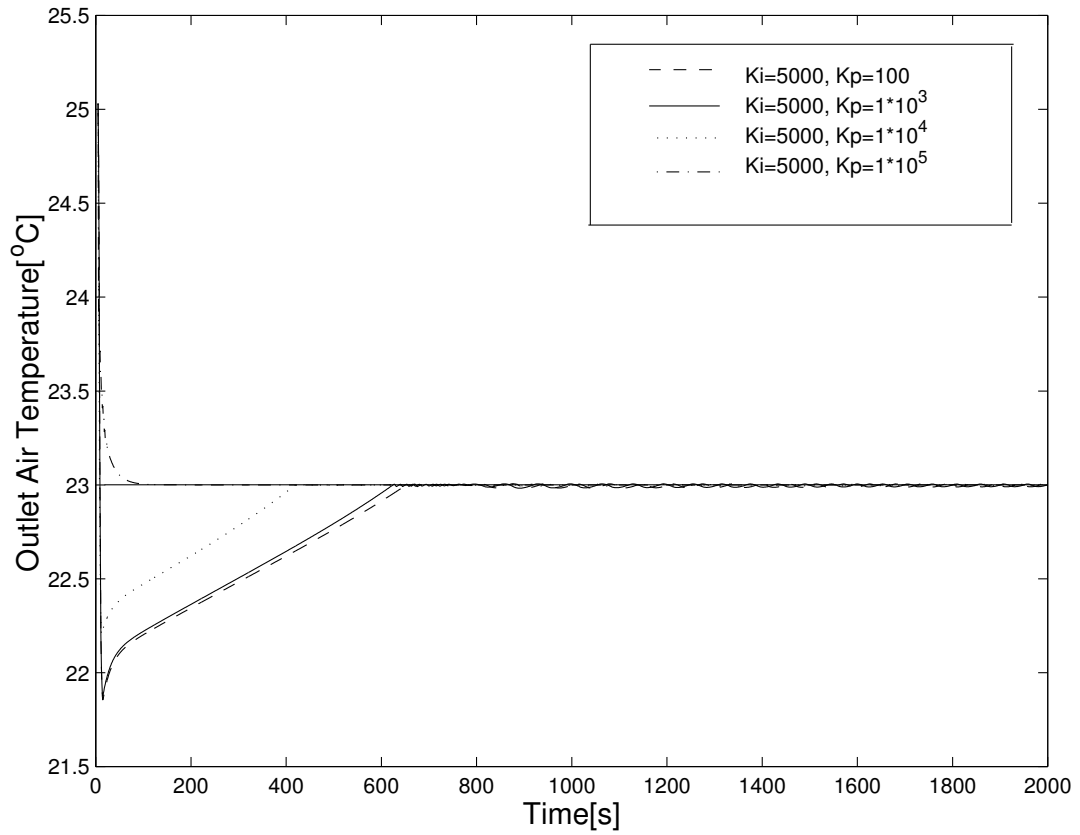


Figure 5.12. Behavior of outlet air temperature as function of time at constant K_i and different K_p .

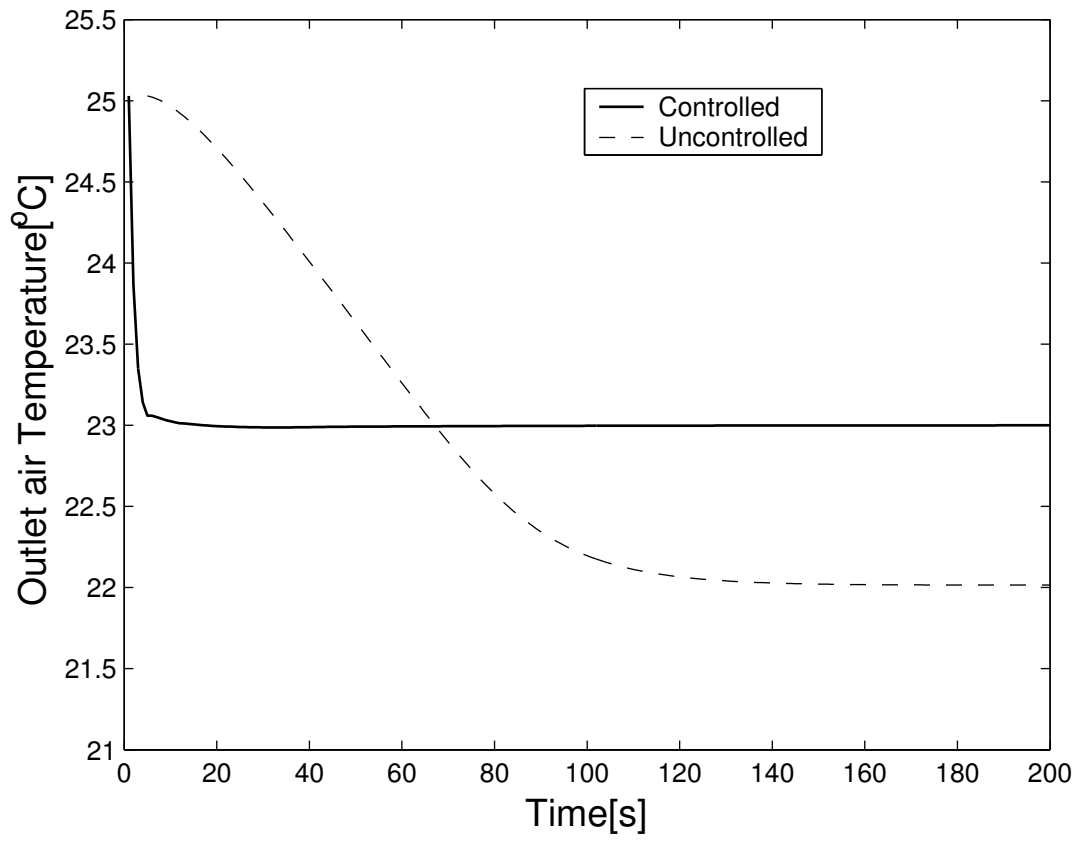


Figure 5.13. Controlled and uncontrolled outlet air temperature.

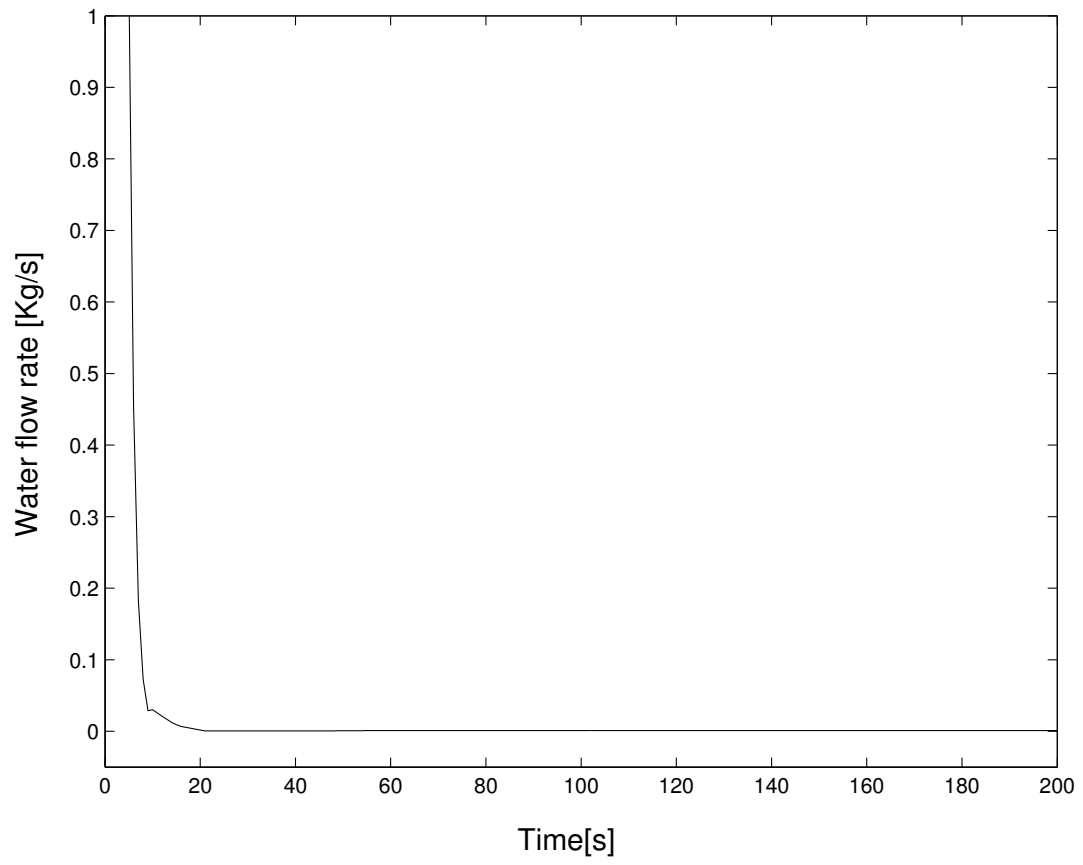


Figure 5.14. Variation of water flow rate with control.

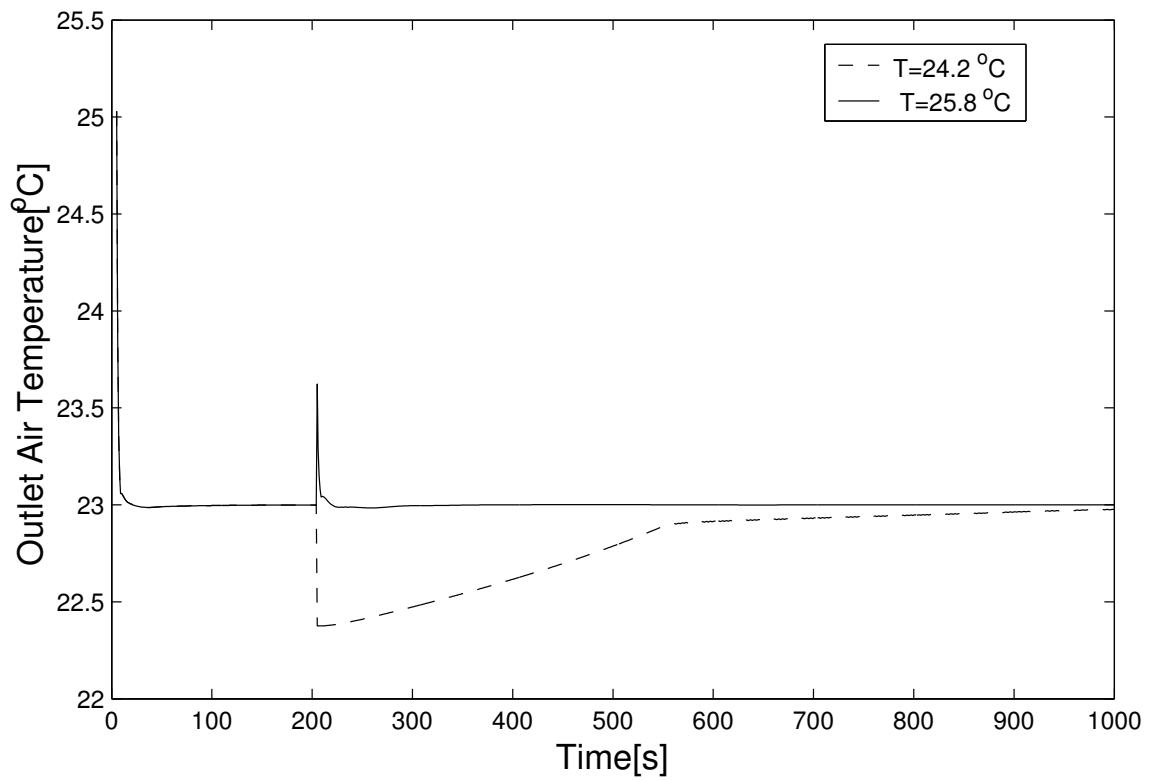


Figure 5.15. Behavior of outlet air temperature with control and disturbance at 200 sec. due to a step change in air inlet temperature from 25°C to 24.2°C and 25.8°C.

air. Also, Figure 5.16 shows another disturbance introduced by increasing the air inlet flow rate from 20% to 40% of the full flow rate. The control scheme is quick to respond to the disturbance by increasing the water flow rate, and the temperature returns quickly to the set-point without any overshoot. On further increasing the air inlet flow rate to 75% of the maximum, the system responds quickly but is unable to provide the exact temperature as shown in Figure 5.17 where the controlled steady state temperature is at 23.2°C.

5.3.4 Step change in set point

At 200 s the target temperature is changed from 23°C to 22° as shown in Figure 5.18. Here, the controller provides the correct value of the water flow rate quickly, and the temperature reaches the new set-point as soon as the change in the set-point is made. The corresponding water flow rates are shown in Figure 5.19. The next change in the set-point is shown in Figure 5.20 where the target temperature changed, this time to 24°C. The temperature rise from 23°C to 24°C is very slow and takes 500 s to come close to the target temperature. The controller stabilizes the temperature at the new set-point, where the water flow rate is near its minimum value near zero, as shown in Figure 5.21.

This disturbance is repeated for a set-point of 21°C as shown in Figure 5.22, and here the system drops the temperature from 23°C to 21.75°C immediately, but is unable to reach the target temperature. The water flow rate reaches its maximum value as shown in Figure 5.23. It should be pointed out that the system reaches the lowest possible temperature while the flow rate is still increasing, from 200 s to 300 s, but a further increase of the water flow rate no longer improves the performance of the heat exchanger.

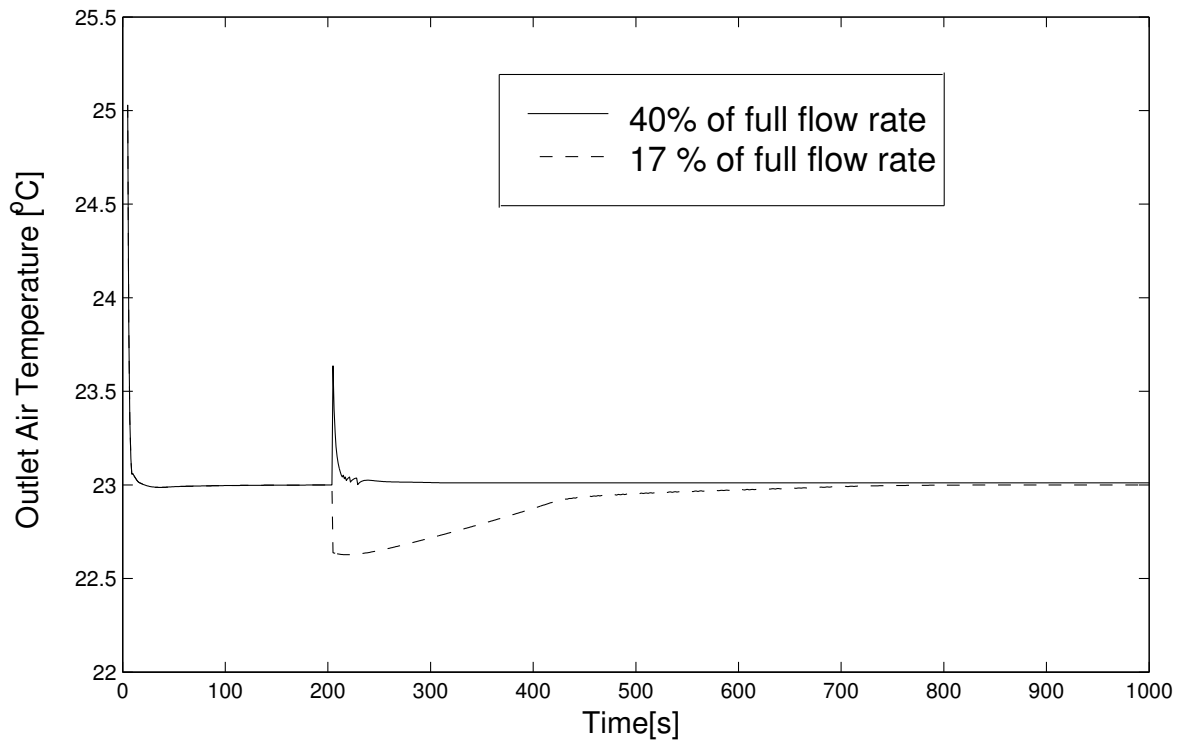


Figure 5.16. Behavior of outlet air temperature with control and disturbance at 200 sec. due to step change in air inlet flow rate from 20% to 17% and 40%.

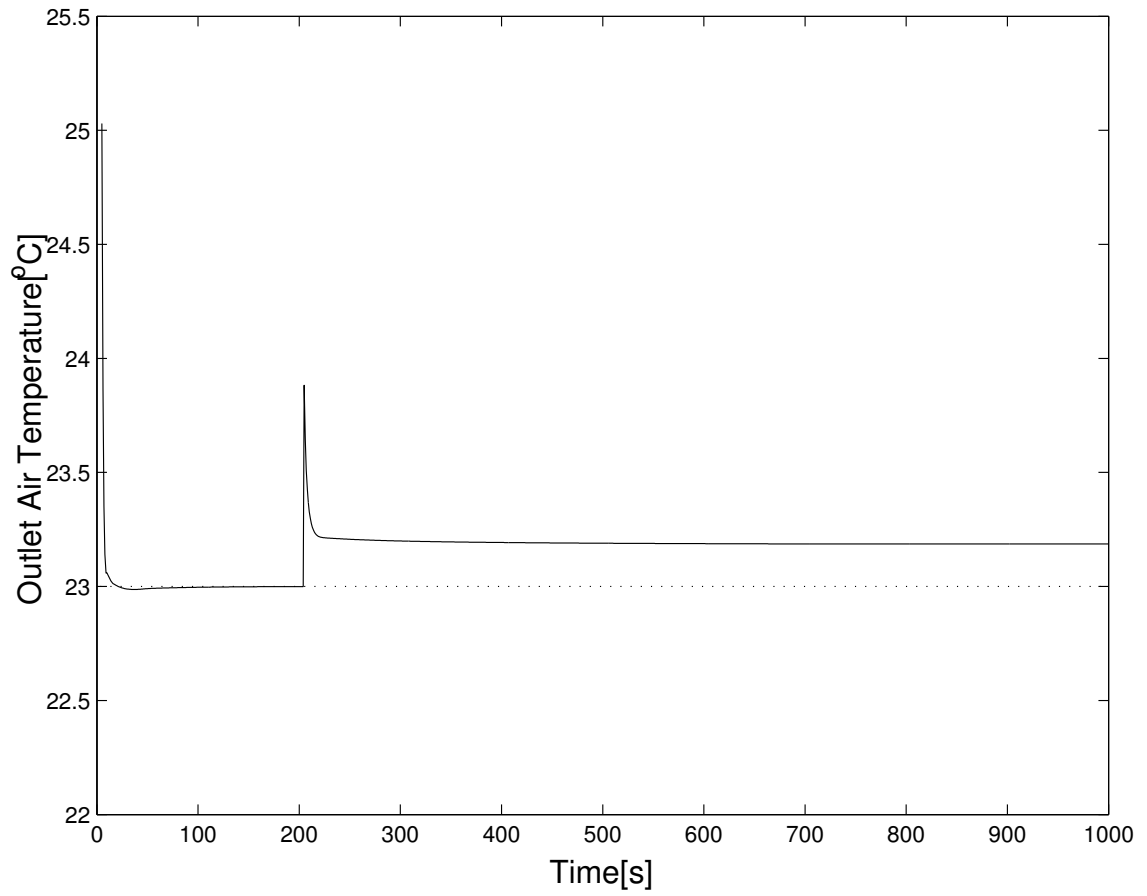


Figure 5.17. Behavior of outlet air temperature with control and disturbance at 200 sec. due to a step change in air inlet flow rate from 20% to 75% of full flow rate.

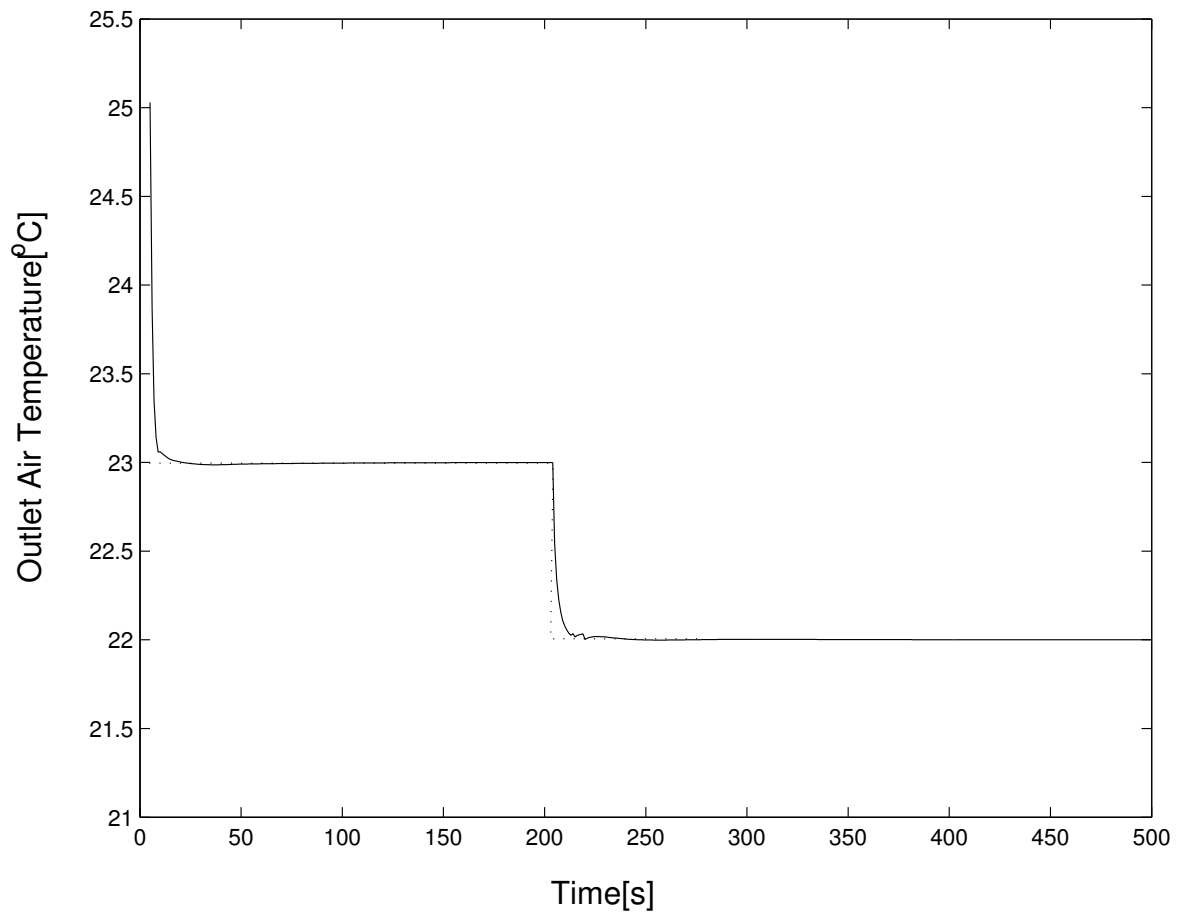


Figure 5.18. Behavior of outlet air temperature with control and disturbance at 200 sec. due to step change in set point from 23°C to 22°C.

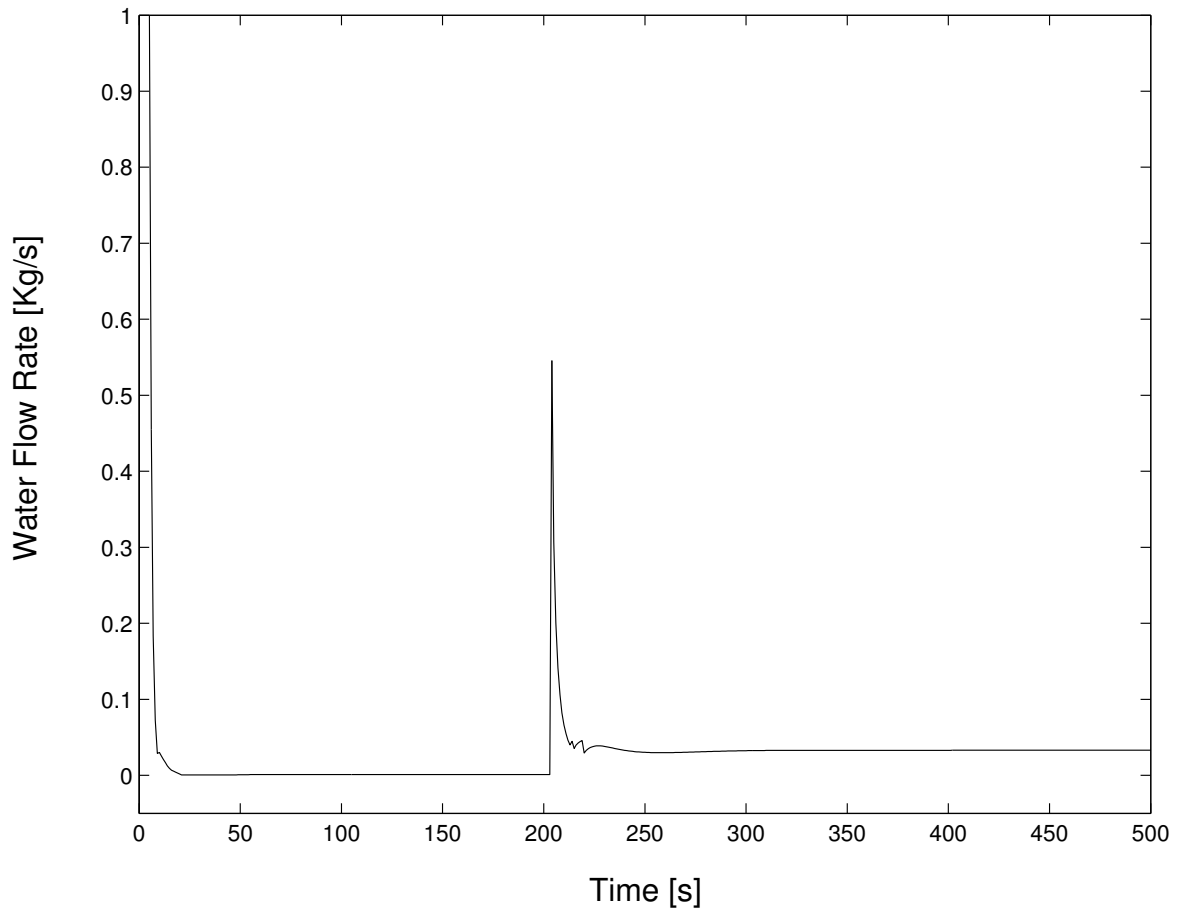


Figure 5.19. Variation of water flow rate with control and disturbance at 200 sec. due to step change in set point from 23°C to 22°C.

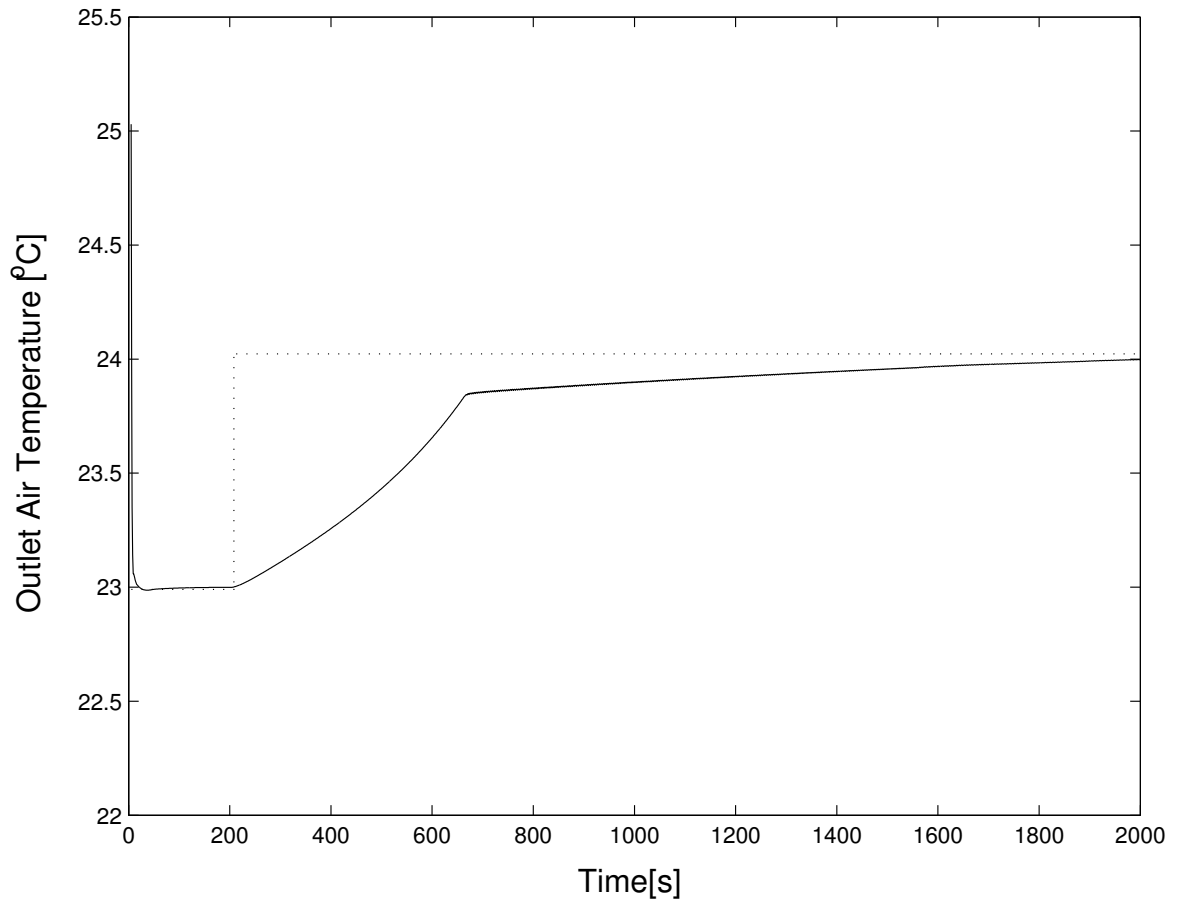


Figure 5.20. Behavior of outlet air temperature with control and disturbance at 200 sec. due to step change in set point from 23°C to 24°C.

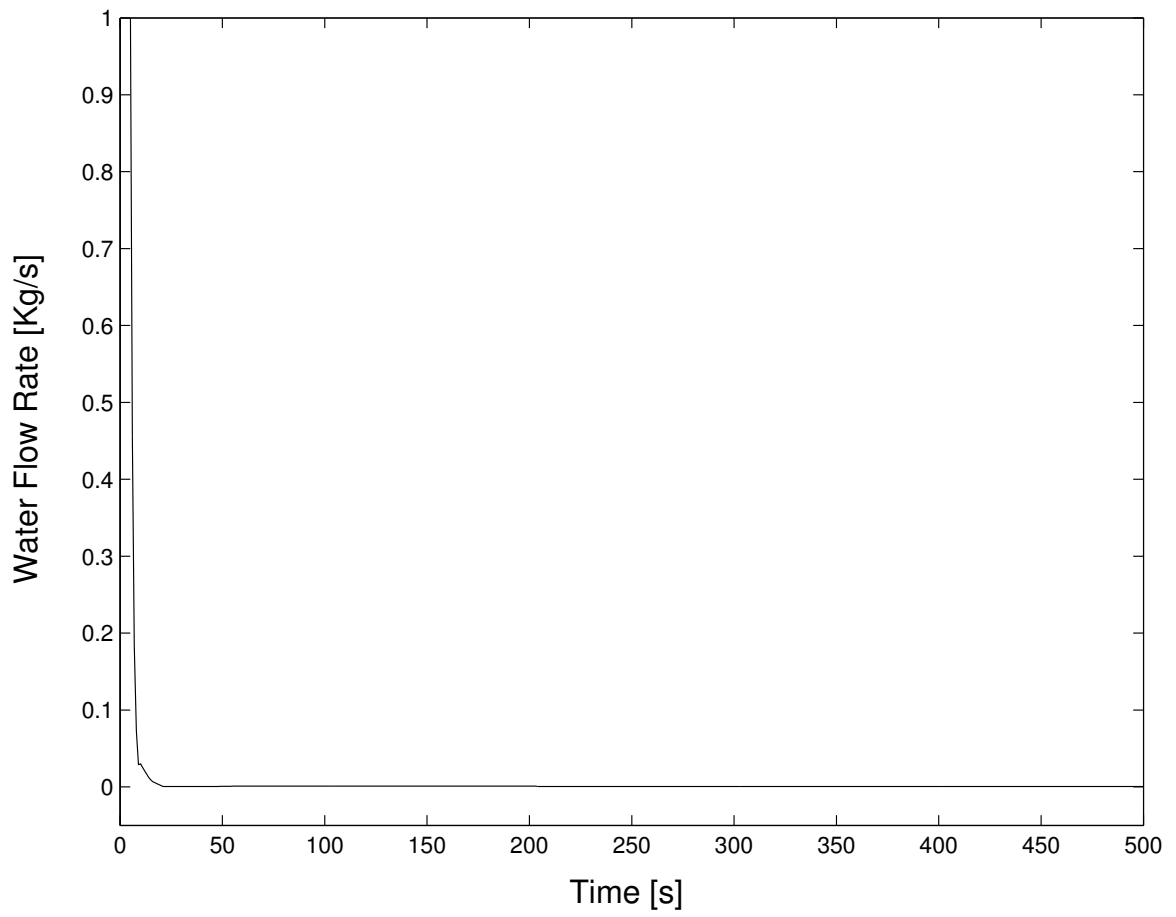


Figure 5.21. Variation of water flow rate with control and disturbance at 200 sec. due to step change in set point from 23°C to 24°C.

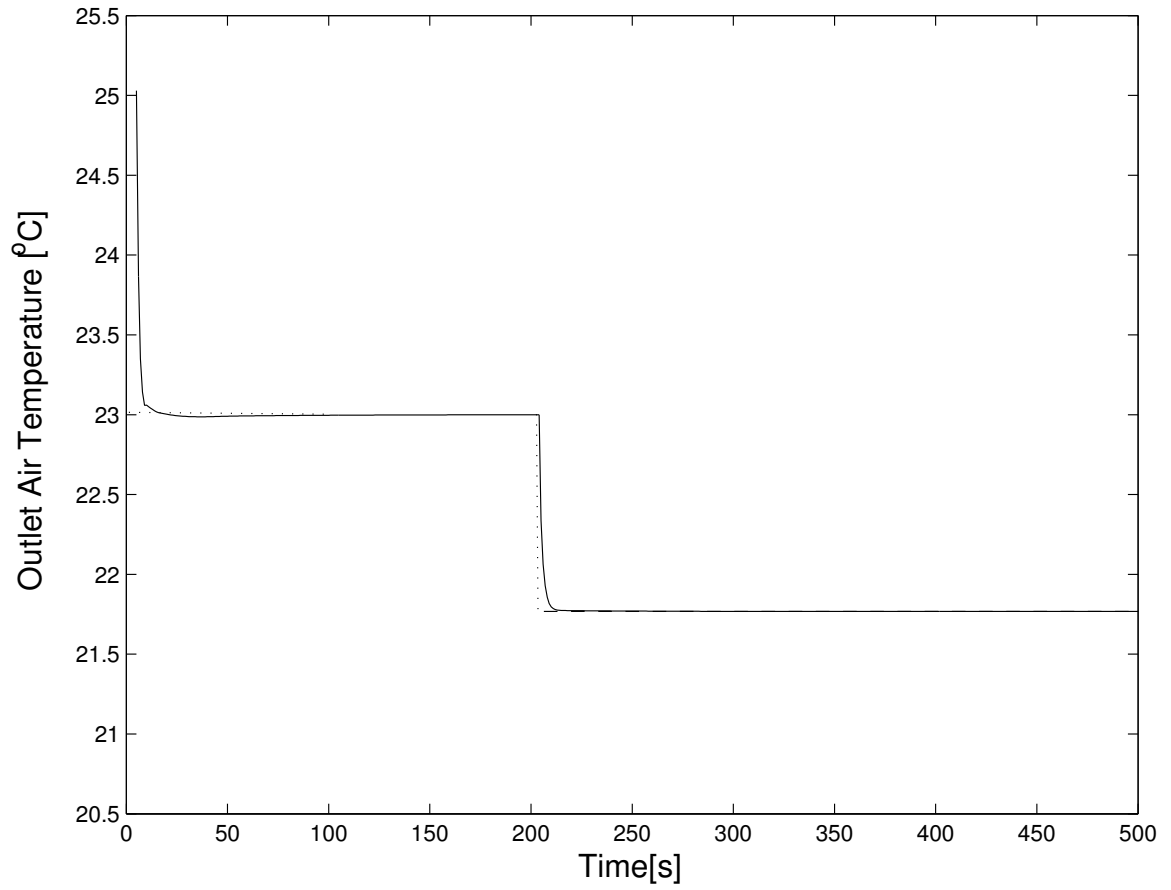


Figure 5.22. Behavior of outlet air temperature with control and disturbance at 200 sec. due to step change in set point from 23°C to 21°C .

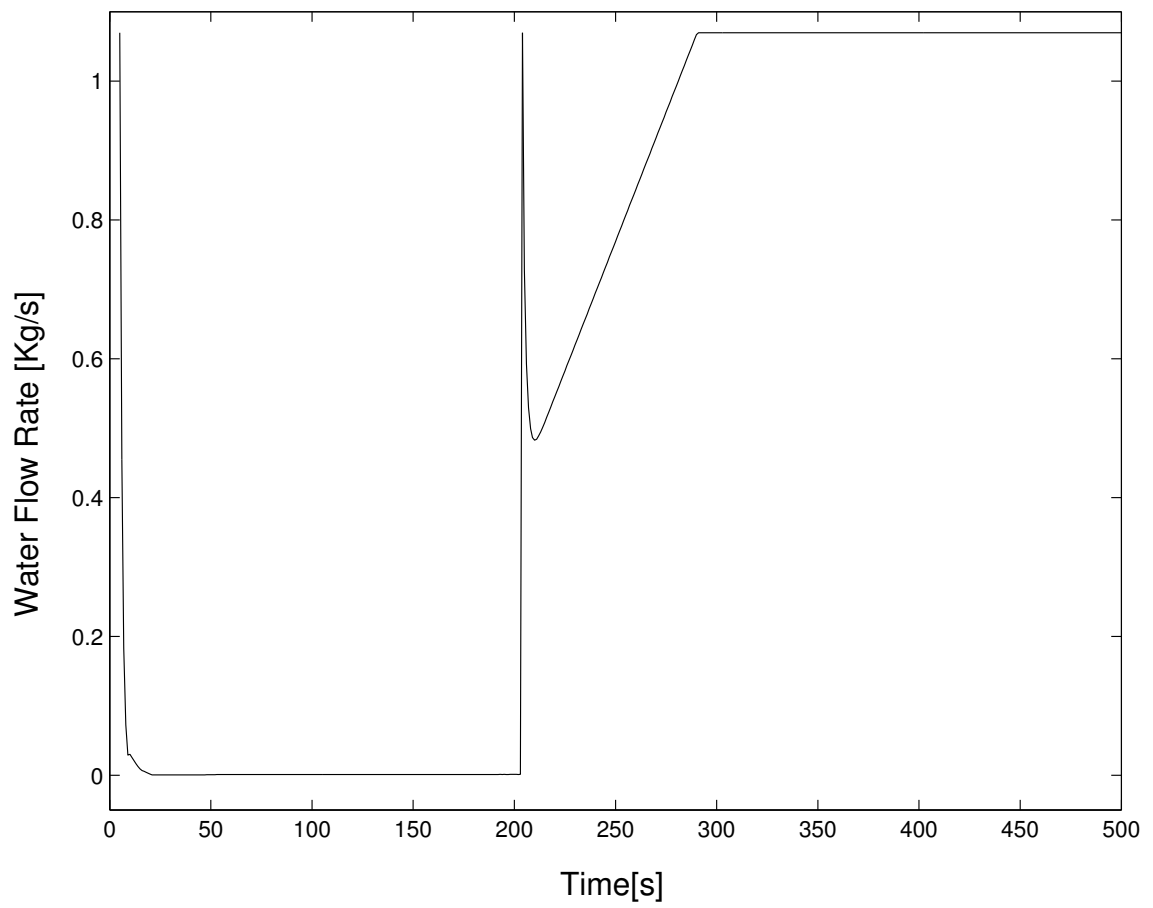


Figure 5.23. Variation of water flow rate with control and disturbance at 200 sec. due to step change in set point from 23°C to 21°C.

5.4 Conclusions

The purpose of this chapter is to develop a mathematical model of cross-flow heat exchangers that can be used for a control. First, a numerical method is developed to simulate the dynamics of the heat exchanger. To develop this model, governing equations have been written for the air side, water side and the tube wall. We have shown that our mathematical model along with the appropriate heat transfer coefficients and the method of finite differences can accurately predict the transient response of the cross-flow heat exchangers. This model was successfully compared with analytical solutions at different physical situations where a analytical solution is possible. Also, this model may be used to study the effects of various cross-flow heat exchangers parameters on the dynamic response of the system.

Second, the performance of PI control of a water-to-air heat exchanger by control of the water flow rate has been examined. The range of control of the air temperature is severely limited by the flow rates achievable. Within these limits the system has a good performance with high temperature and flow rate disturbances on the air side. However, because of limitations due to the water thermal capacity the system becomes very sensitive to small disturbances for low air temperatures and flow rates. For these cases, the outlet air temperature may not achieve the set point value since small disturbances may require the control system to decrease the water flow rate and the air temperature then would take more time to rise to its set value. Therefore, it is desirable to avoid having regions of low water flow rate as an operating point, because of the very low controllability. One possible remedy to improve controllability is to use the highest possible entering cooling water temperature. In general, it is the combined effect of the operating condition, the dynamic behavior, and the sensitivity to disturbances that determine the controllability for these heat exchangers. From the present study, we find that large control efforts are

required for large disturbances. This is not always possible in real situations, when only limited control action is typically available.

CHAPTER 6

FLOW-BASED CONTROL OF TEMPERATURE IN LONG DUCTS

Long heating/cooling ducts are very common. In fact, the cross-flow heat exchanger is a long tube with fins and we may make the tube zig-zag over the face of the heat exchanger so as to make it more compact. Many other applications where flow in long ducts are used can be found. In a long duct the fluid is transported from the site of the actuator to another location where the sensor measures the output of the system. As a result, a delay will occur. This time delay should be taken into account in developing of a model and in designing a control scheme.

For this problem, the effects of delay due to length of the duct have found relatively little place in the literature. Saman and Mahdi [46] analyze the delay in the hot/cold water problem, and Comstock [48] also discusses the delayed hot water problem. Numerical modeling of the thermal behavior of fluid conduit flow with transportation delay has been given in [47]. In general there are many publications on the effect of delay in process engineering; the extensive book by Ogunnaike and Ray [68] provides a nice explanation on the effects of delay in process dynamics and control.

In this chapter we study the effect of delay on the stability of a feedback control loop. We will consider a simple one-dimensional model of heat transfer in a long duct. The objective is to control the outlet fluid temperature by varying the fluid velocity. For the controller, linear and nonlinear stability will be considered. In linear stability, the investigation will be based on applying a small perturbation to the

system followed by analyzing the associated characteristic transcendental equation. For nonlinear analysis the amplitude and the frequency of the controlled temperature are investigated.

6.1 Characteristic solution in duct flow

One of the simplest representations of a heat exchanger is made by considering it as a straight pipe with a flow within it, and which exchanges heat with the surroundings [58, 59, 60]. Usually the flow is driven by a pump located on the pipe. To enable one-dimensional analysis, we make the simplifying assumptions that the flow is laminar, hydrodynamically and thermally fully developed, and that the velocity and temperature are uniform over the cross section of the pipe. The physical properties of the fluid are also constant.

We begin with a model of thermal effects in a duct of circular cross section that is schematically shown in Figure 6.1. The duct is subject to heat loss through its surface. The inlet temperature is $T_{in}(t)$, the velocity of fluid is $v(t)$, and the outlet temperature is $T_{out}(t)$. The duct is subject to heat loss through its surface h , where the local fluid temperature is $T(x, t)$ and the ambient temperature is T_∞ . Thus

$$\frac{\partial T}{\partial t} + v(t) \frac{\partial T}{\partial x} + \gamma (T - T_\infty(t)) = 0, \quad (6.1)$$

where $T(x, t)$ is the fluid temperature, x is the distance along the pipe from the entrance, $\gamma = 4h/D_i\rho c_p$, h is the coefficient for heat transfer to the exterior, c_p is the specific heat at constant pressure of the fluid, and T_∞ is the outside temperature.

Using the method of characteristics, we have the differential equations

$$\begin{aligned} \frac{dt}{ds} &= 1, \\ \frac{dx}{ds} &= v(t), \\ \frac{dT}{ds} &= \gamma(T - T_\infty(t)). \end{aligned} \quad (6.2)$$

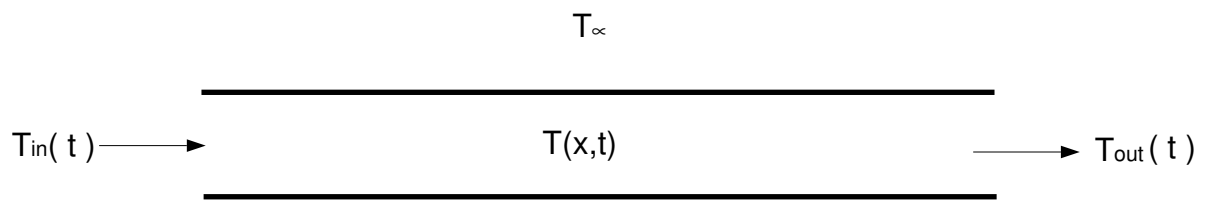


Figure 6.1. Schematic of duct flow.

The first two equations, if put together, give a characteristic ξ in the (x, t) plane, whose slope at time t is

$$\frac{dt}{dx} = \frac{1}{v(t)} \equiv \xi, \quad (6.3)$$

which can be written as

$$x - \int_0^t v(t') dt' = K_1. \quad (6.4)$$

Since $\int_0^t v(t') dt'$ is a function of time, the slope ξ is not constant, i.e. varies with time. The resultant characteristics form a complex wave as shown in Figure 6.2.

Also, from the first and third equations we have

$$dt = \frac{dT}{\gamma T - \gamma T_\infty(t)}, \quad (6.5)$$

which can be solved for T to give

$$T(t) = e^{-\gamma t} \int_0^t e^{\gamma t'} \gamma T_\infty(t') dt' + K_2. \quad (6.6)$$

Now, if we put $f(K_1) = K_2$, the general solution of Equation (6.1) is

$$T(x, t) = \left[f\left[x - \int_0^t v(t') dt'\right] + \gamma \int_0^t e^{\gamma t'} T_\infty(t') dt' \right] e^{-\gamma t}. \quad (6.7)$$

The boundary conditions are $T(0, t) = T_{in}(t)$ and $T(x, 0) = T_0(x)$. Applying the initial condition, the solution for the brief, transient period of time in which the fluid at time $t = 0$ has still not left the duct becomes

$$T(x, t) = T_0\left(x - \int_0^t v(t') dt'\right) e^{-\gamma t} + \gamma e^{-\gamma t} \int_0^t e^{\gamma t'} T_\infty(t') dt' \quad \text{for} \quad \int_0^t v(t') dt' < x. \quad (6.8)$$

The other part of the solution in which $\int_0^t v(t') dt' > x$, which depends on the temperature of the fluid entering at $x = 0$, does not exist analytically if the velocity is a function of time since we need to satisfy

$$T_{in} = \left[f\left[- \int_0^t v(t') dt'\right] + \gamma \int_0^t e^{\gamma t'} T_\infty(t') dt' \right] e^{-\gamma t}. \quad (6.9)$$

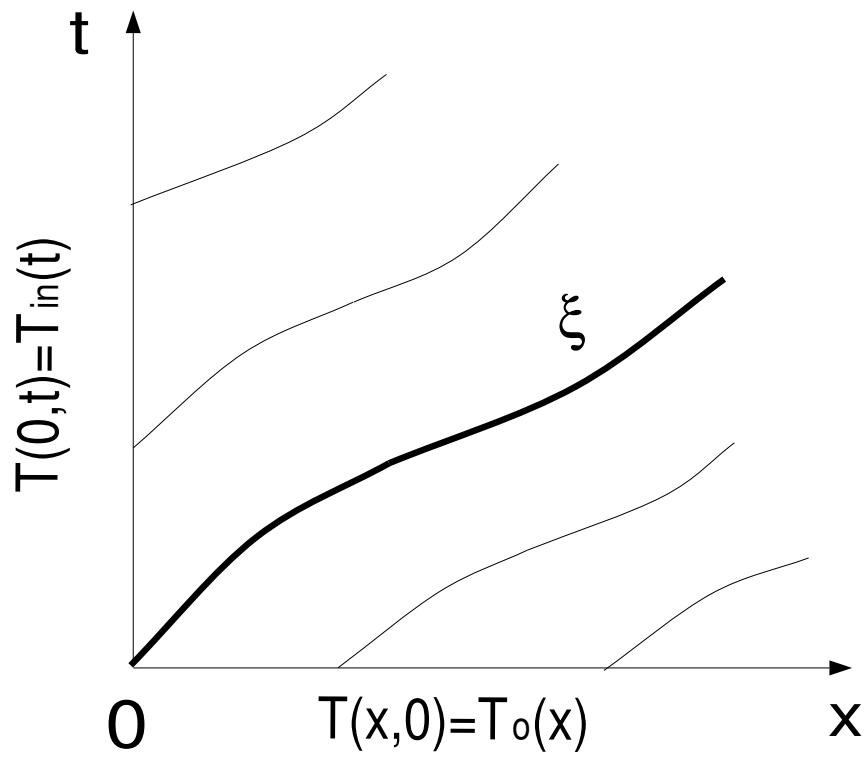


Figure 6.2. Typical characteristic curves.

In Equation (6.9) the boundary condition at the inlet is function of the flow velocity which also function of time. Unless the flow velocity is constant, this boundary condition cannot be satisfied analytically. Also, because it is difficult to get Equation (6.8) into a simple explicit form except for the case of step change in velocity, numerical integration must be used. Therefore, either a numerical integration for this part is performed, or a numerical solution for the original governing Equation (6.1) is needed.

6.2 Governing equations

If the T_∞ is not changing rapidly with time, Equation (6.1) can be written as

$$\frac{\partial T^*}{\partial t^*} + v^* \frac{\partial T^*}{\partial x^*} + \frac{4h}{\rho c D} (T^* - T_\infty^*) = 0, \quad (6.10)$$

where $T^*(x^*, t^*)$ is the fluid temperature, t^* is time, x^* is the distance along the duct measured from the entrance, $v^*(t^*)$ is the flow velocity, h is the coefficient of heat transfer to the exterior, c is the specific heat at constant pressure of the fluid, and D is the diameter of the duct. The inlet temperature, T_{in}^* , and the outside temperature, T_∞^* , are assumed to be constant. The objective is to control the temperature of the fluid coming out of the duct, $T_{out}(t^*)$.

To solve this equation, we nondimensionalized the governing equation Equation (6.10). Using the following nondimensional parameters

$$x = x^*/L,$$

$$T = (T^* - T_\infty^*)/(T_{in}^* - T_\infty^*),$$

$$t = t^*4h/\rho c D,$$

and

$$v = v^* \rho c D / h L,$$

where L is the length of the duct, Equation (6.10) becomes

$$\frac{\partial T}{\partial t} + v \frac{\partial T}{\partial x} + T = 0. \quad (6.11)$$

Ignoring the initial startup period of time in which the fluid within the duct is flushed out, the general solution of this equation is

$$T(x, t) = e^{-t} f \left(x - \int_0^t v(s) ds \right), \quad (6.12)$$

where f is an arbitrary function.

The boundary condition $T^*(0, t^*) = T_{in}^*$ becomes $T(0, t) = 1$, so that

$$1 = e^{-t} f \left(- \int_0^t v(s) ds \right). \quad (6.13)$$

In general, Equations (6.12) and (6.13) cannot be reduced to a single equation since f is an implicit function of t and cannot be inverted. Numerical integration must be used.

The temperature at the outlet of the duct is

$$\begin{aligned} T_{out}(t) &= T(1, t) \\ &= e^{-t} f \left(1 - \int_0^t v(s) ds \right). \end{aligned} \quad (6.14)$$

Since T_{out} is a function of t alone, we can write

$$T_{out}(t) = e^{-\tau(t)}, \quad (6.15)$$

where $\tau(t)$ will be given a physical meaning later. Thus we can write

$$f \left(1 - \int_0^t v(s) ds \right) = e^{t-\tau}, \quad (6.16)$$

from which

$$1 - \int_0^t v(s) ds = g(e^{t-\tau}). \quad (6.17)$$

On the other hand, from Equation (6.13) we get

$$- \int_0^t v(s) ds = g(e^t). \quad (6.18)$$

The difference is

$$\begin{aligned} 1 &= g(e^{t-\tau}) - g(e^t) \\ &= - \int_0^{t-\tau} v(s) ds + \int_0^t v(s) ds \\ &= \int_{t-\tau}^t v(s) ds. \end{aligned} \quad (6.19)$$

To get a physical meaning of the variable $\tau(t)$ we consider a Lagrangian description of the flow. The residence time is the time taken for a fluid particle to travel the length of the duct from inlet to outlet, which in general is a function of t . The fluid exiting the duct at time t was within the duct from $t - \tau$ to the present t so that the residence time for this fluid particle is defined by Equation (6.19). Furthermore, the Lagrangian version of Equation (6.11) is

$$\frac{DT}{Dt} + T = 0, \quad (6.20)$$

where D/Dt is the derivative following the fluid that can be integrated for this time period to give Equation (6.15).

For a given $v(t)$, Equations (6.15) and (6.19) are to be solved together to get $T_{out}(t)$ and $\tau(t)$. However, in a control problem in which $v(t)$ is the manipulated variable, it is unknown and one needs an additional control equation that governs the control process. It must be pointed out also that in that case, Equation (6.11) is nonlinear and Equation (6.19) has a dependent variable $\tau(t)$ in one of the limits.

6.3 Numerical solution

Two different approaches will be used for the numerical simulation of this problem. The first will be based on a finite-difference approximation of the Eulerian governing

equation Equation (6.11), and the second approach an implicit iterative scheme based on the Lagrangian version of the governing equation Equation (6.20).

6.3.1 Eulerian

The partial differential Equation (6.11) is discretized in space and time. The upwind finite difference scheme for $v > 0$ is

$$T_i^{j+1} = (1 + \Delta t - \varepsilon)T_i^j + \varepsilon T_{i-1}^j, \quad (6.21)$$

where the subscripts denote discretization points in space and superscripts in time, $\varepsilon = v(t)\Delta t/\Delta x$, Δt is the time step, and Δx is the spatial grid size. Since v is always positive, the CFL (Courant, Friedrichs, and Lewy) condition for stability of the numerical scheme is [33]

$$0 \leq \Delta t \leq \frac{\Delta x}{\max |v(t)|}. \quad (6.22)$$

We assume that the duct to be initially at $T = 1$, so that the boundary and initial conditions are $T(0, t) = T(0, t) = 1$.

6.3.2 Lagrangian

In the previous section we considered the Eulerian version of the governing equation. In that equation we considered the changes occur at a fixed control volume in the fluid, so we have to take into account the changes in this control volume.

In this section we consider the Lagrangian version of the governing equation. In this case we have a moving control volume, so we consider changes which occur as we follow a fluid particle, i.e. along a trajectory.

The duct has been discretized in space and time, so that on following a fluid particle, the solution of Equation (6.20) gives

$$T_i^j = T_{i-1}^{j-1} \exp(-\Delta t^j). \quad (6.23)$$

We fix Δx , but Δt^j at each time step is determined from

$$\Delta t^j = \frac{\Delta x}{v}. \quad (6.24)$$

If v is known or $v = v^{j-1}$, then the calculation is explicit. If $v = v^j$, it is fully implicit and iterations are used until there is convergence in v . The correct time step will then be used to calculate the temperature at the outlet T_N^j . A flowchart that describes this procedure is shown in Figure 6.3.

6.3.3 Model validation

Two computer programs were written to test the validity of the above two mathematical models. First, the convergence of each method is studied for a specific case. Second, the two methods are compared with each other for the same case. We are specifically interested in the dynamic behavior of the outlet temperature, $T(1, t)$. For the set of nondimensional parameters, $T_{in}(0, t) = 1$, $T_o(L, 0) = 1$, and $L = 1$ we choose to have a step change in the fluid velocity from 0.5 to 2 at time equal 1. To analyze numerical convergence we refine the spatial discretization and compare the result. Different number of discretizations have been used. The convergence of the Eulerian and Lagrangian methods for this case is shown in Figures 6.4 and 6.5 respectively. In Figure 6.6 we compare the two methods together. It is worth mentioning that in the Lagrangian method we are indeed using the exact solution to compute the particle temperature as it moves. Thus, the Lagrangian method gives more accurate results than the Eulerian method. Analytical solution of the temperature can be found if the velocity is constant. For this case the initial velocity and temperature are 0.5 and 1 respectively. The outlet temperature can be calculated, and the final temperature is the initial temperature for the second part where the velocity changed from 0.5 to 2 at time equal to 1. The results of the analytical solution and the Lagrangian are exactly the same.

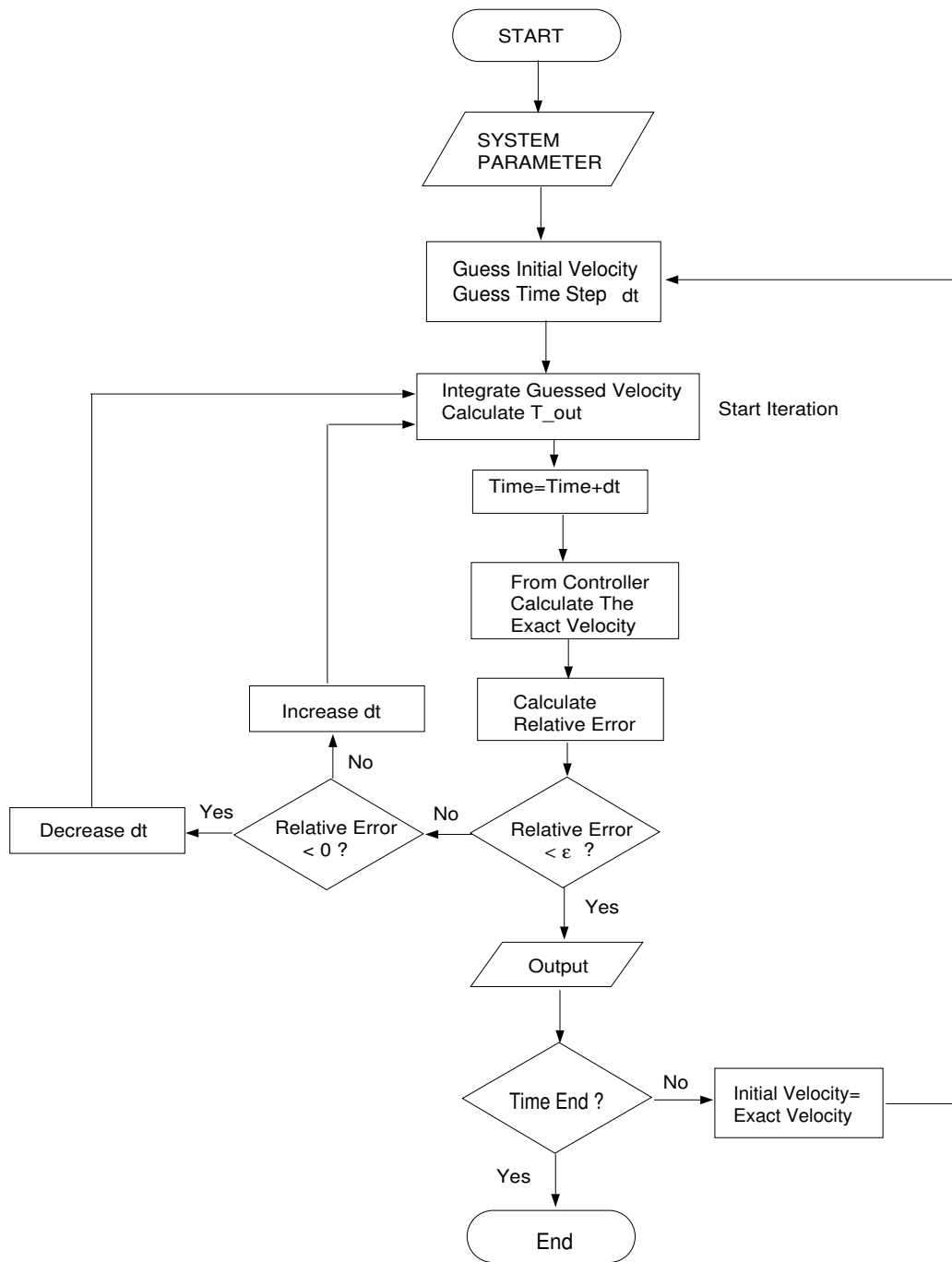


Figure 6.3. Flow chart of implicit iterative scheme.

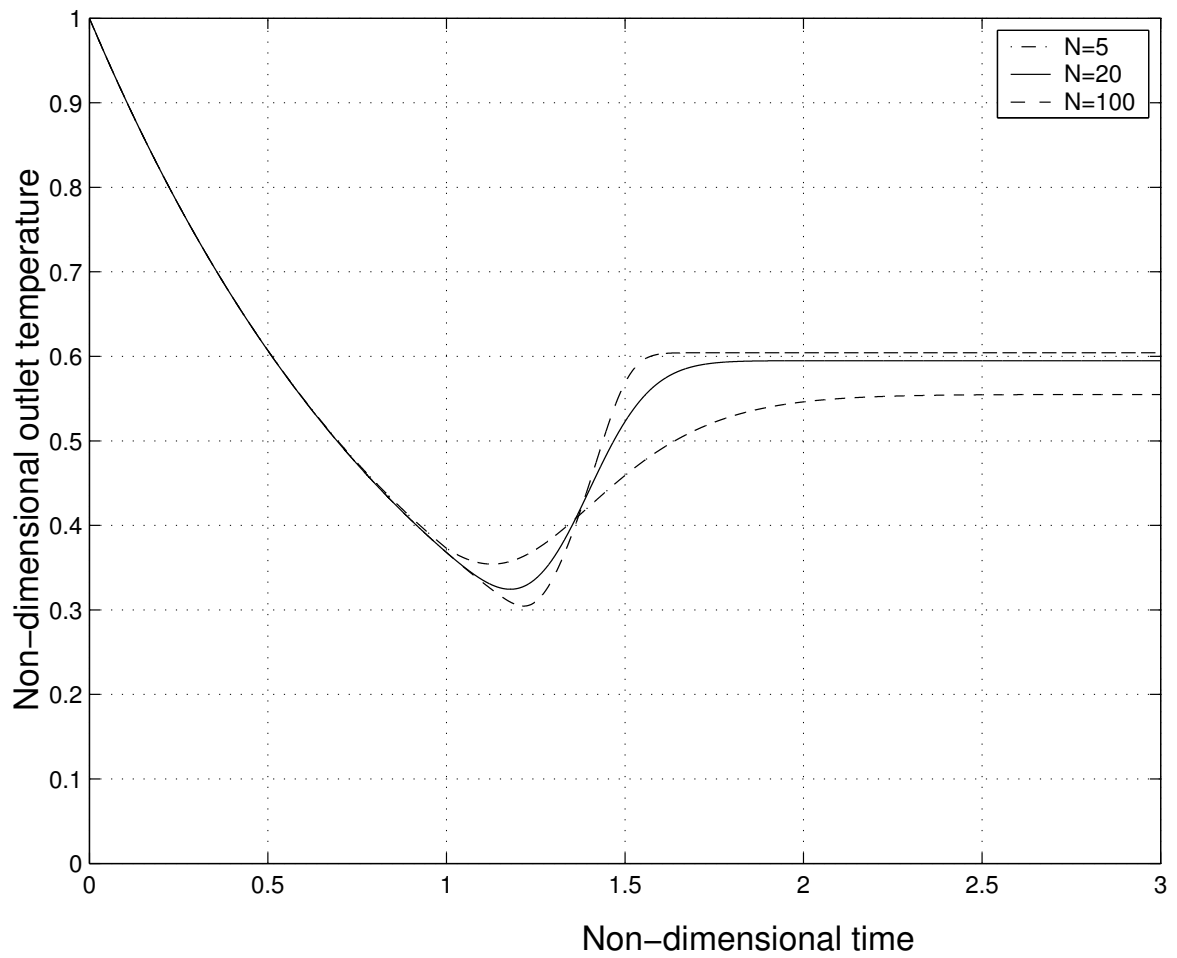


Figure 6.4. Convergence of Eulerian solution.

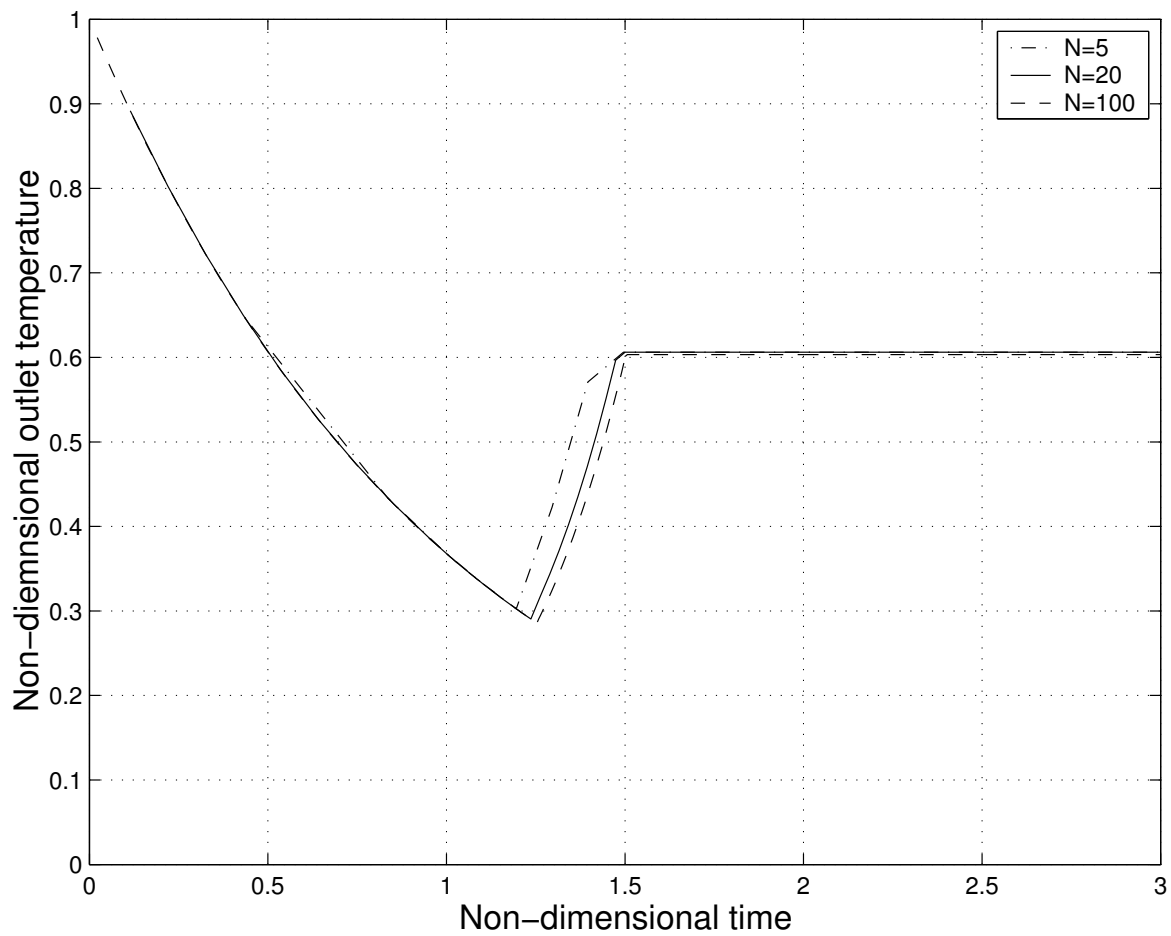


Figure 6.5. Convergence of Lagrangian solution.

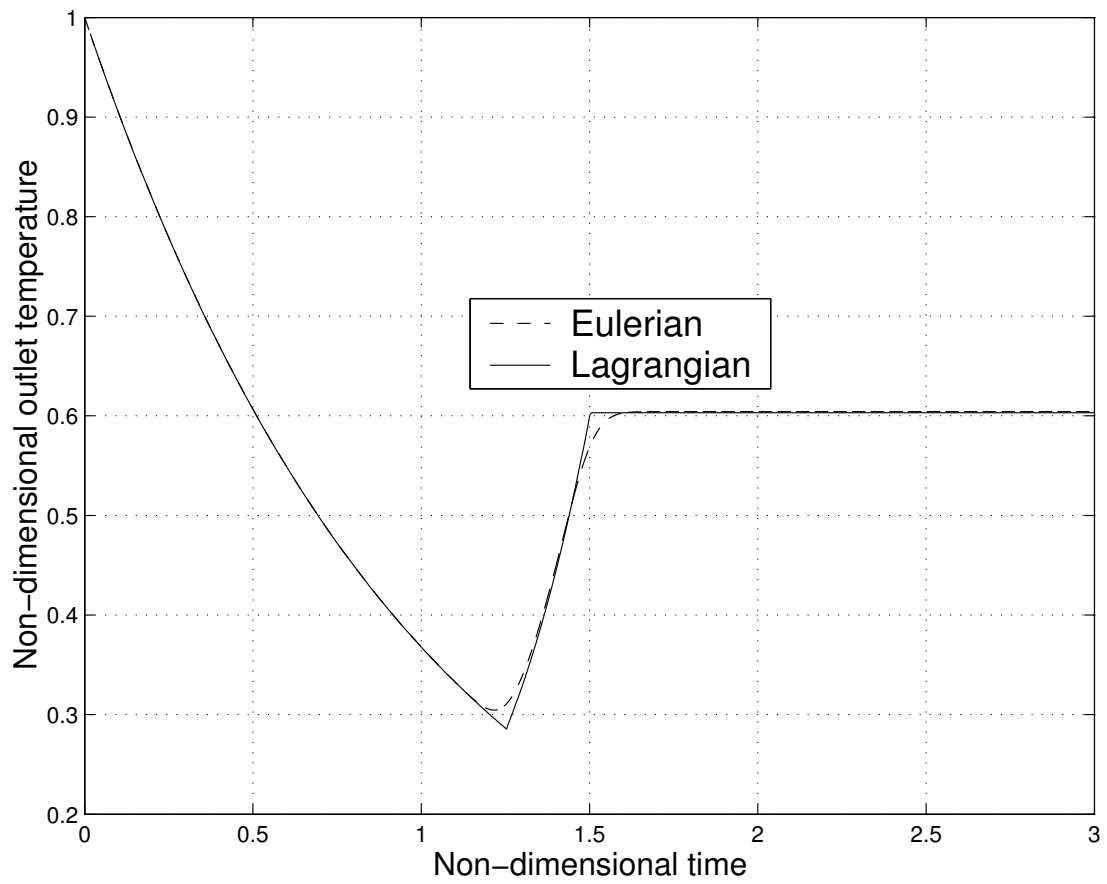


Figure 6.6. Comparison of outlet temperature between Eulerian and Lagrangian methods.

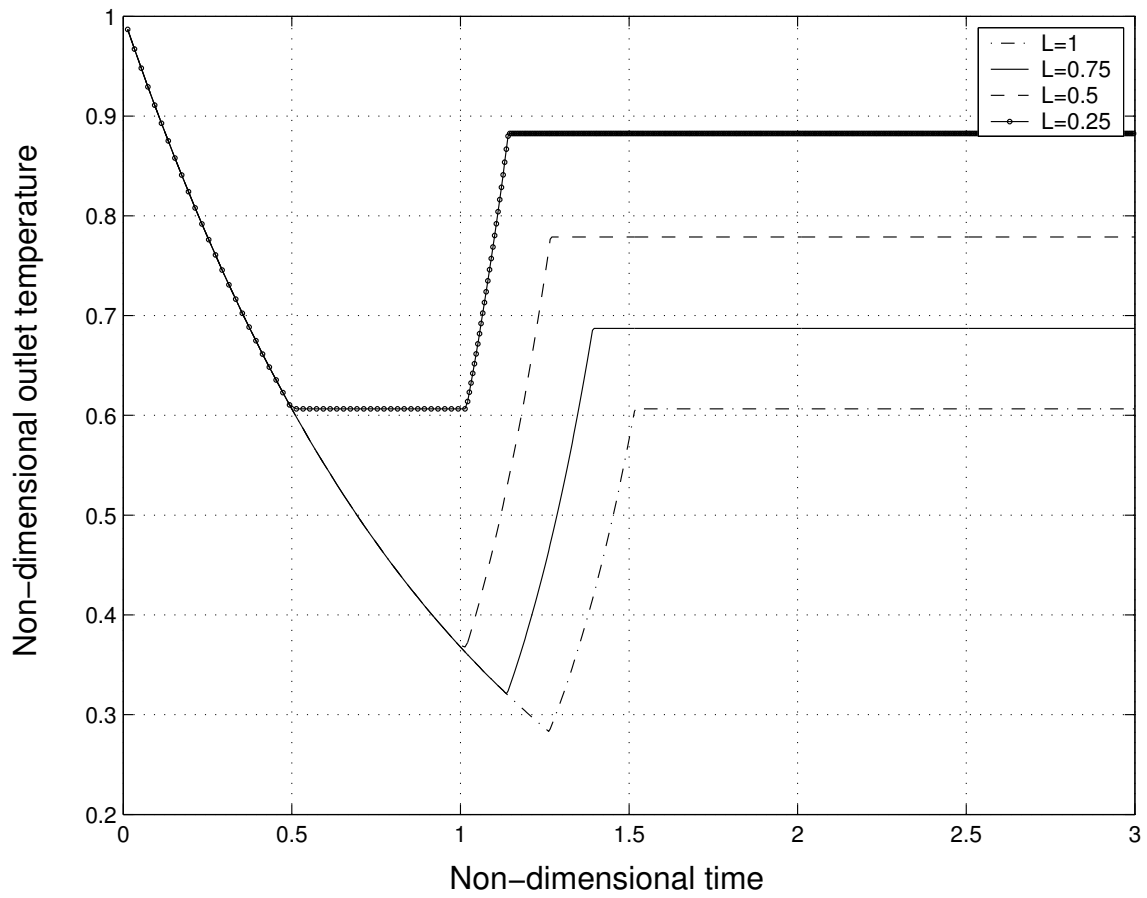


Figure 6.7. Behavior of temperature with time at different locations in duct.

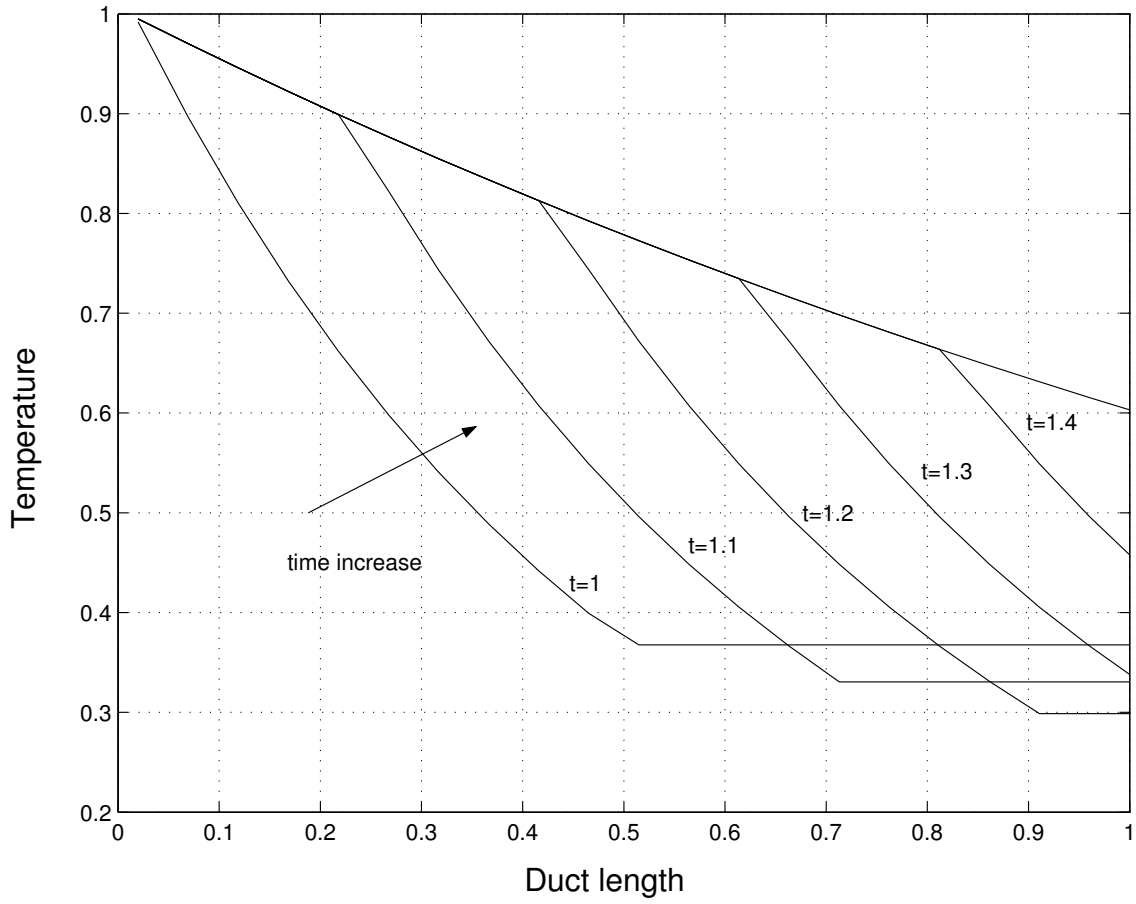


Figure 6.8. Behavior of temperature along duct at different times.

To insure the accuracy of the numerical results, further simulation was performed. Using the Lagrangian solution, the behavior of the temperatures along the duct is tested. Figure 6.7 shows the temperature at different locations in the duct with time. Figure 6.8 presents the temperature along the duct at different times. An agreement between these figures can be found which lends additional support to the accuracy of the above numerical simulation.

6.4 Outlet temperature control

The Lagrangian method developed in the previous section will be used now to simulate the dynamic behavior of the flow. The objective is assumed to be the control of the outlet temperature, T_{out} , by manipulating the velocity v while keeping constant the inlet and surrounding temperatures. Since $0 \leq \tau < \infty$, from Equation (6.15) we find that $0 < T_{out}(t) < 1$. This means that only this range of values of the outlet temperature can be reached by varying the flow velocity, and that it is controllable only within this range.

We begin with the system in the steady state that we want to be at, with the corresponding variables being indicated by overbars. Thus for $v = \bar{v}$, $\tau = \bar{\tau}$ and $T_{out} = \bar{T}_{out}$ in the steady state. From Equations (6.15) and (6.19) these variables are related by

$$\begin{aligned}\bar{T}_{out} &= e^{-\bar{\tau}}, \\ \bar{v} \bar{\tau} &= 1.\end{aligned}$$

We would like to maintain \bar{T}_{out} as the desired outlet temperature in spite of any disturbances by manipulating $v(t)$. To do this many different strategies can be used, but we will employ the commonly used PI control. In this case the flow velocity is related to the error signal $T_{out}(t) - \bar{T}_{out}$ by

$$v(t) = K_p(T_{out}(t) - \bar{T}_{out}) + K_i \int_0^t (T_{out}(s) - \bar{T}_{out}) ds, \quad (6.25)$$

the differential form of which is

$$\frac{dv}{dt} = K_p \frac{dT_{out}}{dt} + K_i (T_{out}(t) - \bar{T}_{out}). \quad (6.26)$$

For numerical purposes the target temperature was set at $\bar{T}_{out} = e^{-1}$.

6.5 Linear stability

The linear stability of this control system can be analyzed by applying small perturbations to the system and hoping the fluctuations will vanish or remain small for all time $t > 0$. Generally, the behavior of these fluctuations is related to the eigenvalues of the associated characteristic equation.

Applying small perturbations of the form $T_{out}(t) = \bar{T}_{out} + T'_{out}(t)$, $\tau(t) = \bar{\tau} + \tau'(t)$ and $v(t) = \bar{v} + v'(t)$, and substituting in Equation (6.15), we get

$$\bar{T}_{out} + T'_{out}(t) = e^{-\bar{\tau} - \tau'}. \quad (6.27)$$

Expanding $e^{-\tau'}$, neglecting the small terms, and subtracting out the steady states, we will have

$$T'_{out}(t) + e^{-\bar{\tau}} \tau' = 0. \quad (6.28)$$

Similarly, substituting the small perturbations in Equation (6.19), we get

$$\begin{aligned} 1 &= \int_{t-\bar{\tau}-\tau'}^t (\bar{v} + v'(s)) ds \\ &= \int_{t-\bar{\tau}-\tau'}^{t-\bar{\tau}} (\bar{v} + v'(s)) ds + \int_{t-\bar{\tau}}^t (\bar{v} + v'(s)) ds. \end{aligned} \quad (6.29)$$

Neglecting the small terms, and subtracting out the steady states, we will have the following perturbation equation

$$\int_{t-\bar{\tau}}^t v'(s) ds + \bar{v} \tau'(t) = 0. \quad (6.30)$$

From this we can write

$$\frac{d\tau'}{dt} = \frac{-1}{\bar{v}} \left(v'(t) - v'(t - \bar{\tau}) \right), \quad (6.31)$$

and from Equation (6.28) we have

$$\frac{dT'_{out}}{dt} = -e^{-\bar{\tau}} \frac{d\tau'}{dt}. \quad (6.32)$$

Now, from the control equation Equation (6.26) and the above we can show that

$$\begin{aligned} \frac{dv'}{dt} &= -e^{-\bar{\tau}} \left(K_p \frac{d\tau'}{dt} + K_i \tau' \right) \\ &= \frac{K_p e^{-\bar{\tau}}}{\bar{v}} \left(v'(t) - v'(t - \bar{\tau}) \right) + \frac{e^{-\bar{\tau}}}{\bar{v}} K_i \int_{t-\bar{\tau}}^t v'(s) ds. \end{aligned} \quad (6.33)$$

If we assume that the perturbation can be written in the form $v' = \widehat{v}e^{\sigma t}$, where v' is the amplitude of the perturbation, and σ is the growth rate, we get a transcendental equation $F(\sigma) = 0$ for the eigenvalue σ where

$$F(\sigma) = \sigma - \bar{\tau} e^{-\bar{\tau}} \left(K_p + \frac{K_i}{\sigma} \right) (1 - e^{-\sigma \bar{\tau}}) = 0. \quad (6.34)$$

The linear stability is a function of the system parameter $\bar{\tau}$ and the control parameters K_p and K_i . The real part of σ should be negative for linear stability; that is, the above perturbation must exponentially vanish in time. Thus, all the eigenvalues must be located in the left-hand side of the complex plane. Since Equation (6.34) is transcendental, it may have an infinite number of roots, some real and some complex, and it is difficult to find them explicitly. Thus we will look at three different typical cases that we can study.

6.5.1 $\bar{\tau} \ll 1$

For small residence times, the exponentials in Equation (6.34) can be expanded to give

$$\sigma = -2 - \frac{K_i}{K_p} - \frac{2}{K_p \bar{\tau}^3} + \frac{2}{\bar{\tau}} - K_i \bar{\tau}^2 + K_i \bar{\tau}^3 + O(\bar{\tau}^4). \quad (6.35)$$

σ is real, and the control system is stable only if $(K_i \bar{\tau}^3 + 2)/K_p > 2(\bar{\tau}^2 - \bar{\tau}^3)$. This is shown in Figure 6.9 for two different small delays. We can see that the range of stability increases as the delay decreases. When there is no delay, the stability

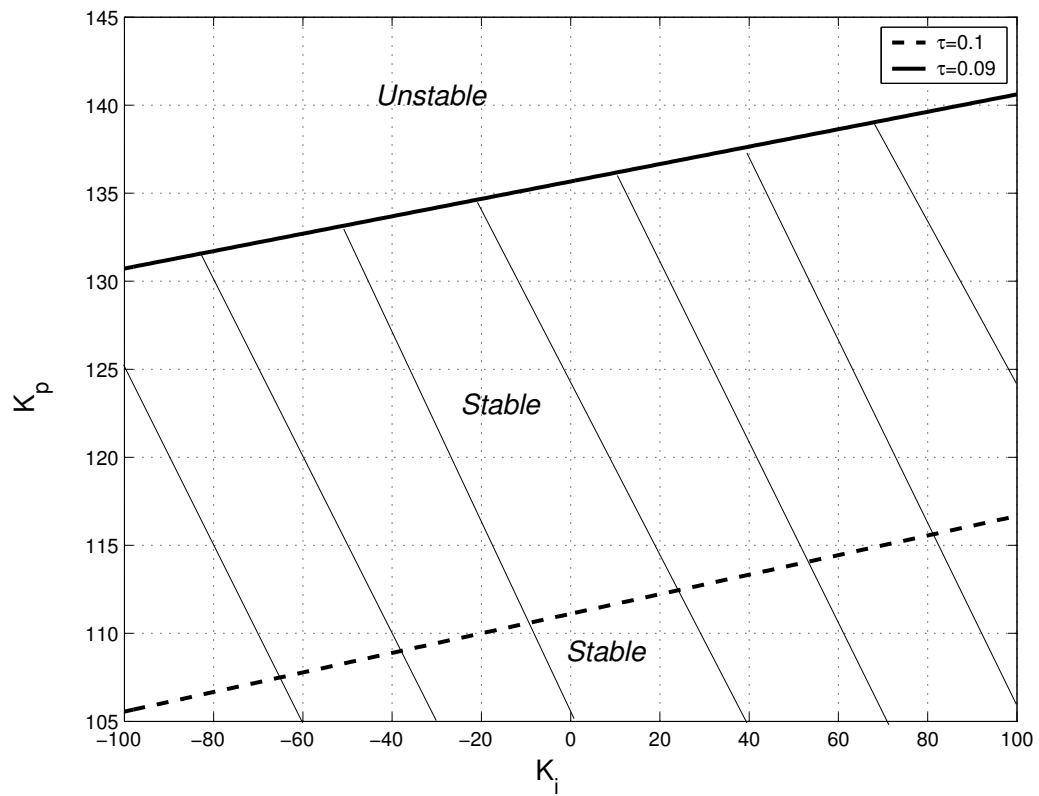


Figure 6.9. Stability regions for $\bar{\tau} \ll 1$; $(K_i \bar{\tau}^3 + 2)/K_p^{cr} > 2(\bar{\tau}^2 - \bar{\tau}^3)$.

region will cover the entire K_p vs. K_i region. In this case the system is stable; this is also clear from Equation (6.34). It should be noted that this is a singular perturbation problem since $\bar{\tau} = 0$ in Equation 6.34 does not give the same result as $\bar{\tau} \rightarrow 0$.

6.5.2 $\bar{\tau} = O(1)$

For a delay of order 1, depending on the control gains K_i and K_p , the transcendental equation may have real and complex roots. In each quarter of the K_p vs. K_i map we will look at the stability of the system.

(a) $K_i > 0, K_p > 0$

Assume σ is real, then Equation (6.34) can be written as

$$(AK_p\sigma + AK_i)e^{-\sigma\bar{\tau}} = -\sigma^2 + (AK_p\sigma + AK_i).$$

Then

$$e^{-\sigma\bar{\tau}} = 1 - \frac{\sigma^2}{\bar{\tau}e^{-\bar{\tau}}(K_p\sigma + K_i)}. \quad (6.37)$$

The graph of $F(\sigma)$ shows that there are real roots, as shown in Figure 6.13. But Equation (6.37) indicates that these roots must be positive. Thus the system is unstable.

(b) $K_i < 0, K_p < 0$

The graph indicates the presence of real roots, but Equation (6.37) shows that a positive real root is not possible. This does not assure stability since additional roots may be complex. Therefore, for stability either these complex roots lie on the left half plane or they do not exist. To check this, we may use Pontryagin's [52] results on the zeros of exponential polynomials. In order to use this result, the order of $e^{-\sigma\bar{\tau}}$ and σ in Equation (6.34) should be greater than zero. Therefore, instead of

$F(\sigma)$ in Equation (6.34) we have $F^*(\sigma) = \sigma F(\sigma)e^{\sigma\bar{\tau}}$, to get

$$F^*(\sigma) = (\sigma^2 - \bar{\tau}e^{-\bar{\tau}}K_p\sigma - \bar{\tau}e^{-\bar{\tau}}K_i)e^{\sigma\bar{\tau}} + \bar{\tau}e^{-\bar{\tau}}(K_p\sigma + K_i) = 0. \quad (6.38)$$

This transformation will only change the roots of the system by adding one extra root at the origin. Thus, the stability of this equation will be equivalent to the one in Equation (6.34). So, according to Pontryagin's results we have a nonzero principal term, i.e. the term with the highest power of σ and e^σ . The following theorem gives necessary and sufficient condition for stability.

Theorem A: *Let $F^*(\sigma)$ be written as $F^*(i\omega) = F_r(\omega) + iF_i(\omega)$, where $F_r(\omega)$ and $F_i(\omega)$ represent, respectively, the real and imaginary parts of $F^*(i\omega)$. Then, $F^*(\sigma)$ has roots in the negative half of the complex plane if and only if the following two conditions are satisfied: (i) $F_r(\omega)$ and $F_i(\omega)$ have only simple real roots and these interlace. (ii) $F_i'(\omega)F_r(\omega) - F_i(\omega)F_r'(\omega) > 0$, for some ω in $(-\infty, \infty)$, where the primes denote the first derivative with respect to ω .*

In order to apply this theorem, we must ensure first that $F_r(\omega)$ and $F_i(\omega)$ have only real roots. This property can be ensured by using the following theorem [52].

Theorem B:

Let M and N denote the highest power of σ and e^σ , respectively, in $F^(\sigma)$, and ϵ be an appropriate constant such that the coefficient of terms of highest degree in $F_r(\sigma)$ and $F_i(\sigma)$ do not vanish at $\omega = \epsilon$. Then for the equations $F_r(\omega) = 0$ and $F_i(\omega) = 0$ to have only real roots, it is necessary and sufficient that in the interval $-2k\pi + \epsilon \leq \sigma \leq 2k\pi + \epsilon$, $F_r(\omega) = 0$ and $F_i(\omega) = 0$ have exactly $4kN + M$ real roots starting with a sufficiently large k .*

First we show that $F_r(\omega)$ and $F_i(\omega)$ satisfies condition **A**(i). From Equation (6.38) since we multiplied by σ , we introduce one extra root at the origin, and this

root must be subtracted from the total number of roots required in any interval by the above theorem. Therefore, we have $N = 1$ and $M = 1$.

Substituting $\sigma = i\omega$ in Equation (6.38), we have

$$\begin{aligned} F_r(\omega) &= -\cos(\omega\bar{\tau})(\omega^2 + \bar{\tau}e^{-\bar{\tau}}K_i) + \bar{\tau}e^{-\bar{\tau}}K_p\omega \sin(\omega\bar{\tau}) + \bar{\tau}e^{-\bar{\tau}}K_i \\ F_i(\omega) &= -\sin(\omega\bar{\tau})(\omega^2 + \bar{\tau}e^{-\bar{\tau}}K_i) - \bar{\tau}e^{-\bar{\tau}}K_p\omega \cos(\omega\bar{\tau}) + \bar{\tau}e^{-\bar{\tau}}K_p\omega, \end{aligned} \quad (6.39)$$

where the principal terms are $-\omega^2 \cos \omega$ and $-\omega^2 \sin \omega$ respectively. With change of variables $z = \omega\bar{\tau}$ the above equations can be written as

$$\begin{aligned} F_r(z) &= -\frac{z}{\bar{\tau}} \cos z \left(\frac{z}{\bar{\tau}} + \frac{\bar{\tau}^2}{z} e^{-\bar{\tau}} K_i \right) + e^{-\bar{\tau}} K_p z \sin z + \bar{\tau} e^{-\bar{\tau}} K_i, \\ F_i(z) &= -\frac{z}{\bar{\tau}} \sin z \left(\frac{z}{\bar{\tau}} + \frac{\bar{\tau}^2}{z} e^{-\bar{\tau}} K_i \right) - e^{-\bar{\tau}} K_p z \cos z + z e^{-\bar{\tau}} K_p. \end{aligned} \quad (6.40)$$

Next we choose $\epsilon = \pi/4$ so that the principal terms do not vanish at ϵ . If we take $k = 1$, then $F_r(z)$ and $F_i(z)$ have five roots in the interval $(-2\pi + \pi/4, 2\pi + \pi/4)$ if we exclude one at $z = 0$. If we increase k from 1 to 2, then the total number of real zeros in the interval $(-4\pi + \pi/4, 4\pi + \pi/4)$ increases by 4 and hence become 9. Similarly, the total number of real zeros continues to increase by 4 as k increases by 1. Therefore, $F_r(z)$ and $F_i(z)$ have the appropriate number of real zeros as required, and hence $F_r(z)$ and $F_i(z)$ have only real roots. From Figure 6.10 and Figure 6.11 we can see the two functions in the above two intervals. In addition, the interlacing properties for $F_r(z)$ and $F_i(z)$ roots are clear from these figures. Next we need to check the inequality in Theorem **A** condition (ii). Simple computation shows that this condition is also satisfied for all z except the origin. This result can be seen in Figure 6.12. Similar results were also obtained for other values of $K_i < 0$ and $K_p < 0$. The two conditions of theorem **A** are now satisfied. Hence we can conclude that the system is stable for some K_i and $K_p < 0$. The stability region in this case is found based on the above theorems.

(c) $K_i > 0, K_p < 0$

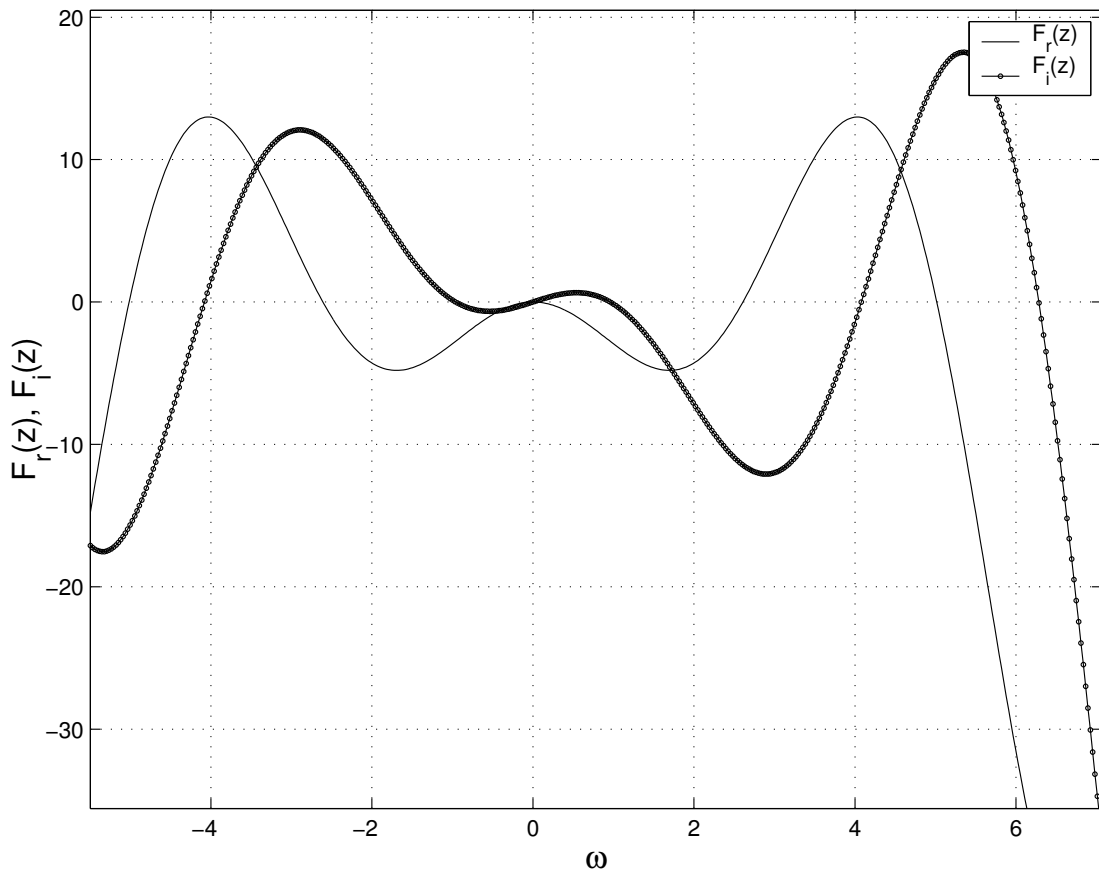


Figure 6.10. $F_r(\omega)$ and $F_i(\omega)$ for $k = 1, -2\pi + \pi/4 < \omega < 2\pi + \pi/4$.

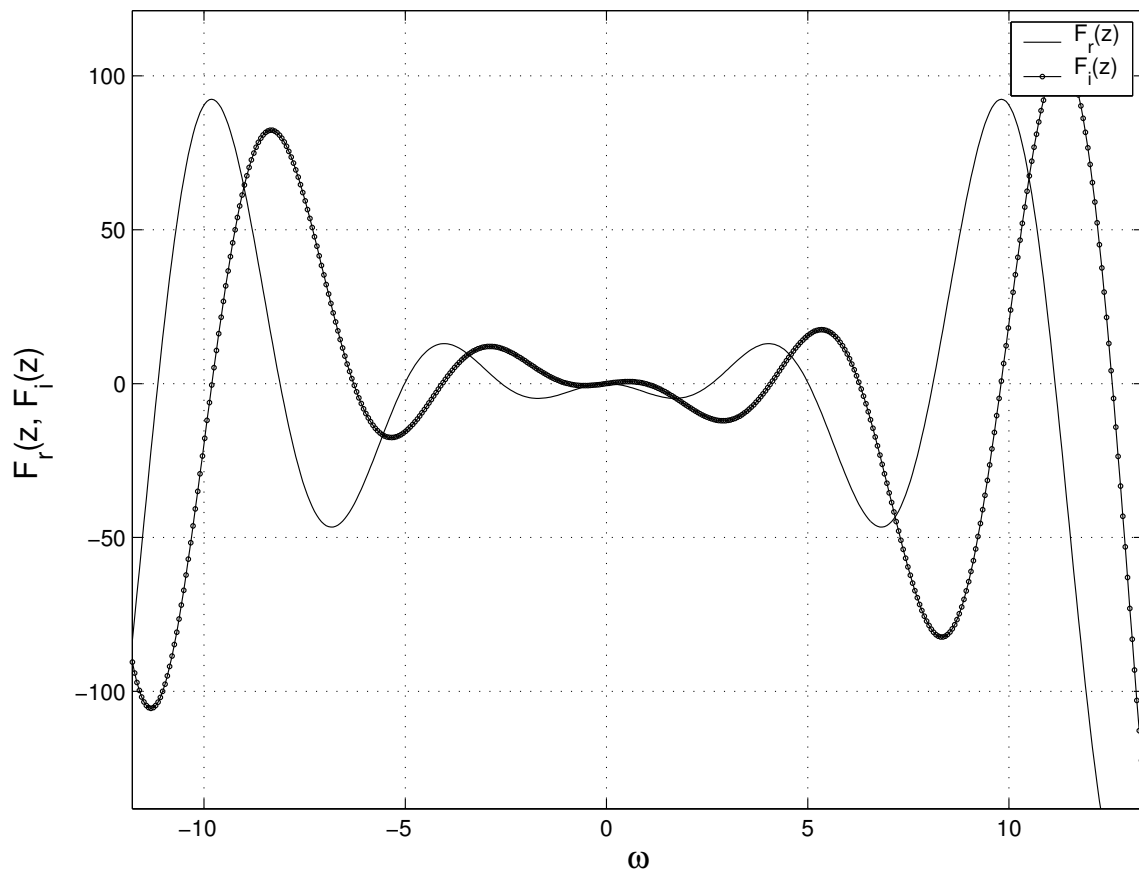


Figure 6.11. $F_r(\omega)$ and $F_i(\omega)$ for $k = 2$, $-4\pi + \pi/4 < \omega < 4\pi + \pi/4$.

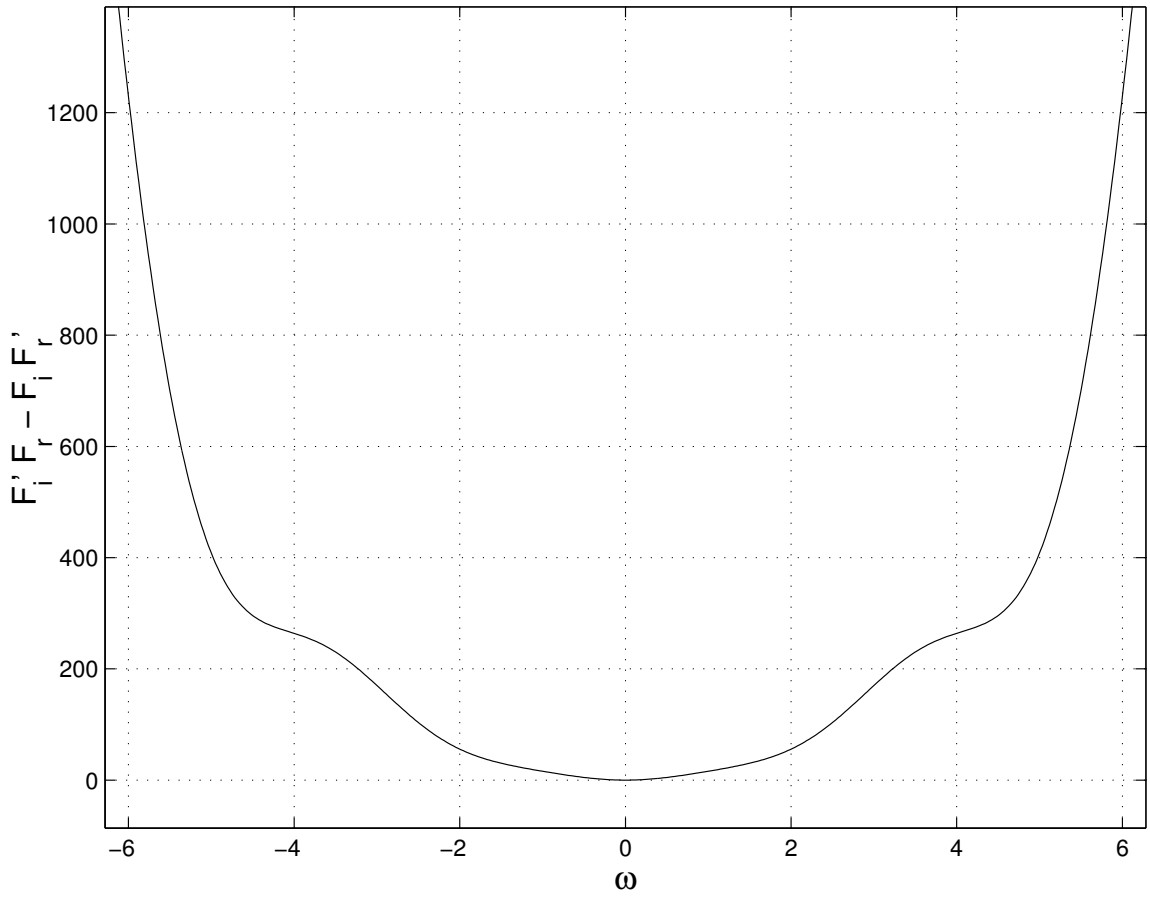


Figure 6.12. Condition (ii) in theorem A. $F'_i(\omega)F_r(\omega) - F_i(\omega)F'_r(\omega) > 0$.

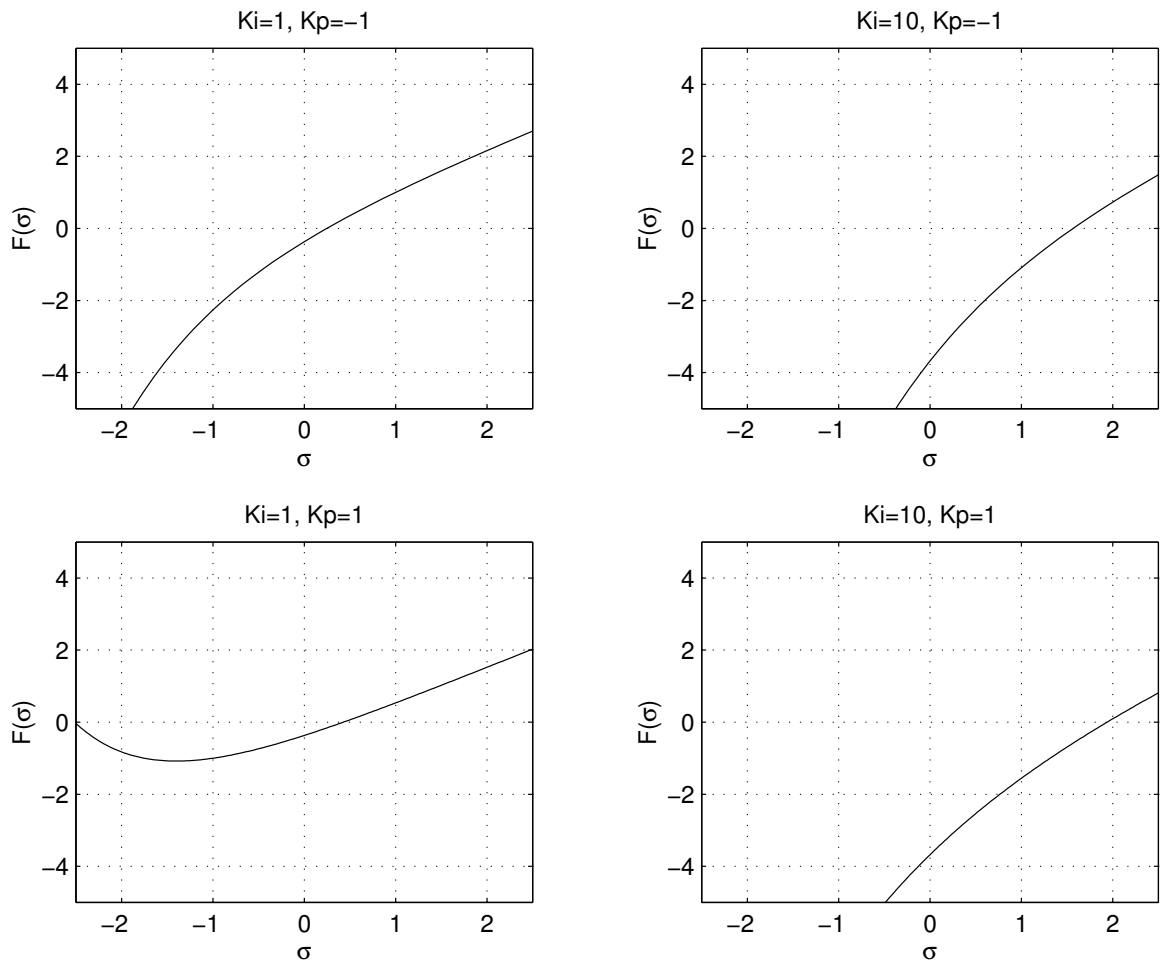


Figure 6.13. Real roots of transcendental equation at $K_i > 0$.

Positive real roots are observed in this case as shown in Figure 6.13. We noticed that from the $\bar{\tau} \ll 1$ result, this case is not a stable set for the system with small delay. Most likely the system will be unstable in the presence of delay. But further investigation is worth doing to make sure that this choice of K_p and K_i leads to instability in the system.

Using the stability condition in the above theorems shows that this system has complex unstable roots. To check the eigenvalues for this case, let σ and $F(\sigma)$ in Equation (6.34) be separated into their real and imaginary parts. We get

$$\begin{aligned} \sigma_r - \bar{\tau}e^{\bar{\tau}}K_p - \frac{\bar{\tau}e^{\bar{\tau}}K_i\sigma_r}{\sigma_r^2 + \sigma_i^2} + \frac{\bar{\tau}e^{\bar{\tau}}K_i}{\sigma_r^2 + \sigma_i^2} \left(\sigma_r \cos(\sigma_i\bar{\tau}) - \sigma_i \sin(\sigma_i\bar{\tau}) \right) + \bar{\tau}e^{\bar{\tau}}K_p \cos(\sigma_i\bar{\tau}) &= 0, \\ \sigma_i + \frac{\bar{\tau}e^{\bar{\tau}}K_i\sigma_r}{\sigma_r^2 + \sigma_i^2} - \frac{\bar{\tau}e^{\bar{\tau}}K_i}{\sigma_r^2 + \sigma_i^2} \left(\sigma_i \cos(\sigma_i\bar{\tau}) + \sigma_r \sin(\sigma_i\bar{\tau}) \right) - \bar{\tau}e^{\bar{\tau}}K_p \sin(\sigma_i\bar{\tau}) &= 0, \end{aligned} \quad (6.41)$$

where $\sigma = \sigma_r + i\sigma_i$. For neutral stability $\sigma_r = 0$, so that the above equations become

$$-\frac{\bar{\tau}e^{\bar{\tau}}K_i}{\sigma_i} \sin(\sigma_i\bar{\tau}) + \bar{\tau}e^{\bar{\tau}}K_p \cos(\sigma_i\bar{\tau}) - \bar{\tau}e^{\bar{\tau}}K_p = 0, \quad (6.42)$$

$$\sigma_i - \frac{\bar{\tau}e^{\bar{\tau}}K_i}{\sigma_i} \cos(\sigma_i\bar{\tau}) - \bar{\tau}e^{\bar{\tau}}K_p \sin(\sigma_i\bar{\tau}) + \frac{\bar{\tau}e^{\bar{\tau}}K_i}{\sigma_i} = 0. \quad (6.43)$$

Moving the terms of the trigonometric functions into the right-hand side, then squaring and adding these two equations yields

$$\sigma_i^2 + 2\bar{\tau}e^{-\bar{\tau}}K_i = 0, \quad (6.44)$$

from which $\sigma_i = \pm\sqrt{-2\bar{\tau}e^{-\bar{\tau}}K_i}$. Thus, the change from stability to instability and the reverse will depend on K_i only. Since in this case $K_i > 0$, this means there is no solution for σ_i . In this case the roots will not cross the imaginary axis and they will be either on the left half plane (stable) or on the right half plane (unstable) of the imaginary axis. The application of the above theorems shows that this set of K_p and K_i is not a stabilizing set, so the system is not stable in this case.

(d) $K_i < 0, K_p > 0$

In this case real and complex roots are observed. The above theorem shows that not all the roots in this case are real. Actually, from Equation (6.44) we can find where the roots cross the imaginary axis. In this case the system is conditionally stable. The stability map for this case and the above cases can be seen in Figure 6.14.

6.5.3 $\bar{\tau} \gg 1$

For very large $\bar{\tau}$ the exponentials in Equation (6.34) tend to zero, so that $\sigma \rightarrow 0$. In this case the system is stable.

6.6 Discussion of linear stability

In the previous section we investigated the stability of the system for different control gains at small, large and a delay of order 1. It was shown that the system is stable for large delay. If the system is delay-free, then the system is stable, and if there is a small delay the system is conditionally stable.

In this section we will discuss the stability at delay of order one, and examine the effect of changing the delay. As a result of Equation (6.44), it has been found that there is a possibility of occurrence of two types of bifurcation. When $K_i < 0$ there are two real roots for σ_i , so there is a crossing of the imaginary axis. Therefore, a switch in the system stability occurs. This is a Hopf bifurcation. On the other hand when $K_i = 0$, then $\sigma_i = 0$ and a simple bifurcation occurs. When $K_i > 0$, from Equation (6.44) there is no solution for σ_i which means there is no switch in the system stability regardless of K_p . It was shown in these cases that the system is unstable. In Figure 6.14, a stability map is shown as a function of K_p vs. K_i . This map was entirely generated using the above theorems. One can see the range of K_p and K_i where the system is stable. Along the neutral stability line two kinds of bifurcation occur. The first one when $K_i < 0$ is a Hopf bifurcation. The second

when $K_i = 0$ is a simple bifurcation. The effect of changing $\bar{\tau}$ on the system stability is shown in Figure 6.15 and Figure 6.16 as a function of K_p and K_i respectively. In Figure 6.15 a large stability region with small τ can be seen. Then, a decrease and later an increase in the size of the stability region with an increase of τ is observed. When K_i is a variable, a stability region can be found only for $K_i < 0$. This is also shown in Figure 6.16.

6.7 Numerical results

We examine in this section the behavior of the control scheme in response to a small perturbation and verify the analytical stability results numerically.

6.7.1 Linear

After having obtained the stability map, we will compare it with the numerical results obtained at different locations in the K_p vs. K_i map. Because of its accuracy, the Lagrangian model developed in the previous section and given by Equation (6.23) and Equation (6.24) will be used to calculate the outlet duct temperature. After having the system stabilized at a steady-state temperature distribution and velocity, a one percent change in the inlet velocity is introduced about this fixed point. If the system is stable, the controller will bring the system back to the steady-state condition, and the effect of the perturbation will exponentially vanish with time. Figure 6.17–Figure 6.20 show the response of the controller at different locations around the stability map. Stable solutions are shown in solid lines and unstable solutions by dashed lines. The computed results yielded the same stable and unstable regions obtained previously from analyzing the roots of the characteristic equation. In the lower boundary of the K_p vs. K_i map there exists a stable limit cycle. It seems that this limit cycle grows as K_p and K_i decreases. In other words, as K_p and K_i move in a negative direction, there is a subcritical Hopf bifur-

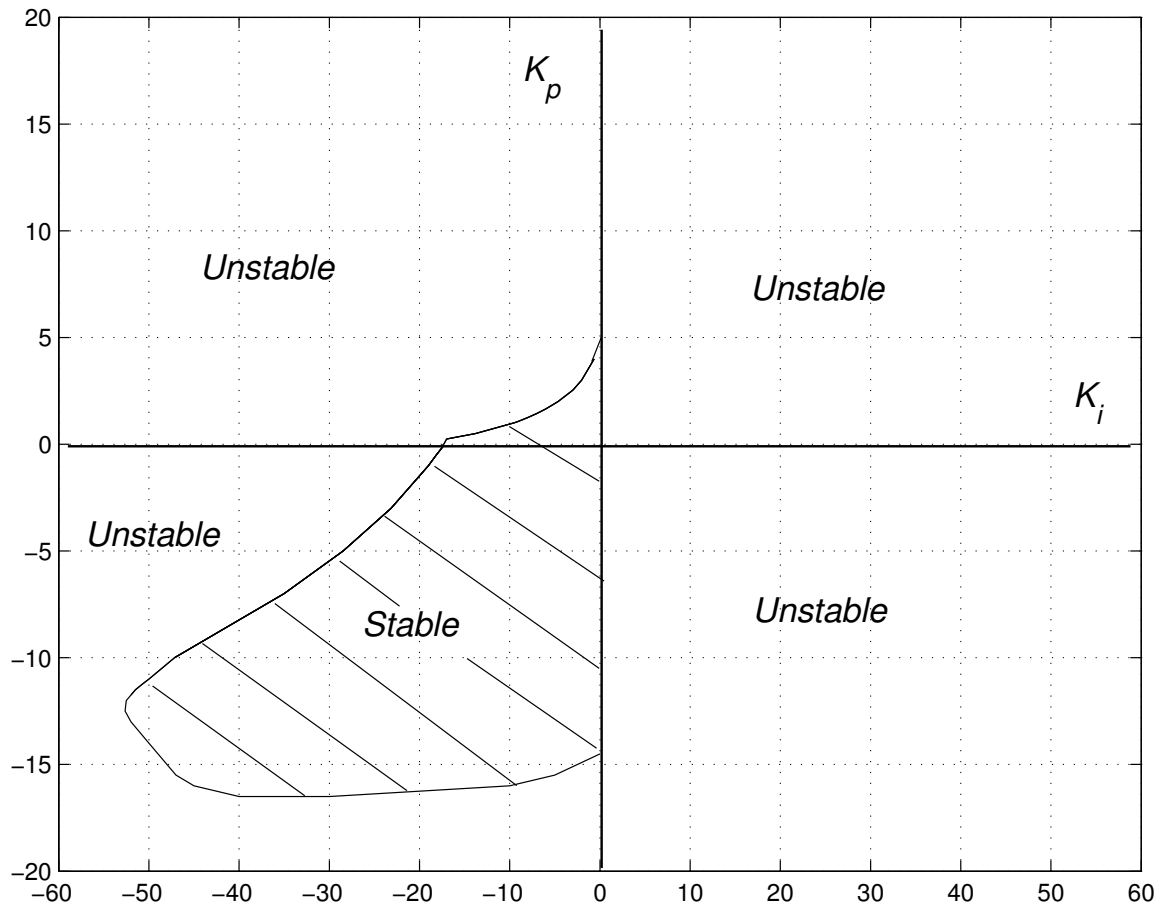


Figure 6.14. Stability map.

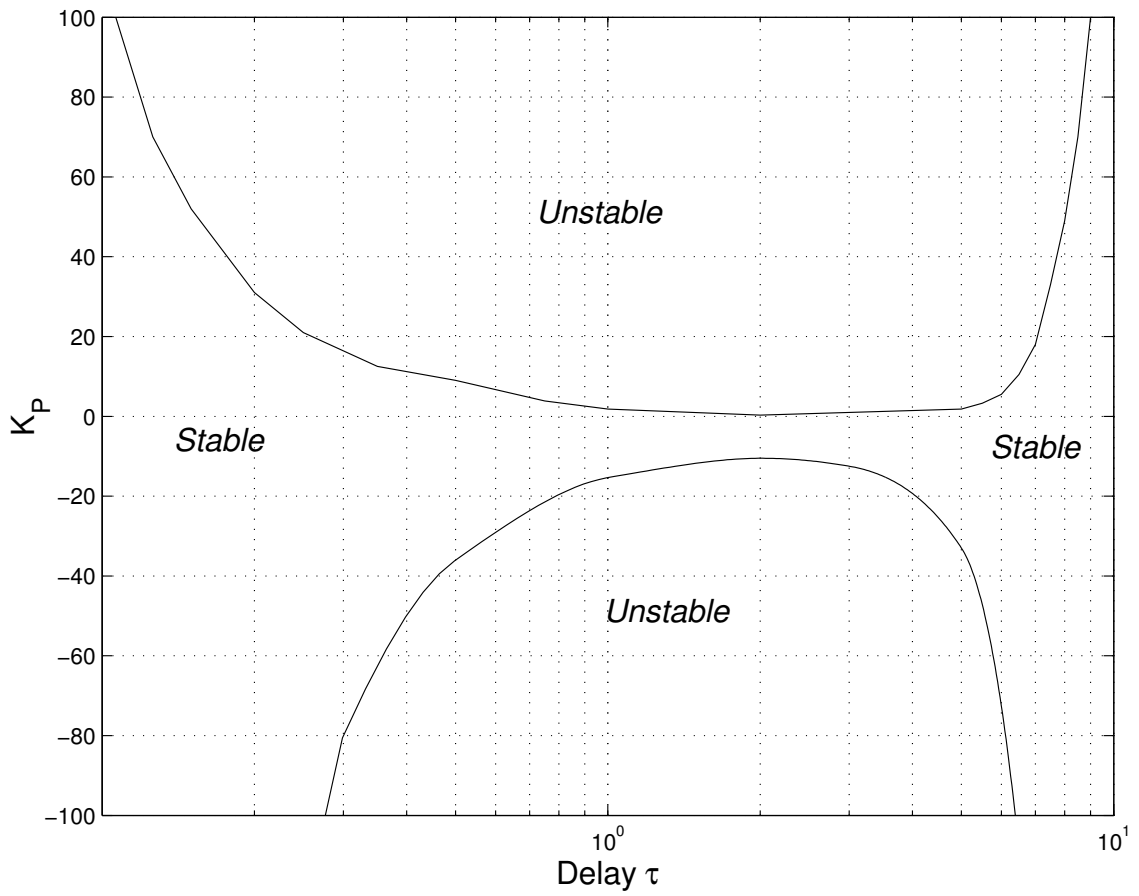


Figure 6.15. Effect of delay at constant $K_i = -5$ and variable K_p .

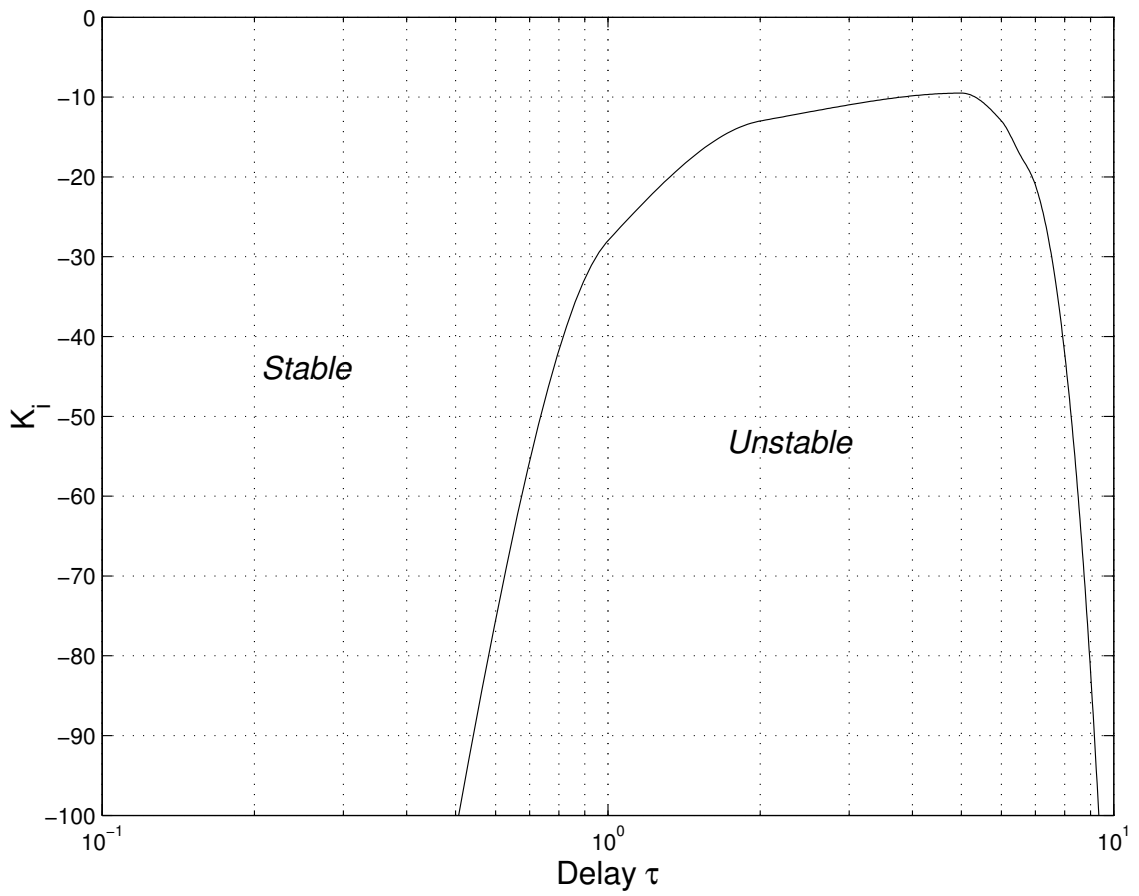


Figure 6.16. Effect of delay at constant $K_p = -5$ and variable K_i .

cation and the limit cycle gets larger in amplitude. To examine this phenomenon, the computed limit cycles are compared with smaller perturbation. The larger limit cycle is expected from the larger perturbation due to the effect of the higher-order terms from the nonlinearities. This can be seen in Figure 6.21 as one moves away from the bifurcation point,

6.7.2 Nonlinear

For certain values of the system parameters K_p and K_i greater than the critical, a limit cycle oscillation around the steady-state condition occurs. This change can be described as a sub- or supercritical Hopf bifurcation. The former is characterized by a unstable limit cycle in the stable region, while the latter has a stable limit cycle in the unstable region. The nature of the bifurcation cannot be predicted by linear analysis.

To obtain insight into the system behavior beyond the critical point, and to analyze the effect of changing the system parameters on the oscillation, numerical amplitude and frequency calculations were performed. Let us consider $K_i = -5$, for which the value of the parameter K_p at the stability boundary is $K_p^{cr} \approx 1.912$. There is a Hopf bifurcation at this point. For $K_p > K_p^{cr}$ the limit cycle expands and lengthens its temporal period and decreases its frequency. The amplitude and frequency can be plotted as a function of the difference $K_p - K_p^{cr}$, as shown in Figure (6.23). Of course K_p greater than the critical can be used in some cases if a small oscillation is acceptable.

6.8 Conclusions

The control and stability of the outlet temperature of a long duct is investigated with consideration to time delay in the system. Two different numerical simulations for the duct flow were tested. Linear and nonlinear stability were analyzed for this

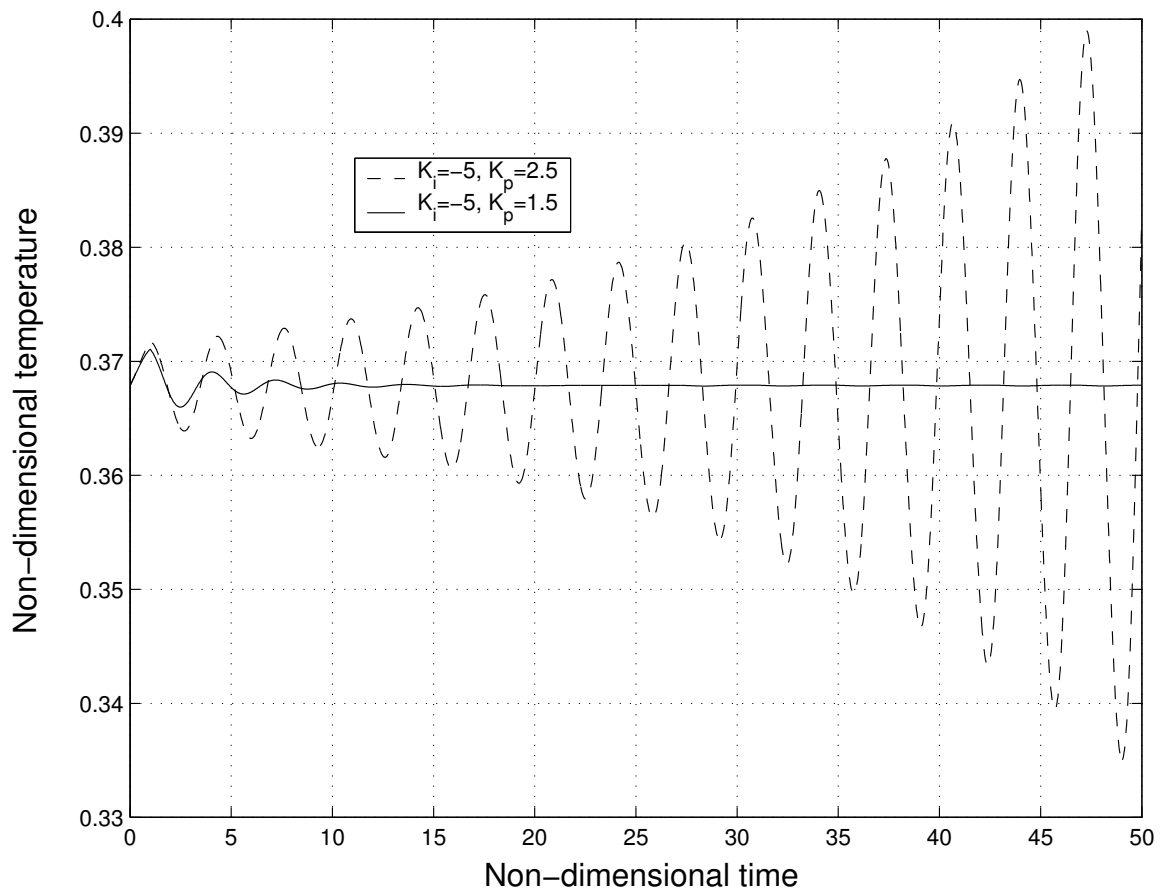


Figure 6.17. Supercritical Hopf bifurcation at $K_i = -5$ and $K_p = 1.5$ and 2.5 .

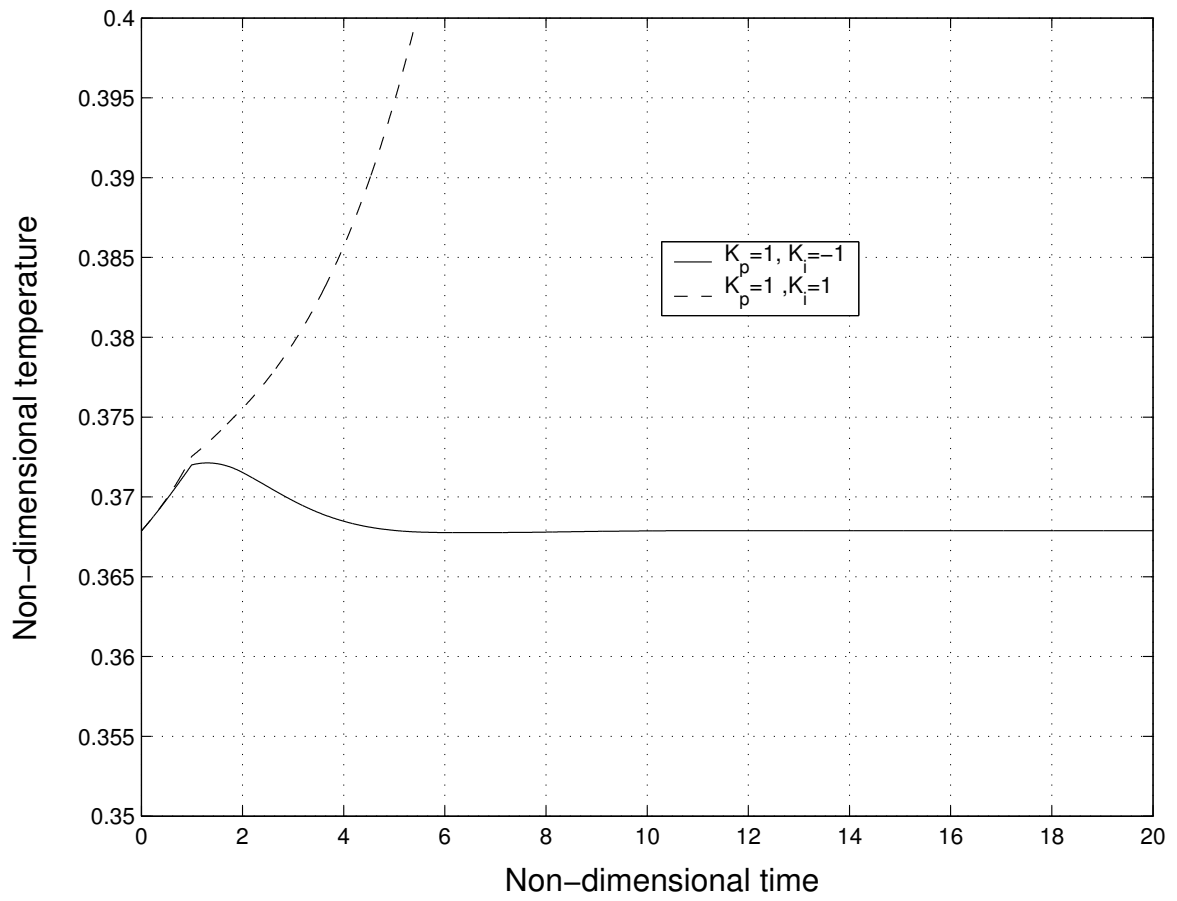


Figure 6.18. Simple bifurcation at $K_p = 1$ and $K_i = \pm 1$.

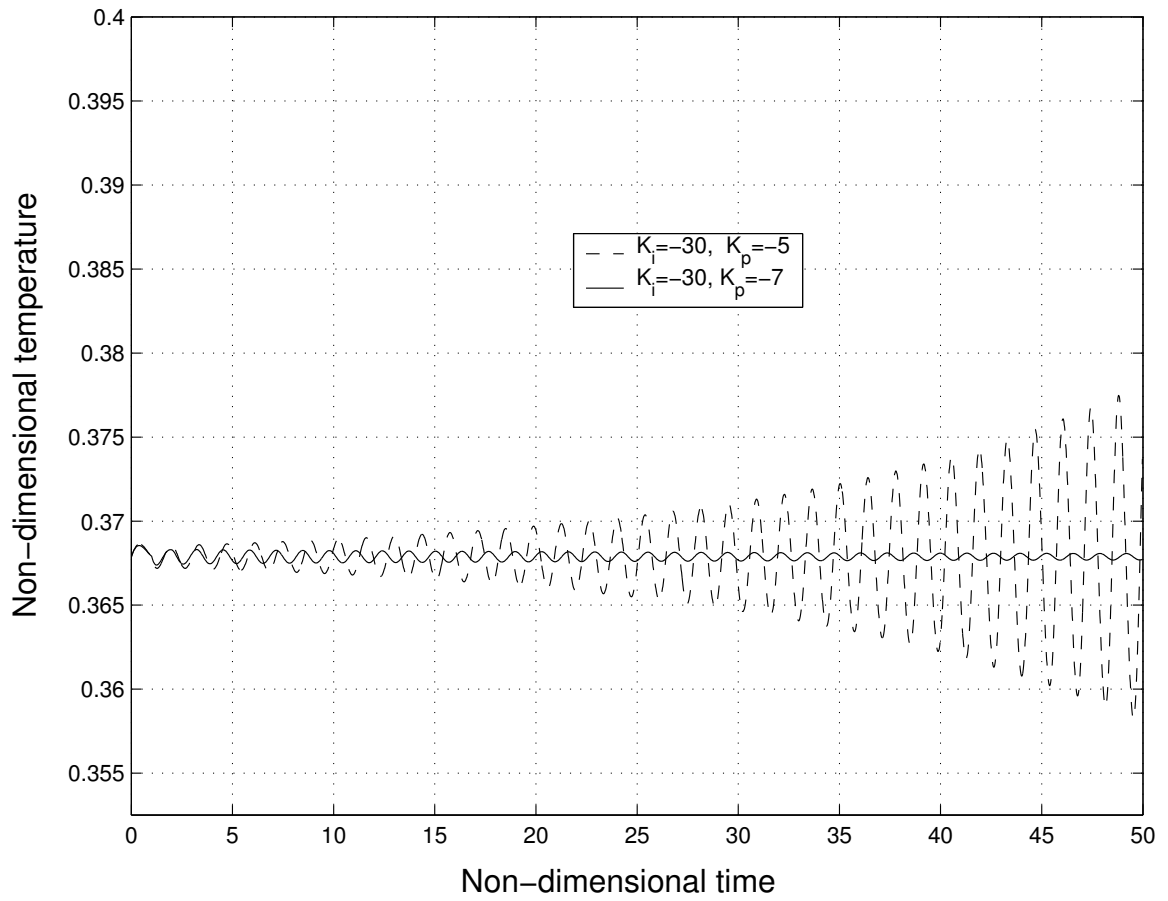


Figure 6.19. Supercritical Hopf bifurcation at $K_i = -30$ and $K_p = -5$ and -7 .

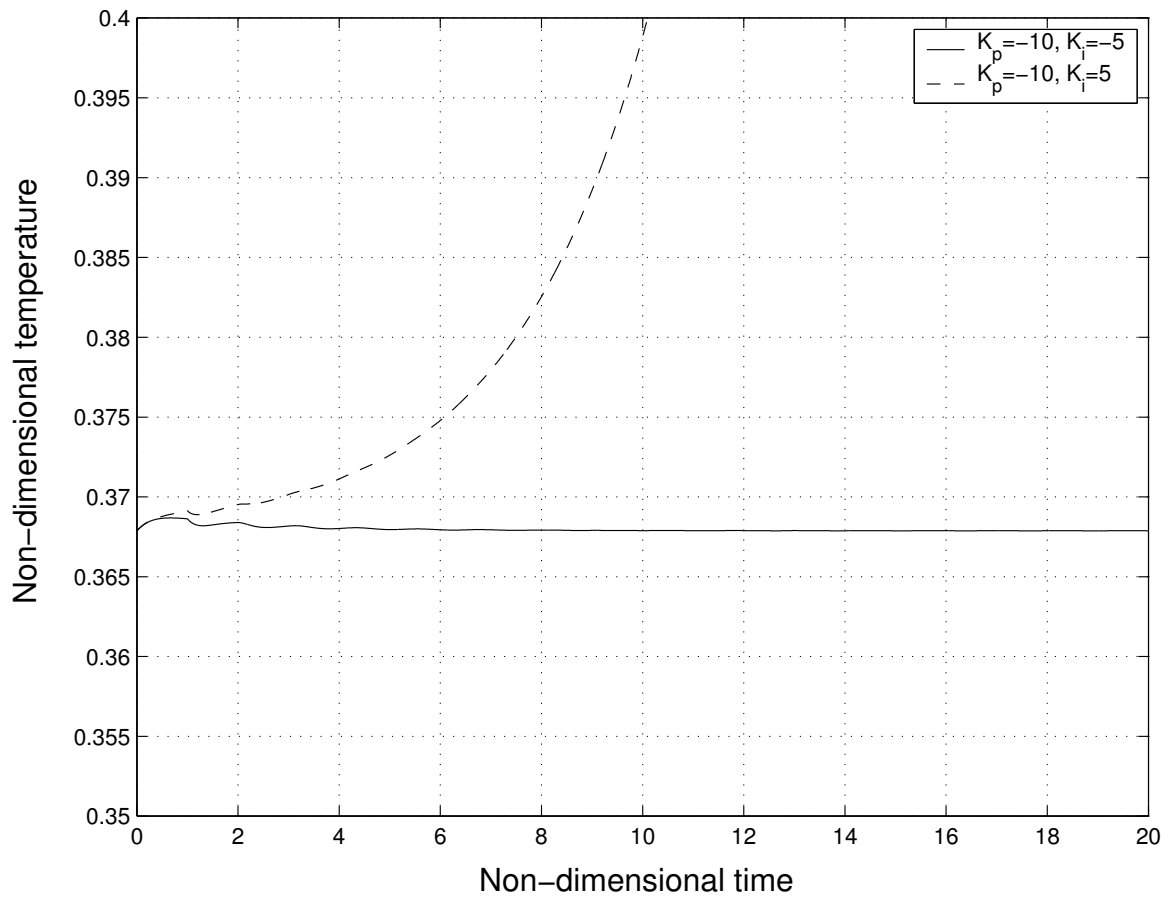


Figure 6.20. Simple Hopf bifurcation at $K_p = -10$ and $K_i = \pm 5$.

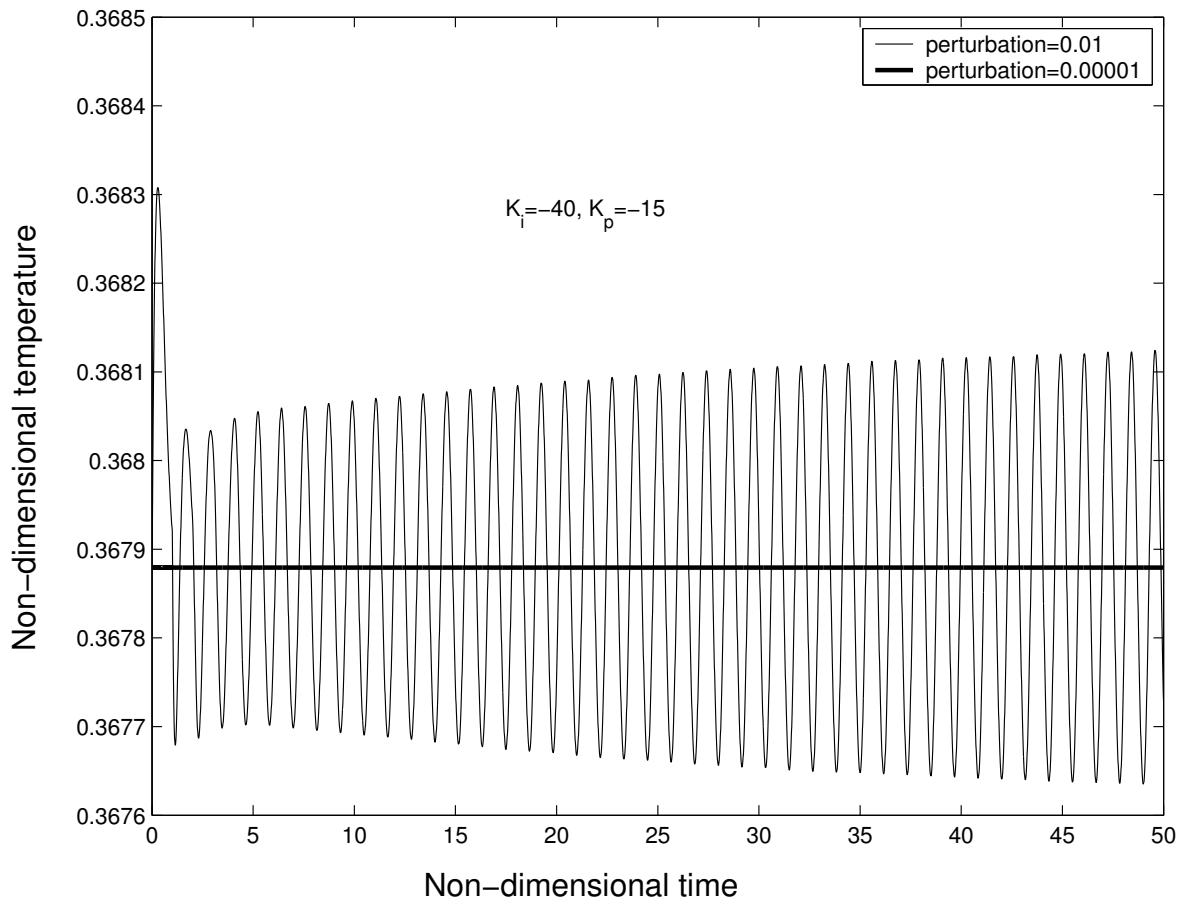


Figure 6.21. Subcritical Hopf bifurcation at $K_p = -15$ and $K_i = -40$.

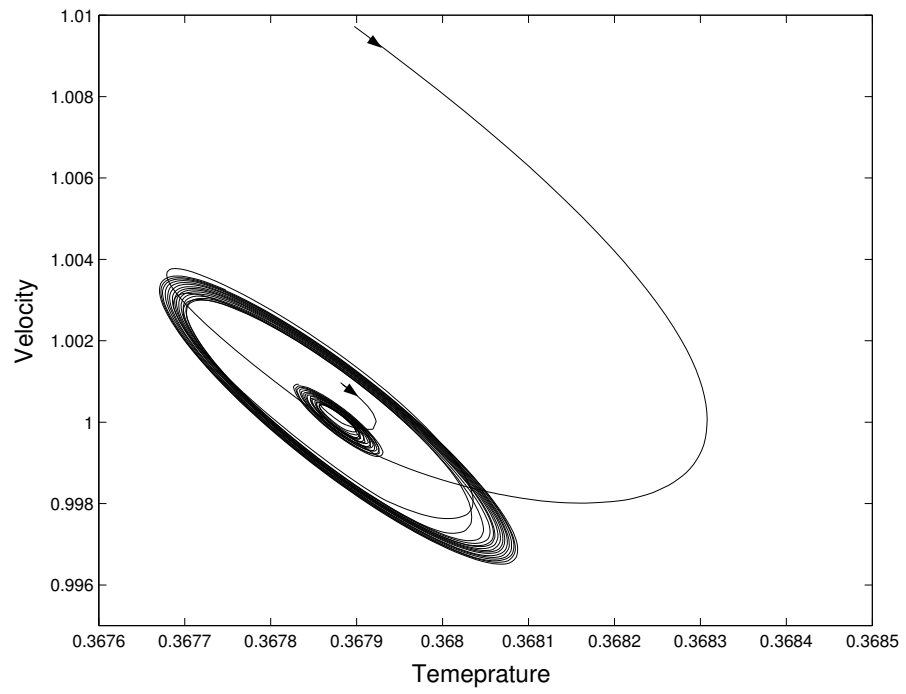


Figure 6.22. Limit cycles at subcritical Hopf bifurcation at $K_p = -15$ and $K_i = -40$

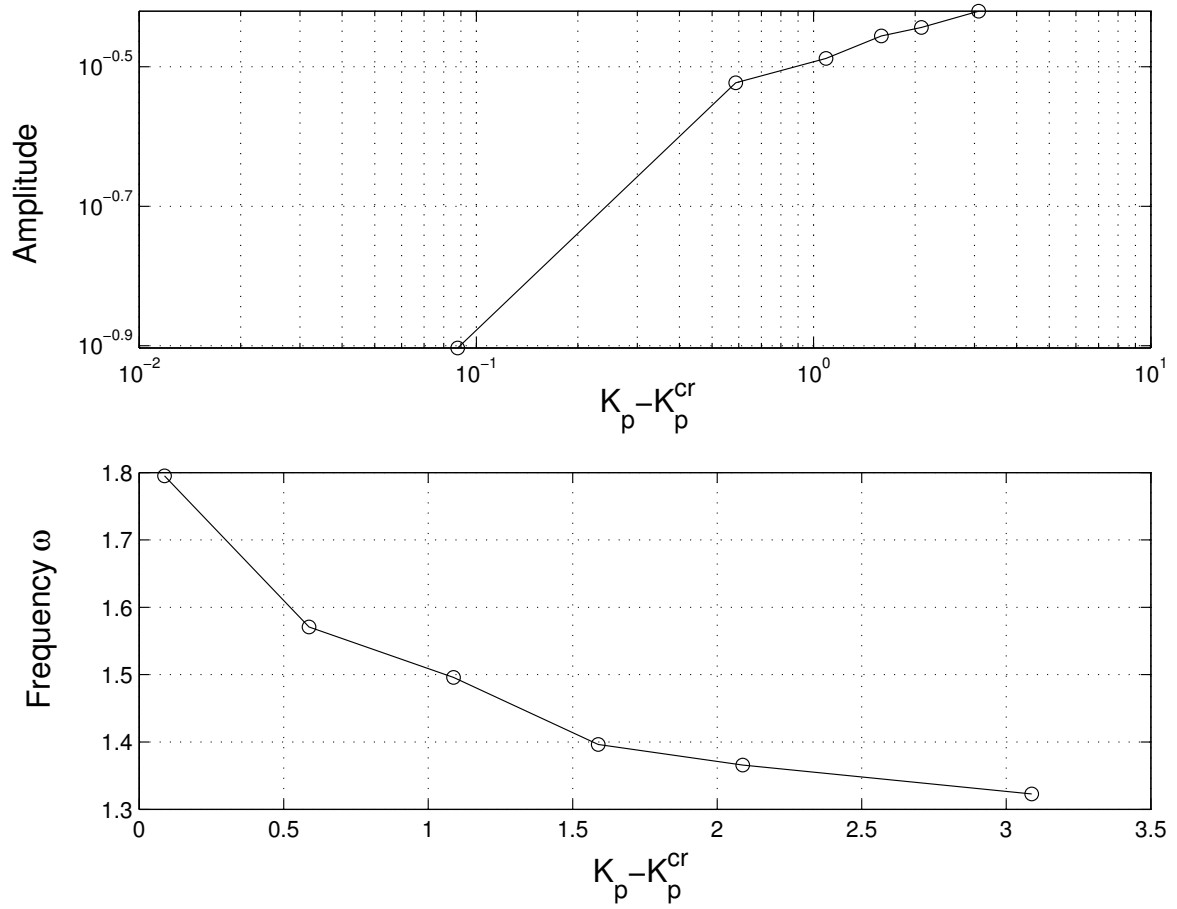


Figure 6.23. Nonlinear amplitude and frequency.

problem. The main results of the present work are the observation of a limited stability region for a delay of order one, and stability at the two extremes of no delay and large delay. Usually the delay destabilizes the system. In this case, as the delay increases the system becomes more stable. Also, it is found that the system is not stable for any positive integral gain K_i , and when the K_i is negative K_p does not appear in the stability criterion. Finally, Hopf bifurcation can take place with a negative and zero integral gain.

CHAPTER 7

CONCLUSIONS AND RECOMMENDATIONS

7.1 Conclusions

The dynamic behavior and controllability of cross-flow heat exchangers and flow in long ducts have been examined. The overall goal of this research is to gain a better understanding of these issues from a thermal engineering point of view. Through this, we may better identify these systems and design effective control schemes for building and district heating and cooling.

A controllability study for a conductive-convective system and cross-flow heat exchanger is presented. A numerical method based on finite-differences is developed for the study of infinite-dimensional equations and tested for a conduction-convection system. The state and output controllability of a single-pass cross-flow heat exchanger with simultaneous advection, convection and conduction, in which water and air are the in- and over-tube fluids is presented. This provides a useful design tool to determine the controllability of a heat exchanger. It is found that there is an optimum water flow rate at which the heat exchanger is the most controllable.

A more accurate mathematical model for cross-flow heat exchanger has been presented. A finite-difference method was used to solve this model numerically. This model was then used to simulate the response of the heat exchanger to feedback control. The results of this transient model based on spatially distributed parameters of the cross-flow heat exchanger show that the control behavior can be accurately simulated and that this control methodology is effective.

Finally, a numerical simulation of the flow in long ducts that takes into account the delay in the system is presented. This allows insight into its dynamic behavior and provides a useful design tool for control systems. In addition, the effect of delay on the stability of this long duct flow has been examined and a stability limits were obtained for PI controller.

In conclusion, this dissertation exploits some interesting research areas and presents some innovations to the study thermal control problems. This is achieved as a result of combining the two fields of heat transfer and control theory.

7.2 Recommendations for future work

The following recommendations can be made for future research efforts in extending the current results.

- The controllability of dynamical systems governed by partial differential equations has been shown to be one of the difficult problems in mathematical control theory. Even for a linear system the analysis is far from being trivial. Therefore, approximation of the governing equation to reduce its order is needed. In this dissertation the finite-difference method was adopted to perform this task and a system of ordinary differential equations was obtained. The rank condition can now be used to check the controllability of the system. It would be interesting to see how the controllability of different approximations methods will differ from the results obtained in this work. Also, in practical situations the parameters of the system may be temperature dependant. It is reasonable in such situations to consider a time-varying parameter model in studying the controllability of the system.

In the analysis of the controllability of the cross-flow heat exchanger, we used a single control input. The extension of these results to a multi-input system, and the linearization around an operating condition when a nonlinear behavior exists

are important.

Can the controllability be improved by slightly changing the structure of the heat exchanger? It would be extremely interesting to study the interaction of optimal design and the controllability of the cross-flow heat exchanger.

- In the numerical simulation of cross-flow heat exchangers, two recommendations for future modeling can be made where the model is still simple and effective enough to reflect the main characteristics of the cross-flow heat exchanger. First, to include condensation of ambient humidity. This will evaluate the psychrometric properties of humid air and the possibility of cooling the air below its dew point temperature. In this work we dealt with dry air where we maintained the air temperature to be above its dew point temperature. This modification to the model is very practical and will increase the operating range of the heat exchanger. The second point is to incorporate a gradient analysis in the air-side control volume. This will result in one more partial differential equation for the air side. Also, an average of the inlet and outlet air temperatures was used to calculate the air side heat transfer coefficient and to reduce the number of unknowns in the system. This average temperature can be eliminated to have the air side heat transfer coefficient and other properties like thermal conductivity to be temperature-dependent.

- In the control of cross-flow heat exchangers, we chose the well known and widely used PI controller to study the response of this distributed parameter system to a control strategy. This was just a starting point to test the feasibility of this method. This computational methodology can be extended to more complex control schemes to be used with more complicated systems which may have more than one heat exchanger.

- Flow in long ducts is a very practical problem. In this dissertation we considered

the effect of delay on the response and stability of flow in a single duct. Dual-duct systems are widely used in HVAC and other industrial application. Therefore, the analysis of dual-duct flow is worth carrying out. The effect of delay in each duct on the overall performance is a very interesting problem. Also, it would be important to control a dual-duct system where the interaction between two different control loops and the presence of delay are included.

APPENDIX A

NONDIMENSIONALIZATION OF CROSS-FLOW HEAT EXCHANGER GOVERNING EQUATIONS

A.1 Air-side equation

In the air side we have

$$\frac{\dot{m}_a}{L} c_a (T_a^{in} - T_a^{out}) = h_o 2\pi r_o (T_a - T_t). \quad (\text{A.1})$$

Let $\theta = (T - T_w^{in}) / (T_a^{in} - T_w^{in})$, and multiply both sides of Equation (A.1) by LD_o/k_a to give

$$\frac{\rho V_a c_a A D_o}{k_a} (\theta_a^{in} - \theta_a^{out}) = (2\pi r_o L) \frac{h_o D_o}{k_a} (\theta_a - \theta_t). \quad (\text{A.2})$$

Divide by the frontal area A , so that

$$Pe_a (\theta_a^{in} - \theta_a^{out}) = \beta_1 \left(\frac{\theta_a^{in} + \theta_a^{out}}{2} - \theta_t \right), \quad (\text{A.3})$$

where $Pe_a = Re_o Pr_a$, $\beta_1 = A_o Nu_o / A$, $Re_a = V_a D_o / \nu$, and $Pr_a = \nu \rho c_a / k_a$.

A.2 Tube-wall equation

For the tube wall we can write

$$\rho_t c_t \pi (r_o^2 - r_i^2) \frac{\partial T_t}{\partial t} = k_t \pi (r_o^2 - r_i^2) \frac{\partial^2 T_t}{\partial x^2} + 2\pi r_o h_o (T_a - T_t) - 2\pi r_i h_i (T_t - T_w). \quad (\text{A.4})$$

Divide by $k_t A_t$ and then defining the dimensionless quantities: $x^* = x/L$, $\tau = t\alpha_w/L^2$, and θ as in above, Equation (A.4) can be written as

$$\frac{\alpha_w}{\alpha_t L^2} \frac{\partial \theta_t}{\partial \tau} = \frac{\partial^2 \theta_t}{\partial x^{*2} L^2} + \frac{2\pi r_o h_o}{k_t A_t} (\theta_a - \theta_t) - \frac{2\pi r_i h_i}{k_t A_t} (\theta_t - \theta_w). \quad (\text{A.5})$$

from which

$$\frac{\alpha_w}{\alpha_t} \frac{\partial \theta_t}{\partial \tau} = \frac{\partial^2 \theta_t}{\partial x^{*2}} + \frac{2\pi r_o h_o L h_o L k_a D_o}{A_t k_t k_a D_o} (\theta_a - \theta_t) - \frac{2\pi r_i h_i L h_i L k_w D_i}{A_t k_t k_w D_i} (\theta_t - \theta_w). \quad (\text{A.6})$$

This can be written as

$$\frac{\alpha_w}{\alpha_t} \frac{\partial \theta_t}{\partial \tau} = \frac{\partial^2 \theta_t}{\partial x^{*2}} + \frac{A_o}{A_t} Nu_o \frac{k_a L}{k_t D_o} (\theta_a - \theta_t) - \frac{A_i}{A_t} Nu_i \frac{k_w L}{k_t D_i} (\theta_t - \theta_w). \quad (\text{A.7})$$

Therefore, we have

$$\gamma \frac{\partial \theta_t}{\partial \tau} + \beta_2 (\theta_t - \theta_w) = \frac{\partial^2 \theta_t}{\partial x^{*2}} + \beta_3 \left(\frac{\theta_a^{in} + \theta_a^{out}}{2} - \theta_t \right). \quad (\text{A.8})$$

A.3 Water-side equation

This is

$$\rho_w c_w \pi r_i^2 \frac{\partial T_w}{\partial t} + \dot{m}_w c_w \frac{\partial T_w}{\partial x} = h_i 2\pi r_i (T_t - T_w). \quad (\text{A.9})$$

Divide Equation (A.9) by $A_w k_w$, and using the above nondimensional parameters, we have

$$\frac{\rho_w c_w}{k_w} \frac{\partial \theta_w}{\partial t} + \frac{\rho_w V_w c_w}{L k_w} \frac{\partial \theta_w}{\partial x^*} = \frac{2\pi h_i r_i}{A_w k_w} (\theta_t - \theta_w). \quad (\text{A.10})$$

Using the nondimensional time parameter

$$\frac{\rho_w c_w \alpha_w}{k_w L^2} \frac{\partial \theta_w}{\partial \tau} + \frac{\rho_w V_w c_w}{L k_w} \frac{\partial \theta_w}{\partial x^*} = \frac{2\pi r_i h_i}{A_w k_w} (\theta_t - \theta_w), \quad (\text{A.11})$$

this gives

$$\frac{\partial \theta_w}{\partial \tau} + \frac{L V_w \nu D_i}{\alpha_w \nu D_i} \frac{\partial \theta_w}{\partial x^*} = \frac{2\pi r_i h_i L D_i L h_i}{A_w D_i k_w} (\theta_t - \theta_w), \quad (\text{A.12})$$

which can be written as

$$\frac{D_i}{L} \frac{\partial \theta_w}{\partial \tau} + Re_i Pr_w \frac{\partial \theta_w}{\partial x^*} = Nu_i \frac{A_i}{A_w} (\theta_t - \theta_w). \quad (\text{A.13})$$

BIBLIOGRAPHY

- [1] Antsaklis, P.J., and Michel A.N. *Linear Systems.*, McGraw-Hill, 1997.
- [2] Butkovsky, A.G. *Distributed Control System*, Elsevier, Amsterdam, 1969.
- [3] Lions, J. L. On the controllability of distributed systems. *Proc. Natl. Acad. Sci. USA*, Vol. 94, pp. 4828-4835, 1997.
- [4] Rosenbrock, H.H. *State-Space and Multivariable Theory*. John Wiley and Sons, New York, 1970.
- [5] Fattorini, H. O., and Russel, D. L. Exact controllability theorems for linear parabolic equations in one space dimension. *Archive For Rational Mechanics & Analysis*, 1971.
- [6] Fattorini, H. O. *The Cauchy Problem*, Addison-Wesley, U.S.A., 1983.
- [7] Triggiani, R. Controllability and observability in banach space with bounded operators. *SIAM J. Control*, Vol. 13, No. 2, Feb. 1975.
- [8] Klamka, J. *Controllability of Dynamical Systems*, Kluwer Academic Publishers, Netherlands, 1991.
- [9] Daniel, R. L., and David, B. Controllability analysis of an industrial polymerization reactor. *Computers Chem. Engng.*, Vol. 20. pp. S871-S876, 1996.
- [10] Vargra, E. I., Hangos, K. M., and Szigeti, F. Controllability and observability of heat exchangers networks in the time-varying parameter case. *Control Engineering Practice*, Vol. 3. No. 10, pp. 1409-1419, 1995.
- [11] Kequn, L., Xing, L., and Niemeyer, B. Controllability analysis of multistream heat exchangers. *Proceeding of the International Symposium on Compact Heat Exchangers.*, pp. 163-167, Grenoble, August 24, 2002.
- [12] Wilfried, R., Yimin, X. *Dynamic Behaviour of Heat Exchangers*, WIT Press, UK, 1999.
- [13] Gartner, J. R. and Harrison, H. L. Frequency response transfer functions for a tube in cross flow. *ASHRAE Trans.*, vol. 69 pp. 323-330, 1963.
- [14] Gartner, J. R., and Harrison, H. L. Dynamics characteristics of water to air cross-flow heat exchanger. *ASHRAE Trans.*, vol. 71 pp. 212-224, 1965.
- [15] Myers, G. E., Mitchell, J. W. and Nagaoka, R. A method of estimating cross flow heat exchanger transients. *ASHRAE Trans.*, vol. 71 pp. 225-230, 1965.

- [16] Tamm, H. Dynamics response relations for multi-row cross flow heat exchangers. *ASHRAE Trans.*, vol. 75, Part 1, pp. 69–80.
- [17] Gartner, J. R., and Daane, L. E. Dynamics response relations for a serpentine cross flow heat exchanger with water velocity disturbance. *ASHRAE Trans.*, vol. 75, Part 2, pp. 53–68, 1969.
- [18] Tamm, H., and Green, G. H. Experimental multi-row cross flow heat exchangers. *ASHRAE Trans.*, vol. 79 Part 2, pp.9-18, 1973.
- [19] Thal-Laresen, H. Dynamics of heat exchanger and their models. *ASME J. of Basic Eng.*, pp. 489–504, 1960.
- [20] Boot, J. L., Pearson, J. T., and Leonard, R. G. An Improved dynamics response model for finned serpentine cross-flow heat exchangers. *ASHRAE Trans.*, vol. 83 Part 1, pp. 218–239, 1977.
- [21] Sundén, B. Transient conjugate forced convection heat transfer from circular tubes in cross-flow. *Numerical Methods in Heat Transfer*, vol. 3, Chap. 11, Wiley, New York, 1985.
- [22] Underwood, D. M., and Crawford, R. R. Dynamics nonlinear modeling of a hot water-to-air heat exchanger for control application. *ASHRAE Trans.*, pt 1, pp. 149–155 0001-2505, 1991.
- [23] Yamashita, H., Izumi, R., and Yamaguchi, S. Analysis of the dynamic characteristics of cross-flow heat exchangers with both fluid unmixed. *Bulletin of the ASME*, vol. 21, No. 153, pp. 479-485.
- [24] Spiga, M., and Spiga, G. Two-dimensional transient solution for cross-flow heat exchanger with neither gas mixed. *Journal of Heat Transfer*, vol. 109, pp.281–286, 1987.
- [25] Spiga, M., and Spiga, G. Transient temperature field in cross flow heat exchanger with finite wall capacitance. *Journal of Heat Transfer*, vol. 110, pp.49–53, 1988.
- [26] Spiga, M., and Spiga, G. Step response of the cross flow heat exchanger with finite wall capacitance. *Int. J. Heat Mass Transfer*, vol. 35, No. 2, pp. 559–565, 1992.
- [27] Kabelac, S. The transient response of finned crossflow heat exchangers. *Int. J. of Heat and Mass Transfer*, vol. 32, No. 6, pp. 1183–1189, 1989.
- [28] Gane, C. R., and Stephenson, P. L. An explicit numerical method for solving transient combined heat conduction and convection problems. *Int. J. Num. Methods Eng.*, vol. 14, p. 1141, 1979.
- [29] Katayama, T., Ito, T., Ogawa, O., and Yamamoto, H. Optimal tracking control of a heat exchanger with change in load condition. *Proceedings of the IEEE Conference on Decision and Control*, vol. 3, 1990.
- [30] Das, S. K., and Dan, T. K. Transient response of a parallel flow shell-and-tube heat exchanger and its control. *Heat Mass Transfer*, vol. 31, pp. 231–235, 1996.

- [31] Peter, B., Martin, F., Dominik, F., Oliver, N., and Rolf, I. Integrated control, diagnosis and reconfiguration of a heat exchanger. *IEEE Control System Magazine*, vol. 18, No. 3, pp. 52–63 0272–1708, 1998.
- [32] Diaz, D. Simulation and control of heat exchanger using artificial neural network. *Ph.D Thesis*, Department of Aerospace & Mechanical Engineering, University of Notre Dame., IN, 2000.
- [33] Morton, K.W., and Mayers. *Numerical Solution of Partial Differential Equations*, Cambridge University Press, 1994.
- [34] Rhee, H. K., Amundson, N. R. *First-Order Partial Differential Equations*, Prentice-Hall, Englewood Cliffs, NJ, U.S.A., 1986.
- [35] Russel, D. Quadratic performance criteria in boundary control of linear symmetric hyperbolic systems. *SIAM J. Control*, Vol. 11, No. 3, pp. 475–509, 1973.
- [36] Ito, A., Kanoh, H., and Masubuchi, M. MWR approximation and modal control of parallel and counterflow heat exchangers. *Proc, 2nd IFAC Symposium on Distributed-Parameter Systems*. Pergamon, Oxford, 1978.
- [37] Marian, W. Application of orthogonal collocation to simulation and control of first order hyperbolic systems. *Mathematics and Computers in Simulation.*, pp. 335-345, 1983.
- [38] Ray, W. H. *Advanced Process Control*. McGraw-Hill, New York, U.S.A, 1981. Netherlands, 1991.
- [39] Christofides, P.D., and Dautidis P. Feed-back control of hyperbolic PDE systems. *A.I.Ch.E., J.* Vol. 42, 3063.
- [40] Irena, L., and Triggiani, R. Deterministic Control Theory for Infinite Dimensional Systems vols. I and II, Encyclopedia of Mathematics. *Cambridge University Press*, 1999.
- [41] Munk, W. The delayed hot-water problem. *ASME J. Applied Mechanics* Brief Notes, Vol. 21, 1954.
- [42] Henryk, G., Piotr, G., and Adam, K. *Analysis and Synthesis of Time Delay Systems*, John Wiley Sons, Chichester, 1989.
- [43] Huang, G., Nie, L., Zhao, Y., Yang, W., Wu, Q., and Liu, L. Temperature control system of heat exchangers. An application of DPS theory. *Lecture Notes in Control Information Sciences*, vol. 159, pp. 68–76, 1991.
- [44] Zhang, Z., and Nelson, R. M. Parametric analysis of a building space conditioned by a VAV System. *ASHRAE Transactions*, vol. 98, No. 1, pp. 43–48, 1992.
- [45] Antonopoulos, K.A., and Tzivanidis, C. A correlation for the thermal delay of building. *Renewable Energy.*, vol. 6, No. 7, pp. 687–699, 1995.
- [46] Saman, N., and Mahdi, H. Analysis of the delay hot/cold water problem. *Energy*, vol. 21, No.5, pp. 395–400, 1996.

- [47] Tin-Tai, C. Numerical modeling of thermal behavior of fluid conduit flow with transport delay. *ASHREA Transactions.*, vol. 102, n. 2, 1996.
- [48] Comstock, C. On the delayed hot water problem. *J. Heat and Mass Transfer.*, vol. 96, pp. 166–171, 1974.
- [49] Chu, J. Application of a discrete optimal tracking controller to an industrial electrical heater with Pure Delay. *J. Proc. Cont.*, vol. 5, No. 1, pp.3–8, 1995.
- [50] Chu, J., Su H., and Hu, x. A time-delay control algorithm for an industrial electrical heater. *J. Proc. Cont.*, vol. 3, No. 4, pp. 220–224, 1993.
- [51] Baruch, C, and Darrell, S. On stability of systems of delay differential equations. *J. Comp. Appl. Math.*, Vol. 117, pp. 137–158, 2000.
- [52] Bellman, R., and Cooke, K.,L. *Differential Difference Equations (Mathematics in Science and Engineering)*, Academic Press, 1963.
- [53] Margarete, B. On the stability of some exponential polynomials. *J. Math. Anal. appl.* Vol. 205, pp. 259–272, 1997.
- [54] Silviu-lulian, N. *Delay Effects on Stability.*, Lecture Notes In Control And Information Sciences, Springer, London, 2001.
- [55] Guillermo, J. S., Aniruddha, D., and Bhattacharyya, S.P. PI stabilization of first-order systems with time delay. *automatica*, Vol. 37, pp. 2020–2031, 2001.
- [56] Diaz, D., Sen, M., Yang, K.T., and Mc Clain, R.L. 2003. Effect of delay in long heating and cooling systems.
- [57] Curain, R. F., and Zwart, H. J. An Introduction to Infinite-Dimensional Linear Systems Theory. *Springer-Verlag*, New York, 1995.
- [58] Alotaibi, S., Sen, M., Goodwine, J.W., and Yang, K.T. Numerical simulation of the thermal control of heat exchangers. *Numerical Heat Transfer*, Vol. 41, pp. 229-244, 2002.
- [59] Alotaibi, S., Sen, M., Goodwine, J.W., and Yang, K.T. Controllability of conductive-convective systems. *The 6th ASME-JSME Thermal Engineering Joint Conference*, March 16–20, Hawaii, 2003.
- [60] Diaz, D., Sen, M., Yang, K.T. and Mc Clain, R.L. Simulation of heat exchanger performance by artificial neural network. *International Journal of HVAC&R Research*, Vol. 5, No. 3, pp. 195-208, 1999.
- [61] Özisik, M. N. *Boundary Value Problems of Heat Conduction* , Dovers Publication, 1989.
- [62] Özisik, M. N., and Orlande, H. R. B. *Inverse Heat Transfer: Fundamentals and Application*, Taylor & Francis, 2000.
- [63] Sontag, E.D. *Mathematical Control Theory*, Springer-Verlag, New York, 1990.
- [64] Naidu, D. S. *Optimal Control system*, CRC Press 2003.

- [65] Xia L., Abreu-Garcia D., and Hartley T. Modelling and simulation of a heat exchanger. *IEEE International Conference on Systems Engineering*, Aug 1-3 1991.
- [66] Sieder, E. N., and Tate, C. E. Heat transfer and pressure drop of liquids in tubes. *Ind. Eng. Chem.*, vol. 28, pp. 1429, 1936.
- [67] Knudsen, J. D., and Katz, D. L. *Fluid Dynamics and Heat Transfer*, McGraw-hill Book Company, New York, 1958.
- [68] Ogunnaike, B. A., and Ray, W. H. *Process Dynamics, Modeling, and Control*. Oxford University Press, New York, 1994.